Ansto

ANSTO/E739

AN ANALYSIS OF MOLYBDENUM-99 EXPIRY TIMES IN SODIUM PERTECHNETATE, DERIVED FROM A DRY-BED GENERATOR

2000

By

R K Barnes
P J Anderson
D Stimson
J Chapman
M Druce

March 2000

ISSN 1030 7745
ISBN 0 642 59977-7

AUSTRALIAN NUCLEAR SCIENCE
AND TECHNOLOGY ORGANISATION

AN ANALYSIS OF MOLYBDENUM-99 EXPIRY TIMES IN SODIUM PERTECHNETATE, DERIVED FROM A DRY-BED GENERATOR

2000

By

R K Barnes
P J Anderson
D Stimson
J Chapman
M Druce

ABSTRACT

Fission-based $^{99}Mo/^{99m}Tc$ generators have undergone evolutionary changes since they were first manufactured at the Lucas Heights Laboratories in the late 1960s for the Australian nuclear medicine community. This study is aimed at understanding the chemistries, which influence the behaviour of the heterogeneous molybdenum-alumina system in a chromatographic generator. The quality of sodium pertechnetate, derived from a dry-bed generator is enhanced when compared with the traditional wet-bed technologies. Data is presented which compare the extent of ^{99}Mo desorption from both wet and dry-bed chromatographic generators. The expiration times for sodium pertechnetate, based on ^{99}Mo breakthrough, are significantly greater for the recently developed dry-bed generators.

ISSN 1030 7745

ISBN 0 642 59977-7

The following descriptors have been selected from the INIS Thesaurus to describe the subject matter in this report for information retrieval purposes. For further details please refer to IAEA-INIS-12 (INIS: Manual for Indexing) and IAEA-INIS-13 (INIS Thesaurus) published in Vienna by the International Atomic Energy Agency.

INIS descriptors:

ACTIVITY LEVELS; ADSORPTION; ALUMINIUM OXIDE; CHARGE DENSITY; CHEMICAL STATE; COMPILED DATA; DATA ANALYSIS; DESORPTION; DRUGS; ELUTION; GAMMA SPECTROSCOPY; HIGH PURITY GERMANIUM DETECTORS; IMPURITIES; ION EXCHANGE CHROMATOGRAPHY; ISOTONI SOLUTIONS; ISOTOPE RATIO; LIFETIME; MOLYBDENUM-99; NEUTRON FLUX; NUCLEAR REACTION KINETICS; PERTECHNETATE; POROSITY; QUALITY CONTROL; RADIATION DOSES; RADIOACTIVITY; RADIOISOTOPE GENERATORS; REGULATORY GUIDES; STATISTICS; SURFACES; TECHNETIUM-99M; URANIUM-235

Additional descriptors:

ALPHA ALUMINA; AMPHOTERIC OXIDES; BRAUNER EMETT TELLER; EXPIRY TIME; GAMMA ALUMINA; SODIUM PERCHNETATE; ZERO POINT OF CHARGE

SUMMARY

FIGURES

AN ANALYSIS OF MOLYBDENUM-99 EXPIRY TIMES IN SODIUM PERTECHNETATE, DERIVED FROM A DRY BED GENERATOR

1. INTRODUCTION

Fission-based, $^{99}Mo/^{99m}Tc$ generators have been manufactured by the Lucas Heights laboratories since the late 1960's for the nuclear medical community. Since then, the generator has undergone evolutionary changes in design to accommodate firstly, pharmacopoeial requirements and secondly the commercial markets. The current development of a commercial dry-bed generator concept brings Australia into line with other major international manufacturers who introduced dry-bed technology in the early 1980's.

One important measure of pertechnetate quality is the radionuclidic purity, that is, the extent to which ^{99m}Tc is contaminated with other trace radionuclides. With the exception of the ubiquitous long-lived isomer ^{99}Tc, ^{99}Mo is generally the major radiocontaminant measured in pertechnetate, eluted from chromatographic generators. Pharmacopoeia monographs therefore specify strict limits for ^{99}Mo impurity (see Section 2).

The chemical separation technology employed in commercially available generators is such that the extent of ^{99}Mo contamination in sodium pertechnetate is some orders of magnitude lower than the prescribed limits in the pharmacopoeias. Commercial manufactures of generators therefore define an 'expiry time' for sodium pertechnetate as being that time in the future when a longer-lived radioisotope meets a specified fraction of the radioactivity of ^{99m}Tc (see Section 2). Longer expiry times for ^{99m}Tc allow greater utility and versatility of product use in busy nuclear medicine departments.

This study is aimed at understanding the factors which influence ^{99}Mo desorption from chromatographic generators and hence expiration times of sodium pertechnetate. Comparisons are made between the wet-bed and dry-bed technologies.

One outcome of our study into the chemistry of the molybdenum-alumina system for generators indicated that the dry-bed chromatographic technology had superior performance, in relation to ^{99}Mo desorption, to the older wet-bed technology. Based upon this observation, ANSTO proposes to increase the specification for expiration time of sodium pertechnetate, derived from a dry-bed generator, from the current 8 hours to 12 hours. This specification shall be met for unusual elution scenarios.

2. EXPIRATION TIMES OF SODIUM PERTECHNETATE

Pharmacopoeia monographs define the minimum requirements of radionuclidic purity for sodium pertechnetate, vis:

- The British and European Pharmacopoeias define that ^{99}Mo content should be "not greater than 0.1% at the date and hour of administration"
- The United States Pharmacopoeia defines the ^{99}Mo content should "not be greater than 0.15 KBq/MBq [of ^{99m}Tc] in the injection at the time of administration". ie 0.015% at expiry.

To be of utility to nuclear medicine, sodium pertechnetate is expected to meet pharmacopoeial standards up to a definite time, post-generator elution. This time is defined as the expiry time. The current expiry-time prescribed for ^{99m}Tc eluates, derived from ANSTO manufactured, wet-bed generators, is 8 hours. The current dry-bed generator is expected to have a minimum expiration time of 12 hours.

Derivation of a general function for Expiry Time estimate.

From simple half-life considerations the ratio of a long-lived radionuclide to a shorter lived isotope in the same sample increases with time. The expiry time for a long-lived radionuclidic contaminant in a shorter lived radioisotope, is that time in the future when the longer-lived species reaches a defined fraction of the shorter-lived isotope.

A general equation for expiry time can be derived:

$$A_1 = A_{1,0}\, e^{-\lambda_1 t}$$

$$A_2 = A_{2,0}\, e^{-\lambda_2 t}$$

Where:

A_1 = activity of long lived isotope at time t

$A_{1,0}$ = activity of longer lived isotope at t = 0

A_2 = activity of short-lived isotope at time = t

$A_{2,0}$ = activity of shorter lived isotope at time t = 0

λ_1 = decay constant for long lived isotope.

λ_2 = decay constant for shorter lived isotope

then,

$$t_{exp} = (1/\lambda_2 - \lambda_1)\ \ln (f \,.\, A_{2,0}/A_{1,0})$$

where:

t_{exp} = expiry time (expressed in the same units of time used to compute λ_1 and λ_2)

f = radioisotopic ratio of the longer-lived contaminant to the shorter lived radioisotope ,

f = 0.001 for ^{99} Mo in ^{99m} Tc.

The expiry time for ^{99} Mo in ^{99m} Tc is given by:

$$t_{exp} = 9.56 \ln (0.001 A^{99m}_{Tc}/A^{99}_{Mo})$$

In this study the radioactivity's of ^{99m} Tc and ^{99} Mo were measured in each generator eluate using a calibrated γ- spectrometer (see Section 3).

3. EXPERIMENTAL

Overview of Generator Manufacture and QC

The chromatographic alumina column, used in ANSTO manufactured generators, is prepared by sedimentary deposition of the bottom strata of 1.5 g of medium grained (53 μm mesh) alumina. This step is followed by the deposition of 0.5 g of coarse (125μm mesh), heat-treated, alumina. The deposition is performed under gravity in 0.5 mol.L^{-1} nitric acid. The chromatographic column is then allowed to drain under gravity. The column height of alumina is 15 mm.

Small volumes (<1mL) of FP ^{99}Mo are sorbed onto the top, coarse-alumina strata of the column. This loading step is followed with a conditioning bolus of 0.5mL of 0.5mol.L^{-1} nitric acid and a 250 mL wash with isotonic saline. The generator is terminally sterilised by autoclaving.

As 'in-process' quality check, each production generator is allowed an appropriate ingrowth time, followed by an elution with 10 mL of isotonic saline. ^{99}Mo breakthrough is measured by γ-spectroscopy.

Wet Bed Generators

Wet Bed generators produced by ANSTO are typically eluted with 10 mL volumes of 0.9% w/v isotonic saline, contained in a vinyl sachet. The saline is spiked with 90 μg.mL^{-1} sodium nitrate as a weak oxidant. During the quiescent ingrowth phase between elutions, the chromatographic column is in continuous contact with the eluting solution.

Normal elution regimes for the generator may vary, depending upon demand of the relevant nuclear medicine department however, a typical elution regime would involve a minimum of once per day over a maximum fourteen day cycle.

Dry Bed Generators

Dry-Bed generator technology involves eluting ^{99m}Tc from the alumina column, using bottled saline, into a sterile evacuated vial. The receptacle vial has sufficient vacuum

to pull filtered air, via a 0.22 um membrane filter, through the chromatographic column after the ^{99m}Tc desorption. This operation expunges mobile phase from the interstitial volume of the alumina stationary phase, hence the term 'dry-bed'.

Elution regimes are similar to the Wet Bed generator, however the dry-bed technology is such that the generator can be eluted with any saline volume up to a maximum of 20 mL.

Experimental studies have shown that although the 'dry-bed' technology removes eluate from the void volume of the column, surface adhesion of saline to the stationary phase is indicated to the extent of approximately 0.1 mL/g alumina.

Measurement of Expiry Times

γ-emitting radiocontaminants in sodium pertechnetate were measured in each eluate by γ-spectrometry, employing an intrinsic germanium detector. To reduce the flux of 140 keV γ-photons of ^{99m}Tc, on the detector, samples were shielded in a suitable lead attenuator during counting. The expiry times for ^{99}Mo were computed from these measurements.

The current expiry time specification for generator derived sodium pertechnetate is 8 hours.

Elution Profiles of ^{99m}Tc

Elution profiles were established by monitoring successive 1 mL fractions eluted from generator columns. Elution profiling for ^{99m}Tc was conducted on the smallest commercial generator (20GBq) and the largest generator (120 GBq) for both the wet and dry-bed technologies.

Generator Sets

One component of the development work for the dry-bed generator involved a direct study of the performance characteristics of the dry-bed compared with that of wet-bed generators of equal radioactivity.

Ten sets of generators were produced covering the range of commercial interest from 20 GBq at calibration to 120 GBq at calibration. Each set constituted one wet-bed and one dry-bed generator, both of the same activity.

All generators manufactured by ANSTO are eluted within the production laboratories, before dispatch. This elution is defined as the "zero elution" in this study.

4. RESULTS AND DISCUSSION

An analysis of pertechnetate quality, in relation to ^{99}Mo breakthrough, requires an understanding of the physico-chemical interaction between high specific-activity radiomolybdenum/daughter and the alumina stationary phase, during the manufacturing and operating cycles of the generator.

4.1 Chemistry of the ^{99}Mo-Alumina System in ^{99}Mo/^{99m} Tc Generators

4.1.1 Fission-based ^{99}Mo solutions

Fission-based ^{99}Mo is produced at the ANSTO laboratories by irradiating approximately 240 g of sintered uranium dioxide, enriched to 2.2 % in ^{235} U, in an average neutron flux of $7 * 10^{13}$ for 4 -7 days. The target is 'cooled' ex-reactor, for a period of approximately 4 hours before chemical processing.

The specific activity of FP ^{99}Mo is significantly less than the carrier free value of $4.8 * 10^5$ Ci g^{-1} due to the presence of stable molybdenum isotopes, formed concurrently during the irradiation process[1]. The average specific activity of ^{99}Mo at the time of generator manufacture is approximately $5 * 10^4$ Ci g^{-1} ($1.85 * 10^6$ GBq g^{-1}).

The concentration of ^{99}Mo in the stock "load" solutions, at the time of generator manufacture, varies from approximately $1 * 10^{-3}$ mol.L^{-1} to $5 * 10^{-3}$ mol L^{-1}.

Fission-produced ^{99}Mo, in nitric acid stock solutions have been shown to exist in the hexavalent oxidation state using paper chromatography [2].

Molybdenum Speciation

The aqueous chemistry of Mo(V1) is complex and considerable effort has been dedicated to defining its nature[3]. Potentiometric measurements followed by complex computer modelling are used to assess the extent and type of Mo(V1) species[3]. Consistent with the higher atomic number elements of Group 6B, Mo(V1) can exist in a number of polymeric oxy-anions. Speciation is a direct function of pH and [Mo(V1)] concentration[3]. Species range from monomeric forms in acid solution such as H_2MoO_4 at lower concentration (0.1 m.mol L^{-1} Mo(V1)) to polymeric forms such as $[Mo_7O_{24}]^{6-}$, $[Mo_7O_{22}(OH)_2]^{4-}$,$[Mo_8O_{26}]^{4-}$,$[Mo_{10}O_{34}]^{8-}$ at higher concentrations (10 m.mol L^{-1} Mo(V1)) [3].

Recent computer modelling of Mo(V1) speciation at our institution, across the range of Mo(V1) concentrations expected in fission-based ^{99}Mo can be seen in Figures 1a,1b,1c [4].

Brown[3] showed that, in general, the kinetics of solution equilibria of Mo(V1) were rapid with the exception of the formation of the octameric species $[Mo_8O_{24}]^{4-}$ from heptameric and monomeric forms.

4.1.2 Chromatographic Alumina used in Generator manufacture

Crystal Structure

Alumina exhibits polymorphism in which different crystalline modifications can occur. Corundum or α-alumina is the most thermodynamically stable structure of Al_2O_3. This alumina has a crystal structure of a hexagonal di-pyramid rhombohedron and is formed at ignition temperatures greater than 1200 °C. Gamma-alumina (γ-alumina) is the cubic close packed crystalline structure formed at lower ignition temperatures < 1000 °C. X-ray diffraction studies on the coarse and medium grained

alumina used in the ANSTO chromatographic generators confirm the stationary phase to be γ-alumina. The X-ray diffraction patterns on the chromatographic alumina further indicated the porus nature of the material.

Surface Area

Surface area determinations, on coarse and medium grained γ-alumina, used in the generator manufacture were determined using the standard Brauner-Emmet-Teller (BET) method.

The BET surface area of the medium and coarse grained alumina were 175.6 $m^2 g^{-1}$ and 158.3 $m^2 g^{-1}$ respectively. Further evidence of the meso-porosity (pore size 2.0 to 50.0 μm) of the alumina was found. The pore volume of the alumina was found to be 0.26 g cm^{-3} for each of the medium and coarse grade alumina.

Surface Charge Densities

At alumina surfaces, where crystal boundaries have been dislocated, alumina can adopt electrically charged surfaces. The sign and magnitude of the surface charge at a solid-solution interface is usually dictated by the nature and concentration of potential determining ions. Potential determining ions being those ions which can freely establish an equilibrium at the solid-solution interface such as H^+ and OH^-. Amphoteric oxides such as alumina have a pH dependent charge resulting from proton transfer across the solution-solid boundary.

Surface charge densities of chromatographic alumina used in generator manufacture smoothly increased to +1C m^{-2} at pH values more acidic than the ZPC (zero point of charge) at pH_{ZPC} 8.6 [2] . At pH values more alkaline than the pH_{ZPC} the surface charge density decreased to approximately - 0.5 C m^{-2} at pH 12.

From a quality perspective in the manufacture and operation of $^{99m}Tc/^{99}Mo$ generators the pH_{ZPC} is sensitive to the presence of impurities. The sorption of some anionic impurities can shift the pH_{ZPC} to more acidic values. This is of particular importance in the maintenance of pertechnetate quality during the elution stage. If the pH_{ZPC} is moved too far in the acidic direction, the surface charge density, which would normally exist at a defined pH, is decreased and ^{99}Mo may be partially desorbed during generator elution. For instance, we have demonstrated that eluting a generator 0.15mol L^{-1} of sodium sulphate instead of isotonic (0.15 mol L^{-1}) saline can result in the desorption of greater than 50 % of the FP ^{99}Mo.

Adsorption Processes in the Manufacture and Operation of Generators.

Mechanisms of the adsorption-desorption processes of ^{99}Mo during generator manufacture and operation are complex. One hypothesis for adsorption involves the attraction of negatively charged Mo(V1) polymers to the positively charged alumina surfaces at the pH of adsorption (pH 0.3-0.5). As the polymeric anions diffuse from the bulk of solution to strongly sorb to the alumina surface the bulk solution concentration of Mo(V1) decreases. Solution equilibria is rapidly re-established [3] at these low pH values in which neutral monomeric species (H_2MoO_4) predominate, in accord with the model in Figures 1a-1c. The observation that greater than 99.8% of

^{99}Mo(V1) is sorbed to the alumina surface suggest that neutral monomeric forms should dissociated and react at the positive alumina surface. The kinetics of Mo(V1) adsorption to alumina [2], [5] is significantly slower than the rapid solution equilibria of Mo(VI) [3].

The sorption processes to alumina are however, more complex than the simple physisorption model above. It is well established that approximately 20% of Mo(V1) bound to an alumina column cannot be removed, even under very strong alkaline conditions (4 mol L^{-1} NaOH). It is therefore apparent that strong chemisorption processes operate for at least a portion of the sorbed Mo(V1).

The sorption capacity of γ-alumina for Mo(V1) has been shown to be a function of both acid and Mo(V1) concentrations [2]. Under the conditions of manufacture the sorption capacity is approximately 2 mg [Mo(V1)]/ gram alumina [2]. The maximum mass of fission-based ^{99}Mo loaded onto a generator at manufacture, is approximately 0.2 mg, calculated for a 120 GBq generator with a 5 day pre-calibration. Adsorption bands can be seen on aged generator columns to a depth of approximately 2 mm indicating that the ^{99}Mo is sorbed in a very narrow strata at the top of the alumina column.

After ^{99}Mo adsorption at pH 0.3-0.5 the alumina column is washed with 250 mL of saline changing the column environment to pH 5.6. The sorption capacity of alumina for Mo(V1) under these conditions increases to approximately 5 mg Mo(V1)/gram alumina.

4.2 Elution Profiles of ^{99m}Tc from Generator Columns

In a routine clinical environment, radioactive concentrations of generator-derived ^{99m}Tc can be varied by varying elution volumes. As the radionuclidic purity of pertechnetate in the eluted volumes is a function of both the eluted activities of ^{99m}Tc and ^{99}Mo, it is important to know the elution characteristics of pertechnetate.

Ion exchange is the most probable mechanism for $^{99m}TcO_4^-$ desorption from alumina in which 0.155 mol.L^{-1} [Cl^-] in isotonic saline exchanges with $^{99m}TcO_4^-$ at positively charged, protonated sites on the amphoteric alumina. The desorption characteristics of $^{99m}TcO_4^-$ from wet and dry-bed columns were compared by conducting a series of elution profiles. Figures 2a and 2b show the elution profiles of 20 GBq generators and 120 GBq generators respectively.

The elution profiles conform to the expected elution characteristics for a generator column of mass of 2.5 g alumina and height 15 mm. The desorption peak-maxima of approximately 3 mL is consistent with the linear relationship between elution volume, required to eluate the maximum concentration (C_{max}), and column height [6].

As expected from a simple equilibrium model, the peak-maxima is independent of generator activity. No significant differences were observed between the wet and dry-bed technologies. The eluted peak width (β) measured at (C_{max}/e) is approximately 2 mL. The peak width of eluted ^{99m}Tc is marginally smaller than the predicted values, obtained by Boyd [6], of linear plots of β versus ($h^{½}$). This indicates the high resolution with which ^{99m}Tc is eluted from both wet and dry-bed generators.

4.3 Molybdenum Breakthrough from Chromatographic Generators and Expiry Time Measurements

In routine clinical operations of a generator, trace quantities of ^{99}Mo are displaced from the generator column during elution. ^{99}Mo 'breakthrough' maybe attributed to both classic desorption processes, at the solid-solution interface, plus molybdenum bound to displaced, sub-micron, particulate alumina. The breakthrough process, however, is significantly more complex than a simple equilibrium model would suggest.

Figures 3a to 3j indicate the ^{99}Mo breakthrough as a percentage of ^{99m}Tc activity, at the time of elution, for ten sets of generators. The 'predicted percentage' of ^{99}Mo in eluted sodium pertechnetate, shown in Figures 3a-3j, are based on a single, pre-dispatch elution. The equilibrium model used in the 'predicted' plots considers that the same fraction of ^{99}Mo is eluted with each 'milking', decay corrected, and that the ^{99m}Tc is eluted with an 85% efficiency. A similar predictive plot in Figures 3a-3j, shows the percentages of parent breakthrough, if the measured ^{99}Mo was multiplied by a factor of 1.5. To simulate a worst-case elution scenario in a clinical environment, the predictive curves in Figures 3a-3j have included a last point in which the time difference between the 17 and 18th elution is considered to be 2 hours.

In each of the ten sets of generators it can be clearly seen that ^{99}Mo breakthrough is significantly greater for the wet-bed generators compared with the dry-bed technology.

^{99}Mo breakthrough can be more fully appreciated when expressed as a fraction of the ^{99}Mo eluted from the column to the ^{99}Mo retained by the chromatographic column, referenced to the time of elution, Figures 4a-4j. Similar to plots 3a-3j, the predicted fractions, shown in plots 4a-4j, are based on the measurement of ^{99}Mo content in a single, pre-dispatch elution. This 'predictive' equilibrium model assumes that the ratio of desorbed ^{99}Mo, to that retained by the alumina stationary phase, remains constant from the first pre-dispatch elution throughout the life of a generator – the figures are corrected for radioactive decay.

The measured ^{99}Mo breakthrough for both the wet and dry bed generator technologies, appears random and does not conform to any simple standard equilibrium isotherm. The extent of ^{99}Mo breakthrough, generally decreases with increasing elution number , and generator age. The extent of deviation of measured ^{99}Mo breakthrough is highlighted against the predictably flat equilibrium model, in Figures 4a-4j.

^{99}Mo Breakthrough as a function of Elution Volume and Time

The high points in the 'zigzag' plots exhibited for dry-bed generators DB-3, DB-4 and DB5 (Figures 4c, 4d and 4e) are attributed to generator elution with a 20 mL volume. Higher elution volumes desorb greater activities of ^{99}Mo.

Figures 5 and 6 show the ^{99}Mo breakthrough from an 80 GBq generator as a function of elution volume, for two separate elution regimes. The elapsed time involved during fraction collection is shown on the abscissa axis of Figure 5.

Compared to the radioactivity of ^{99}Mo eluted in the first 10 mL fraction, at time zero, the extent of molybdenum desorption decreases to a plateau region, in which the breakthrough in subsequent fractions, is a factor of 2 to 3 lower than that desorbed at time zero. The plateau region is reached after a cumulative volume of 50 mL of saline is passed through the alumina stationary phase – Figure 6.

In addition to a volume relationship for the extent of ^{99}Mo breakthrough during generator elution, a kinetic factor is also evident. The plateau region of the ^{99}Mo fraction/volume curve in Figure 5 shows that ^{99}Mo reaches a low plateau after 4-5 minutes during fraction collection, indicating that ^{99}Mo is in kinetic equilibrium between the mobile and stationary phases.

Figure 5, indicates that the desorption kinetics of molybdenum from alumina, although slow, are sufficiently fast to ensure a minor fraction of molybdenum is always available for elution. The position of the plateau on the ordinate axis is a measure of the desorption kinetics, the lower the fraction-time plateau, the slower the desorption kinetics.

Although the kinetic assumptions above are consistent with the forward and reverse rate constants described by Bourikis et al [5] it is unknown as to what extent desorption kinetics of ^{99}Mo is a function of slow, diffusion-controlled processes, from within the extensive meso-porous structures of the γ-alumina.

The chemical nature of the soluble, desorbed ^{99}Mo(V1) species, present during generator elution is probably the monomeric $HMoO_4^-$. This species is based on a column environment of pH 5.6 and a desorbed concentration range of $1*10^{-10}$ to $2*10^{-9}$ mol L^{-1} Mo, as computed from specific activity considerations.

Radiation Doses and Impact on ^{99} Mo Breakthrough

Commercial-based generators, produced by ANSTO, currently range from 20 GBq to 120 GBq at calibration. Some generators are manufactured with a 5 day pre-calibration period. Radiation doses to the top alumina strata of a 120 GBq generator, produced 5 days pre-calibration, are of the order of 30 M.Gy (3 G.Rad) during the life time of a generator [7]. Other generator activities give proportionate doses to the alumina strata.

One area of our investigation considered whether there was a dose-related effect on ^{99}Mo desorption from an alumina column, over the range of generator activities, ie 20 GBq to 120 GBq. Considering the high radiation doses to the solid/solution interface, was there any changes in surface chemistry of alumina which may impact on ^{99}Mo desorption processes?

Table 1 shows the ^{99}Mo activity and the mean expiry times of each generator in the set of ten.

A statistical analysis of the data showed no correlation between generator activity and ^{99}Mo desorption profiles, as indicated by the mean expiration times, for both wet and dry bed technologies. Statistically insignificant correlation coefficients of 0.22 and 0.15 were found for the wet and dry-bed generators respectively.

We concluded that there was no dose-related impact on ^{99}Mo breakthrough from an alumina surface, over the activity ranges studied.

Expiration Times of Wet-Bed and Dry Bed Generator

Application of the t-test criteria, to compare the mean expiry times for the ten sets of generators, shown in Table 1, found that a significant difference existed at the 95% confidence level for nine out of the ten generator sets. The dry-bed generator giving significantly greater expiry times (a pooled mean of 68 hours) than the wet-bed technology (a pooled mean of 55 hours).

Although a 13 hour difference was shown between the pooled means of the dry and wet-bed technologies one set of generators, out of the ten, showed no difference between means. DB-7 and wet bed generator WB-7, showed no statistically significant difference in means indicating expiry times of 50.4 +/- 5.3 hours for DB7 and 48.6 +/- 4.0 hours for WB-7. A statistical F-test indicated that there was no difference in the variances of expiry times between the wet-bed and dry-bed technologies, for each of the ten generator sets.

Individual expiry times for each eluate is shown in Figures 7a to 7j. Each generator was eluted for a minimum of 17 times. Dry-bed generator (DB-1), Figure 7a, shows only twelve points due to elutions 13 to 17 being below the level of ^{99}Mo detection, using routine γ-spectrometric analysis.

Predictive Estimates of ^{99}Mo Expiry Times for Dry-Bed Generators

^{99}Mo(V1) desorption from an alumina column does not conform to any standard equilibrium model but rather appears to elute in an almost random nature, although the general trend, indicated in Figures 4a-4j, is for the extent of breakthrough to decrease during the life of the generator.

Any predictive paradigm must therefore be of an empirical nature. In order to estimate the expiration times from a single, pre-dispatch elution, our laboratories have erred on the cautious side.

The empirical approach we anticipate adopting for the dry-bed generator considers that ^{99m}Tc is eluted with 85% efficiency throughout the generators life and that the ^{99}Mo, eluted in a 10 mL volume 'pre-dispatch', is multiplied by an empirical factor of 1.5. The factor of 1.5 is applied to accommodate elution volumes of up to the maximum of 20 mL.

The pre-dispatch elution, must give a predicted expiration time of greater than 30 hours, for the first clinical elution at calibration. Further, a worst case elution scenario is considered in which a generator is eluted, with a minimum ^{99m}Tc ingrowth of 2 hours, at the end of its effective life. In this situation, ie low ^{99m}Tc activity, high ^{99}Mo activity, the effect of the ^{99}Mo breakthrough is significantly amplified.

Each of the 'expiry time' plots in Figures 7a-7j show three curves, viz: the measured expiry time; the predicted expiry time based on the ^{99}Mo breakthrough in a single pre-dispatch elution and the expiry time based on the ^{99}Mo desorption multiplied by an

empirical factor of 1.5. The last point in each of the 'predicted' curves in Figures 7a – 7j includes the case for a 2 hour ingrowth scenario, as defined above.

Of the ten dry-bed generators in this study, a total of 170 elutions were conducted. Out of the total number of elutions, seven eluates (5 for DB6 and 2 for DB7) were below the empirically predicted values for the specific elution number – see Dry-Bed plots in Figures 7a-7j. Of the 170 test elutions conducted in the dry-bed study, the minimum expiry time found was 36 hours on DB7-6. The measured expiration times for the dry-bed technology, Figures 7a-7j, are well above the current 8 hour specification defined for the wet-bed generator, and the proposed 12 hour limit for the dry-bed generator.

The empirically derived expiration times were lower than the measured values for both wet and dry bed generators toward the end of a standard 14 day elution cycle. Hence the predicted expiration times may be used to estimate the worst case scenario for ^{99}Mo breakthrough for a specific generator elution.

The empirically estimated expiration time for the last point in each of the dry-bed curves, Figures 7a-7j, was greater than 25 hours. The last point indicating an elution with a 2 hour ^{99m}Tc ingrowth. The predicted expiry times on the last elution are significantly greater than the existing 8 hour specification for sodium pertechnetate and the proposed value of 12 hours.

Figures 8a-8c show a series of plots of ^{99}Mo breakthrough for a 14 day elution cycle for an experimental 80 GBq dry-bed generator. In these plots, elution number 15 was conducted 2 hours after the 14th elution, and elution number 16, 3 hours after the 14th elution, in each case the ^{99}Mo breakthrough was measured. In each case the predicted ^{99}Mo breakthrough was significantly greater than the measured breakthrough. Hence the predictive model constitutes a worst case scenario and may be used as a pass/fail criteria for generator quality.

Further it can be shown from the last two points in Figures 8a-8c, that if a dry-bed generator were milked in an unusual manner toward the end of it's life, that the pertechnetate quality is still maintained with respect to ^{99}Mo expiry time.

5. CONCLUSIONS

ANSTO has manufactured commercial ^{99m}Tc/^{99}Mo generators from fission-based ^{99}Mo since the late 1960's. Since then, the generator has undergone evolutionary changes in design to accommodate pharmacopoeial requirements and the commercial markets.

The transition by ANSTO in the late 1990's to dry-bed generator technologies required a comprehensive study to assess generator performance and quality, from a regulatory consideration.

One production imperative for a quality product is the ability of a manufacturer to be able to predict worst-case performance scenarios, below which a generator's performance and quality should not fall. The major non-technetium

radiocontaminant, which may effect the quality of sodium pertechnetate, derived from fission-based $^{99m}Tc/^{99}Mo$ generators, is the parent nuclide ^{99}Mo.

ANSTO expresses the radionuclidic purity of its sodium pertechnetate in terms of an expiration time, that is the time in the future, when a long-lived radionuclide meets a prescribed percentage of the ^{99m}Tc activity. The prescribed limit, set for the ^{99}Mo radiocontaminant in sodium pertechnetate, by the British Pharmacopoeia 1999, is not greater than 0.1%, at the date and time of administration. The current expiry times set for generator derived sodium pertechnetate is 8 hours.

An analysis of the chemistry of the molybdenum-technetium-alumina systems showed that the desorption of $^{99m}TcO_4^-$ from γ-alumina, with an isotonic saline mobile phase, conformed to a simple equilibrium model in which ^{99m}Tc was eluted in a narrow band, with the peak radioactive concentration at 3 mL, for both the wet and dry-bed technologies. This is consistent with published data for an alumina column of mass 2.5g and height of 15mm. In contrast, the washout of ultra-trace quantities of ^{99}Mo from the alumina column did not conform to any simple isotherm but reached a low plateau, which was a function of elution volume and time for a specific elution. Analysis of the data for both wet-bed and dry-bed technologies showed that the desorption of ^{99}Mo was erratic from elution to elution, however, a general trend was evident for the extent of ^{99}Mo desorption to decrease over the life time of a generator.

The sorption of anionic species of Mo(V1) to alumina surfaces, at pH values more acidic than the zero point of charge ($pH_{ZPC} = 8.6$), is strong. The solution-surface equilibrium is highly in favour of the sorbed species. The published rate constants for the desorption kinetics of Mo(V1) from alumina surfaces are low compared with the adsorption rate constants. From our studies, there is evidence that there maybe a diffusion-controlled effect for $^{99}Mo(V1)$ desorption from the extensive meso-porous structures (pore size 2 – 50 μm) within the γ-alumina. This effect may partially account for the erratic desorption characteristics of $^{99}Mo(V1)$ over the life-time of the generator.

Analysis of the data compiled in this study for ten sets of generators, each set consisting of a wet and dry-bed chromatographic column prepared under identical production conditions, show that the dry-bed generator had a mean expiry time of 68 hours compared with the wet-bed technology of 55 hours. The product quality for both the wet and dry-bed technologies is significantly better than the minimum specification of 8 hours expiry time. ^{99}Mo desorption and subsequent expiration times for sodium pertechnetate was shown to be statistically independent of generator activity, up to a maximum of 120 GBq at calibration.

Given the apparently random desorption properties of $^{99}Mo(V1)$ from alumina surfaces, the derivation of an exact paradigm for predicting the expiration time for each elution, over the life time of a generator was not possible. However empirically derived expiration times based on a single pre-dispatch elution, can give the lowest limits for worst case scenarios, below which a generator eluate will not fall. From a clinical perspective, this empirical approach is applicable to unusual elution scenarios, conducted at the end of a generators effective life.

For the future manufacture of dry-bed generators, the empirical derivation involves eluting a generator, pre-dispatch, and measuring the extent of ^{99}Mo breakthrough by gamma spectroscopy. This quantity of ^{99}Mo is multiplied by an empirically derived factor of 1.5 and decayed to the calibration time and date. The ^{99}Mo is expressed as an expiry time at calibration, using the equation in Section 2. For the purposes of calculation, an elution efficiency is assumed in which 85% of the available ^{99m}Tc is recovered. If the pre-dispatch elution shows an expiry time greater than 30 hours for the first elution at calibration, than each elution of the generator throughout a life of 14 days, including unusual elution scenarios, will ensure an expiry time of greater than 12 hours.

It is concluded that the expiration time of generator-based sodium pertechnetate may be safely increased from the current 8 hours to 12 hours to accommodate the clinical needs of the nuclear medicine community.

Acknowledgments

The authors wish to thank Dr Paul Brown of ANSTO for his Mo(V1) speciation modelling and helpful comments on the solution kinetics of Mo(V1) speciation. Similarly we thank Mr Anthony Pandolfo of CSIRO for his analysis of the surface areas of alumina. Finally, we are grateful to Mr Enzo Valenti and Mr Michael Dries from the ARI Laboratories for their contribution to this study.

6 REFERENCES

(1) Barnes R.K, Hetherington E.L.R, Ohkubo. M. Determination of the Specific Activity of Fission-based 99Mo using Differential Pulse Polarography. Int.J.Appl. Radiat.Isot 34, 3, 603-606, 1983.

(2) Barnes R.K, Boyd R.E. Some Aspects of the Chemistry of the Molybdenum-Alumina System. International Atomic Energy Agency, Vienna (Austria). Radionuclide Generator Technology Seminar, Vienna. 13-17 October 1986.

(3) Brown .P L, Shying M.E, Sylva R.N. The Hydrolysis of Metal Ions. Part 10. Kinetic and Equilibrium Measurements of Molybdenum (V1). J.Chem.Soc. Dalton Trans, 2149, 1987.

(4) Brown .P.L. Private Communication. May, 1999.

(5) Bourikas K, Goula M.A, Lycourghiotis A, Kinetics of deposition of the Mo-Oxo Species on the Surface of γ-Alumina. Langmuir, 14, 4819, 1998.

(6) Boyd R.E, Radiopharmaceuticals and Labelled Compounds. Conference, 26-30 March, IAEA, Vienna. 1973.

(7) Hetherington E.L.H, Unpublished data. May, 1999.

Figure 1a

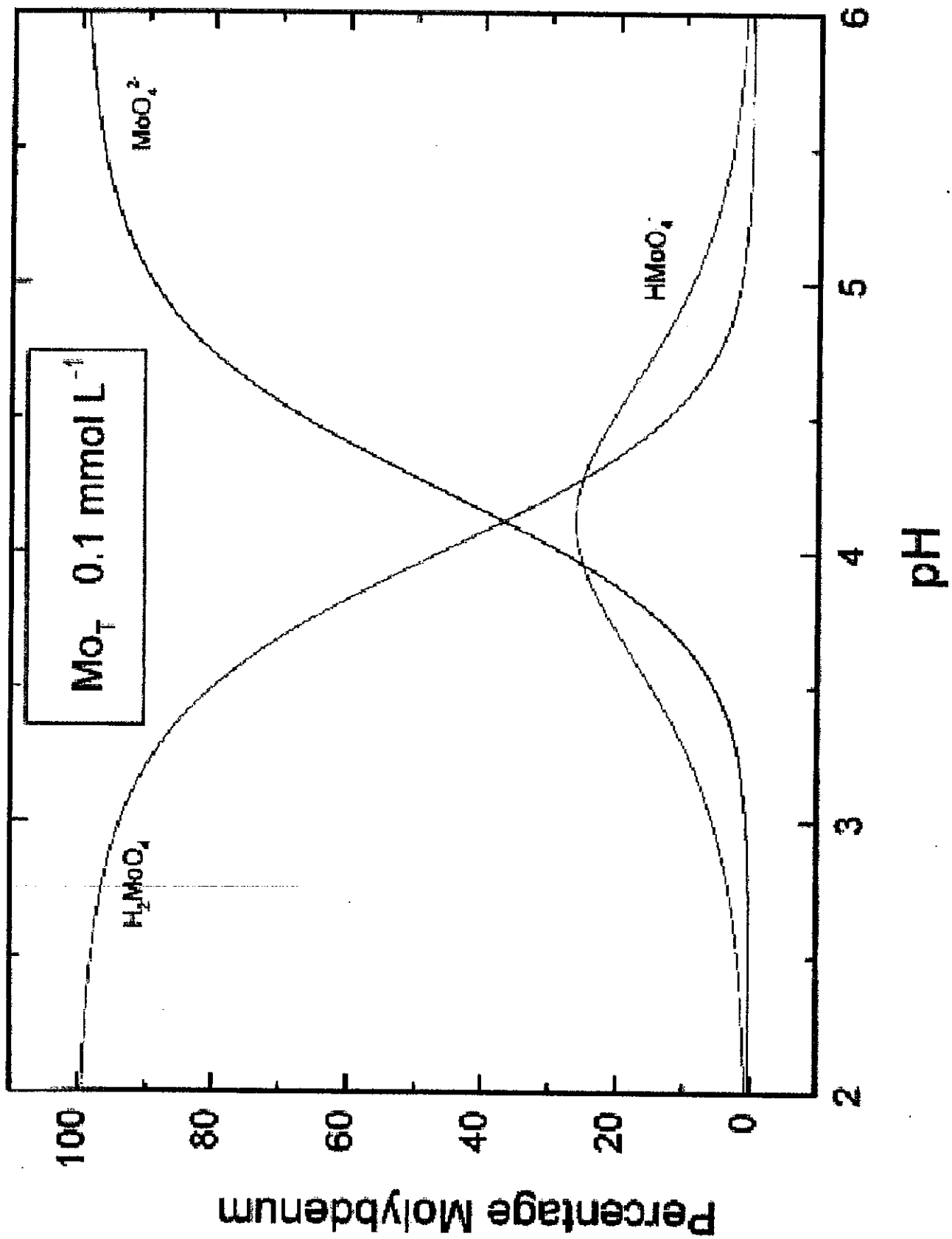
Percentage Molybdenum
pH
Mo_T 0.1 mmol L^{-1}
MoO_4^{2-}
$HMoO_4^-$
H_2MoO_4
100
80
60
40
20
0
2
3
4
5
6

Figure 1c

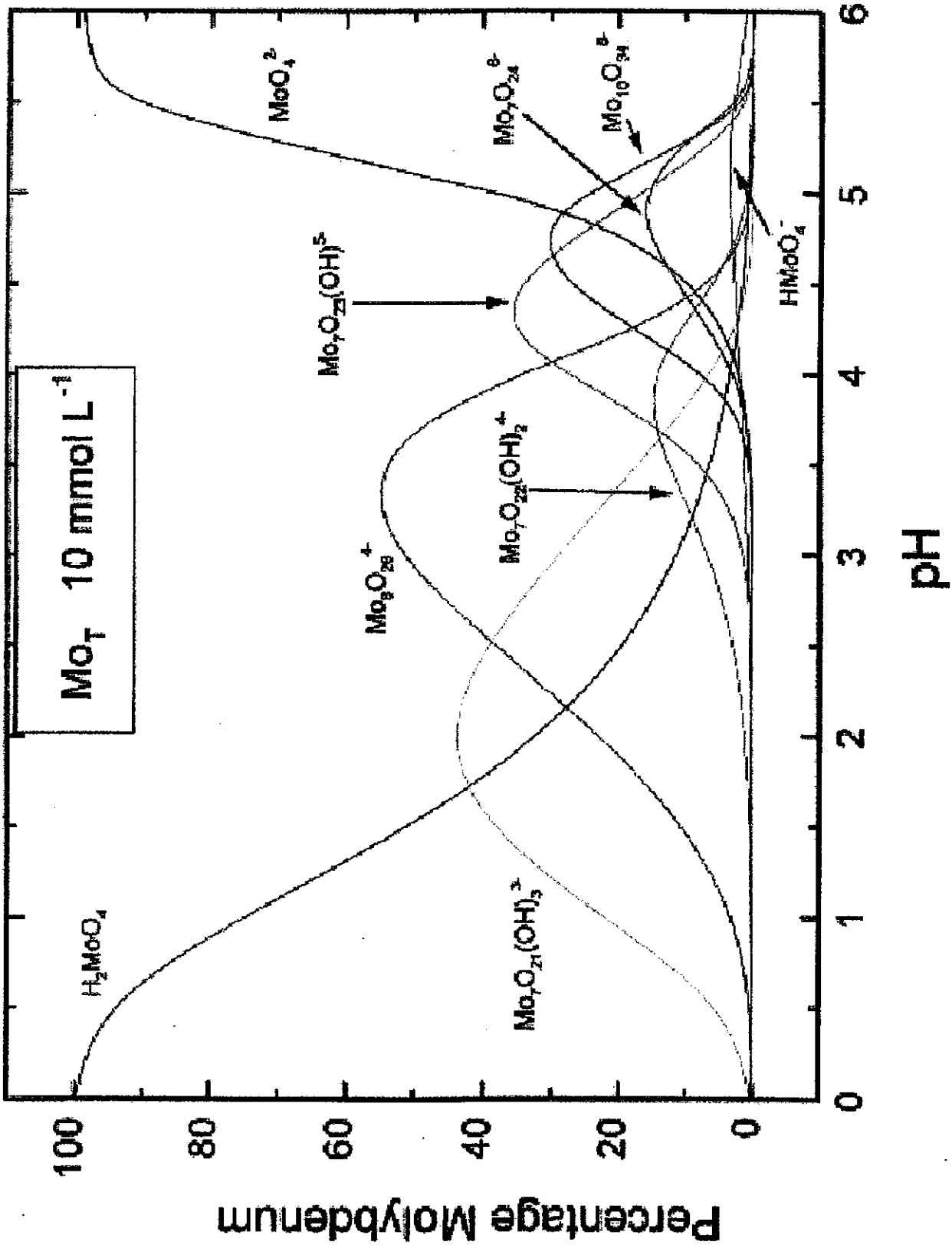
Percentage Molybdenum
pH
Mo_T 10 mmol L^{-1}
H_2MoO_4
MoO_4^{2-}
$Mo_7O_{24}^{6-}$
$Mo_{10}O_{34}^{8-}$
$Mo_7O_{21}(OH)^{5-}$
$Mo_8O_{26}^{4-}$
$Mo_7O_{22}(OH)_2^{4-}$
$Mo_7O_{21}(OH)_3^{3-}$
$HMoO_4^-$

Figure 2a.

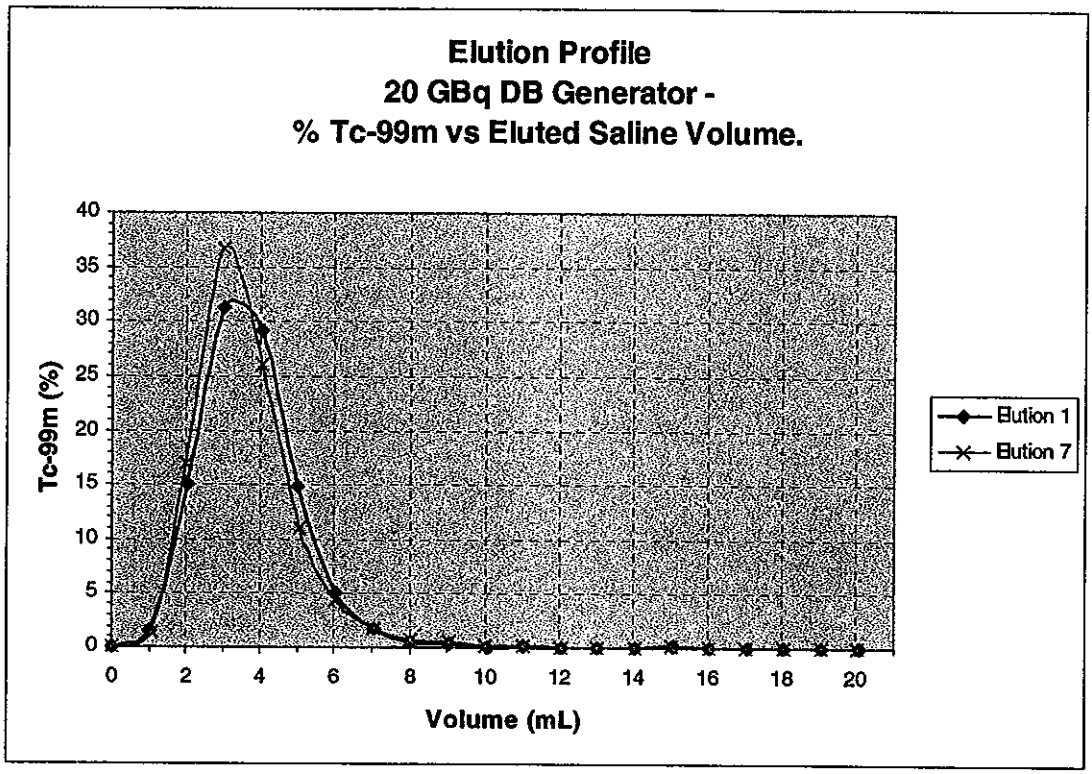
Elution Profile
20 GBq DB Generator -
% Tc-99m vs Eluted Saline Volume.
Tc-99m (%)
Volume (mL)
Elution 1
Elution 7

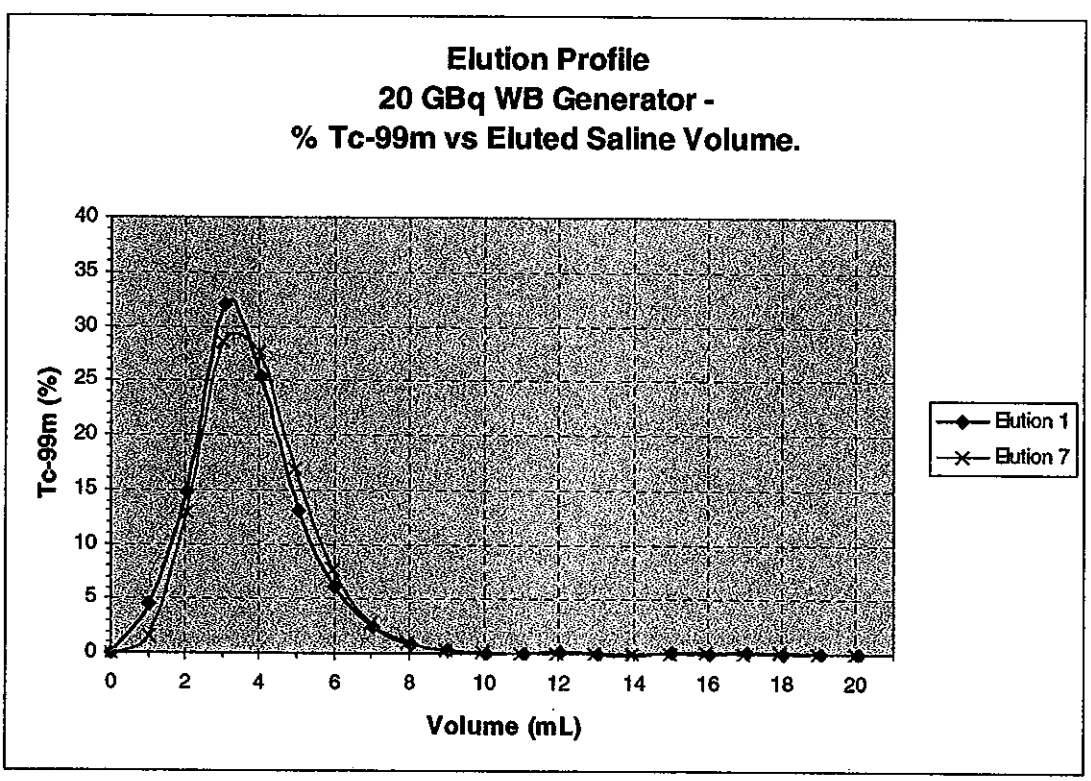
Elution Profile
20 GBq WB Generator -
% Tc-99m vs Eluted Saline Volume.
Tc-99m (%)
Volume (mL)
Elution 1
Elution 7

Figure 2b.

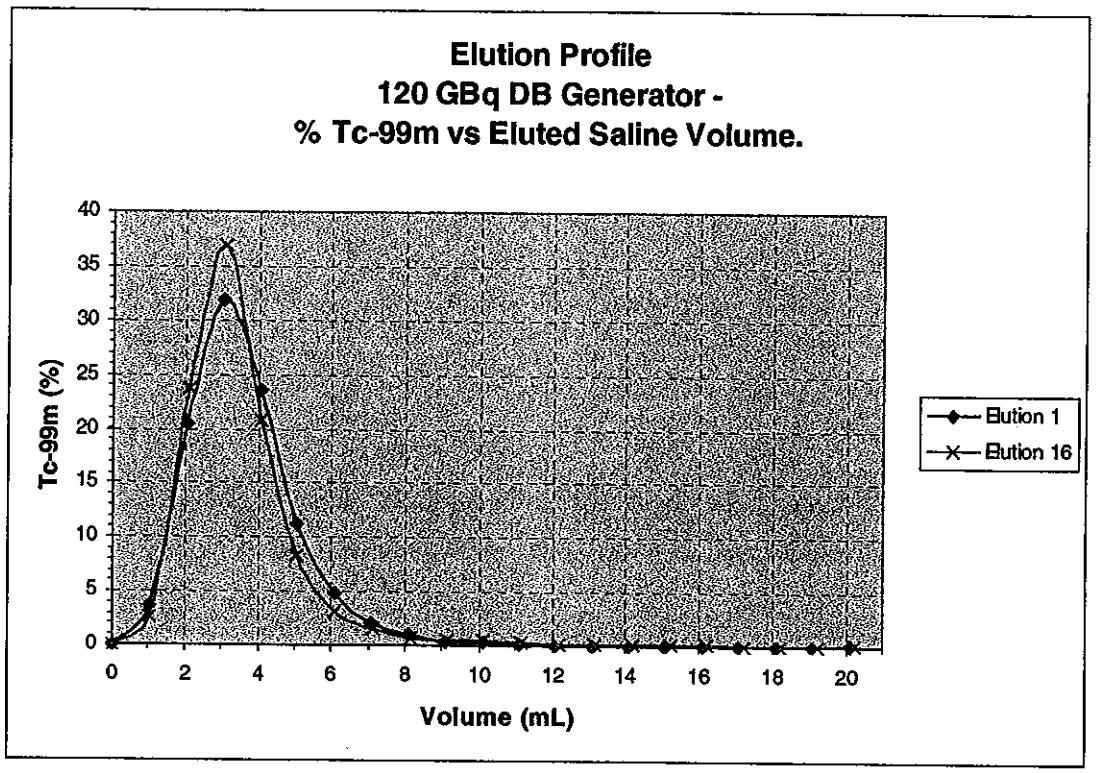
Elution Profile
120 GBq DB Generator -
% Tc-99m vs Eluted Saline Volume.
Tc-99m (%)
Volume (mL)
Elution 1
Elution 16

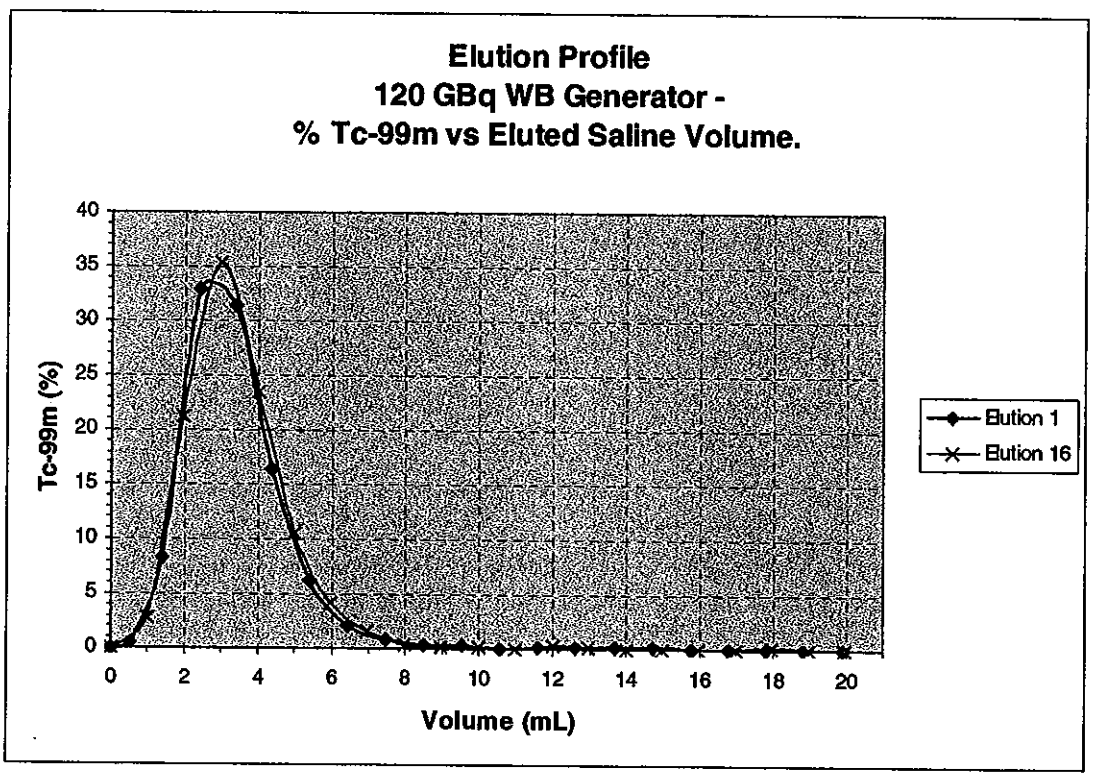
Elution Profile
120 GBq WB Generator -
% Tc-99m vs Eluted Saline Volume.
Tc-99m (%)
Volume (mL)
Elution 1
Elution 16

Figure 3a.

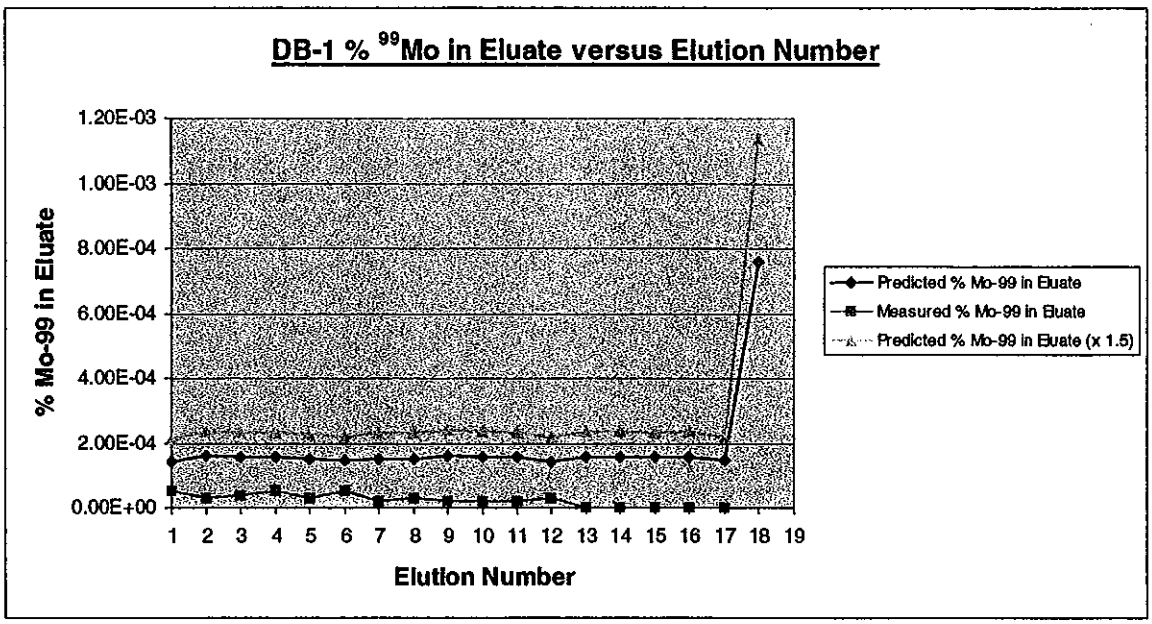
DB-1 % 99Mo in Eluate versus Elution Number
% Mo-99 in Eluate
1.20E-03
1.00E-03
8.00E-04
6.00E-04
4.00E-04
2.00E-04
0.00E+00
1 2 3 4 5 6 7 8 9 10 11 12 13 14 15 16 17 18 19
Elution Number
Predicted % Mo-99 in Eluate
Measured % Mo-99 in Eluate
Predicted % Mo-99 in Eluate (x 1.5)

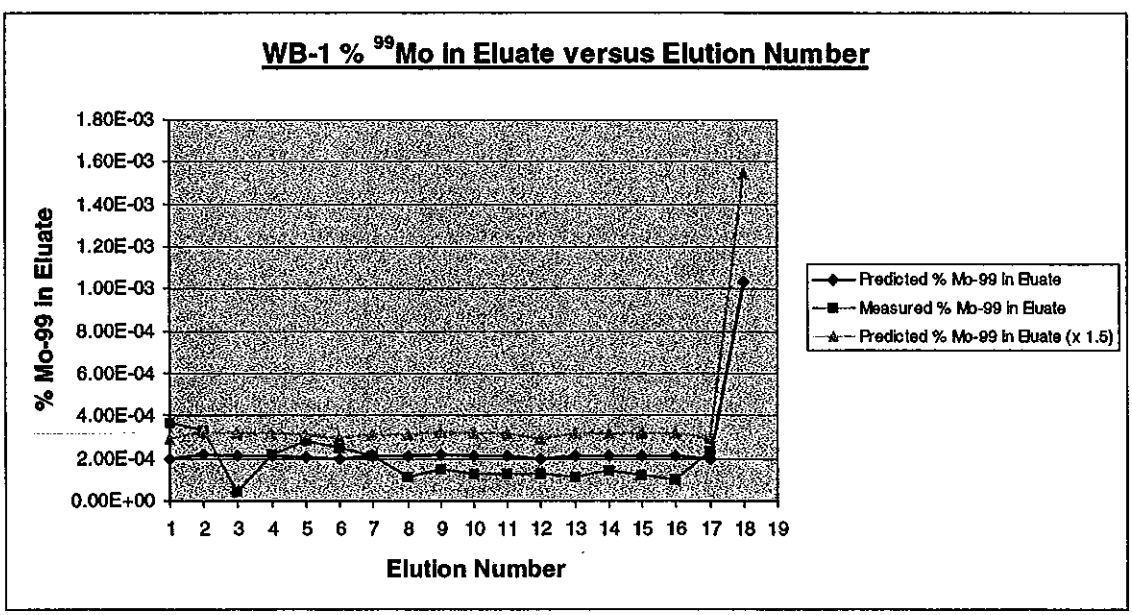
WB-1 % 99Mo in Eluate versus Elution Number
% Mo-99 in Eluate
1.80E-03
1.60E-03
1.40E-03
1.20E-03
1.00E-03
8.00E-04
6.00E-04
4.00E-04
2.00E-04
0.00E+00
1 2 3 4 5 6 7 8 9 10 11 12 13 14 15 16 17 18 19
Elution Number
Predicted % Mo-99 in Eluate
Measured % Mo-99 in Eluate
Predicted % Mo-99 in Eluate (x 1.5)

Figure 3b.

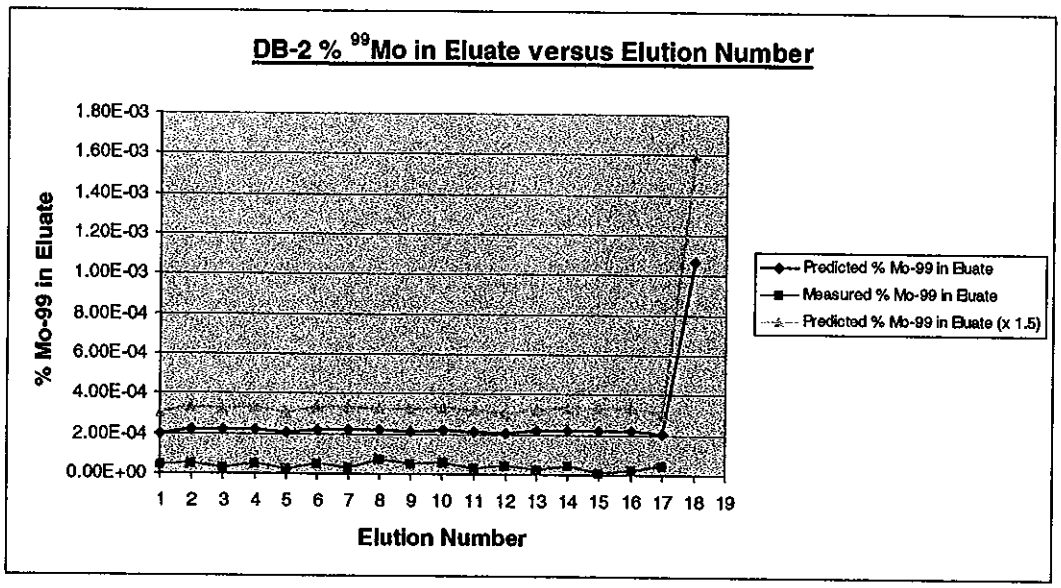
DB-2 % 99Mo in Eluate versus Elution Number
% Mo-99 in Eluate
1.80E-03
1.60E-03
1.40E-03
1.20E-03
1.00E-03
8.00E-04
6.00E-04
4.00E-04
2.00E-04
0.00E+00
1 2 3 4 5 6 7 8 9 10 11 12 13 14 15 16 17 18 19
Elution Number
Predicted % Mo-99 in Eluate
Measured % Mo-99 in Eluate
Predicted % Mo-99 in Eluate (x 1.5)

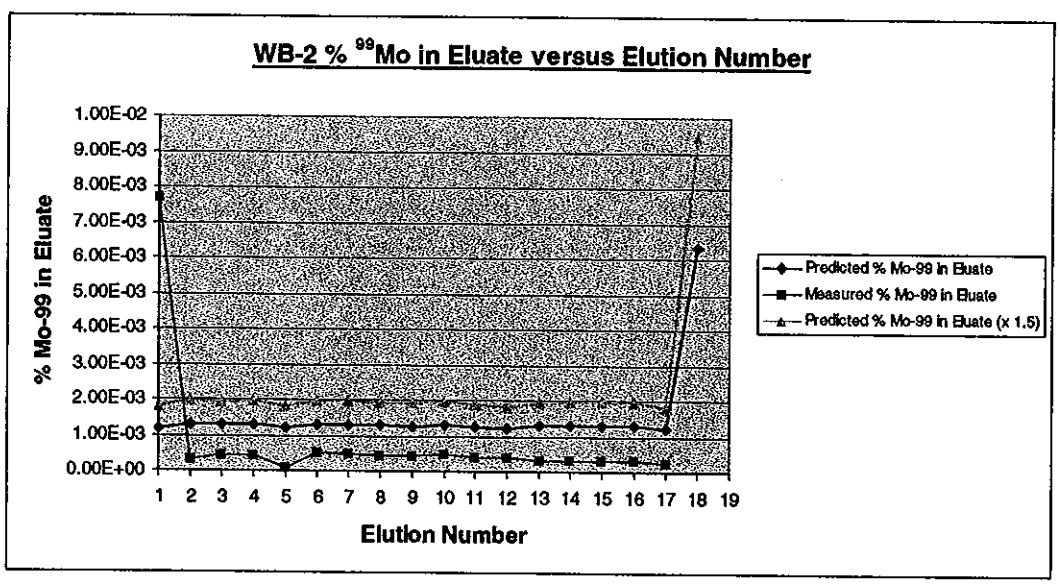
WB-2 % 99Mo in Eluate versus Elution Number
% Mo-99 in Eluate
1.00E-02
9.00E-03
8.00E-03
7.00E-03
6.00E-03
5.00E-03
4.00E-03
3.00E-03
2.00E-03
1.00E-03
0.00E+00
1 2 3 4 5 6 7 8 9 10 11 12 13 14 15 16 17 18 19
Elution Number
Predicted % Mo-99 in Eluate
Measured % Mo-99 in Eluate
Predicted % Mo-99 in Eluate (x 1.5)

Figure 3c.

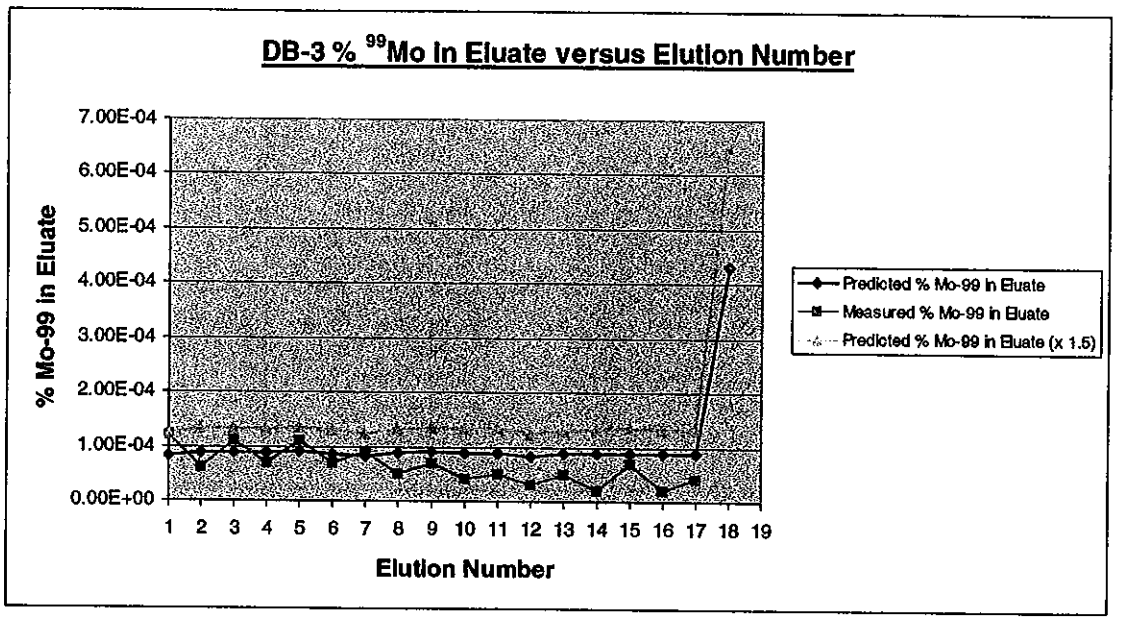
DB-3 % 99Mo In Eluate versus Elution Number
% Mo-99 in Eluate
7.00E-04
6.00E-04
5.00E-04
4.00E-04
3.00E-04
2.00E-04
1.00E-04
0.00E+00
1 2 3 4 5 6 7 8 9 10 11 12 13 14 15 16 17 18 19
Elution Number
Predicted % Mo-99 in Eluate
Measured % Mo-99 in Eluate
Predicted % Mo-99 in Eluate (x 1.5)

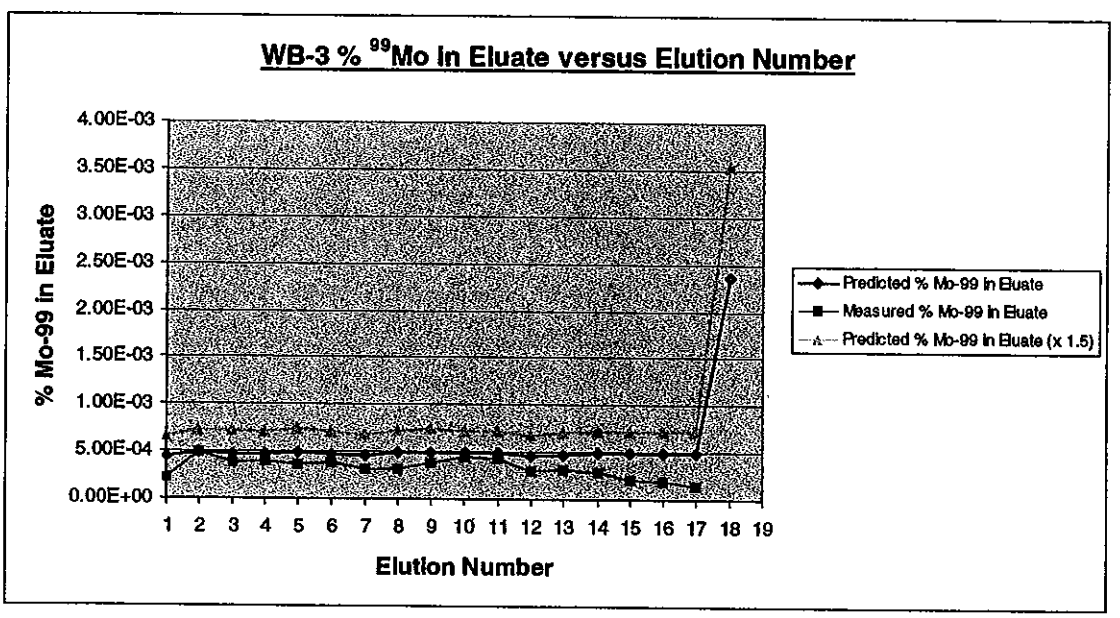
WB-3 % 99Mo In Eluate versus Elution Number
% Mo-99 in Eluate
4.00E-03
3.50E-03
3.00E-03
2.50E-03
2.00E-03
1.50E-03
1.00E-03
5.00E-04
0.00E+00
1 2 3 4 5 6 7 8 9 10 11 12 13 14 15 16 17 18 19
Elution Number
Predicted % Mo-99 in Eluate
Measured % Mo-99 in Eluate
Predicted % Mo-99 in Eluate (x 1.5)

Figure 3d.

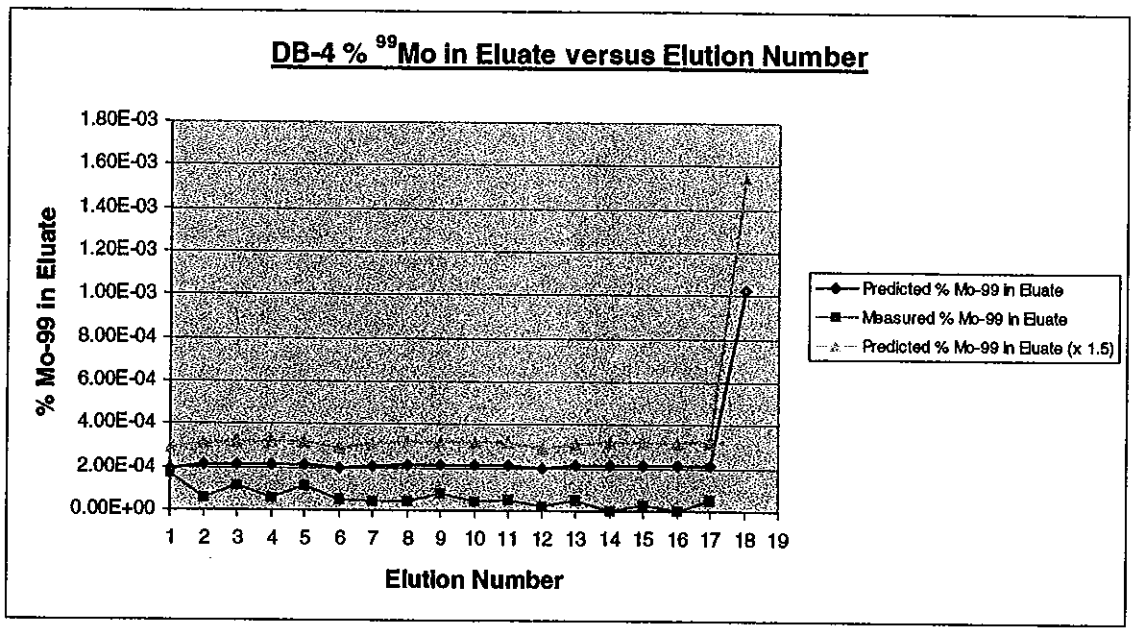
DB-4 % 99Mo in Eluate versus Elution Number
% Mo-99 in Eluate
1.80E-03
1.60E-03
1.40E-03
1.20E-03
1.00E-03
8.00E-04
6.00E-04
4.00E-04
2.00E-04
0.00E+00
1 2 3 4 5 6 7 8 9 10 11 12 13 14 15 16 17 18 19
Elution Number
Predicted % Mo-99 in Eluate
Measured % Mo-99 in Eluate
Predicted % Mo-99 in Eluate (x 1.5)

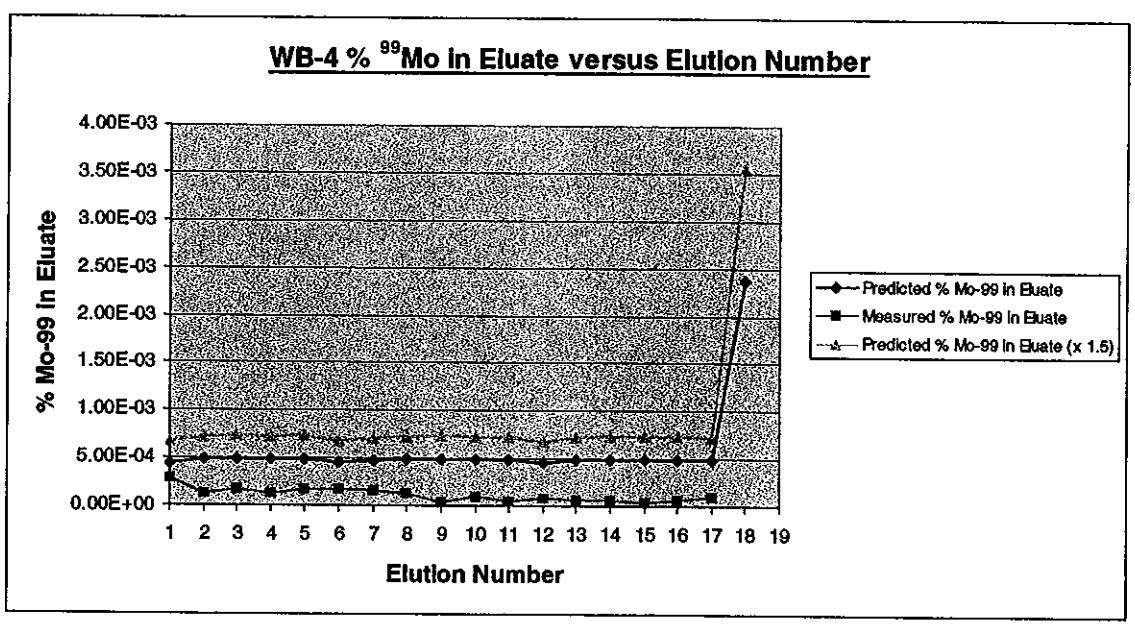
WB-4 % 99Mo in Eluate versus Elution Number
% Mo-99 in Eluate
4.00E-03
3.50E-03
3.00E-03
2.50E-03
2.00E-03
1.50E-03
1.00E-03
5.00E-04
0.00E+00
1 2 3 4 5 6 7 8 9 10 11 12 13 14 15 16 17 18 19
Elution Number
Predicted % Mo-99 in Eluate
Measured % Mo-99 in Eluate
Predicted % Mo-99 in Eluate (x 1.5)

Figure 3e.

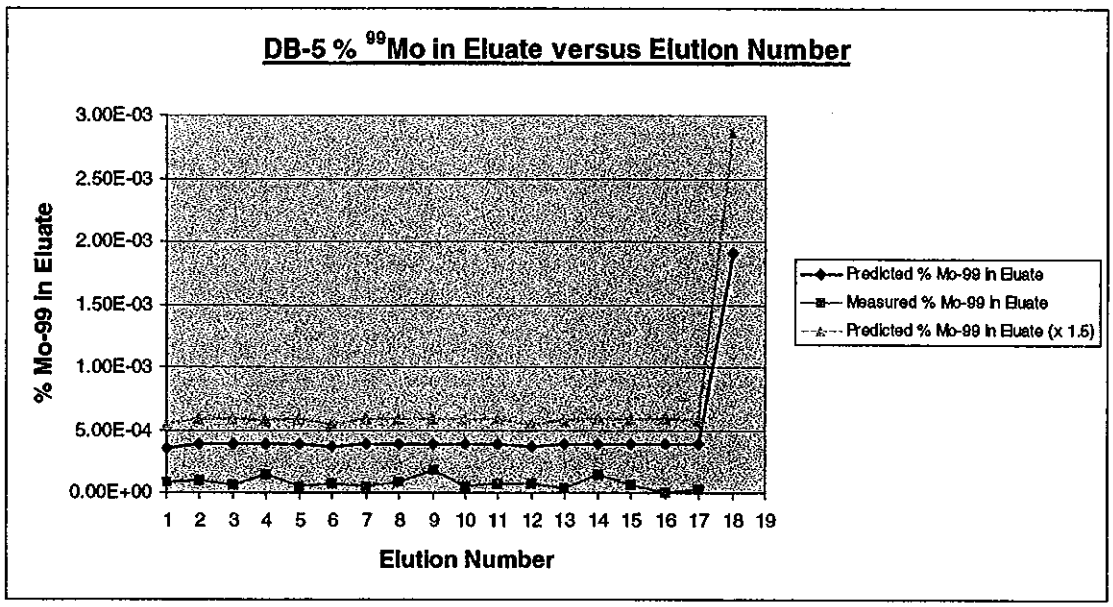
DB-5 % 99Mo in Eluate versus Elution Number
% Mo-99 in Eluate
3.00E-03
2.50E-03
2.00E-03
1.50E-03
1.00E-03
5.00E-04
0.00E+00
1 2 3 4 5 6 7 8 9 10 11 12 13 14 15 16 17 18 19
Elution Number
Predicted % Mo-99 in Eluate
Measured % Mo-99 in Eluate
Predicted % Mo-99 in Eluate (x 1.5)

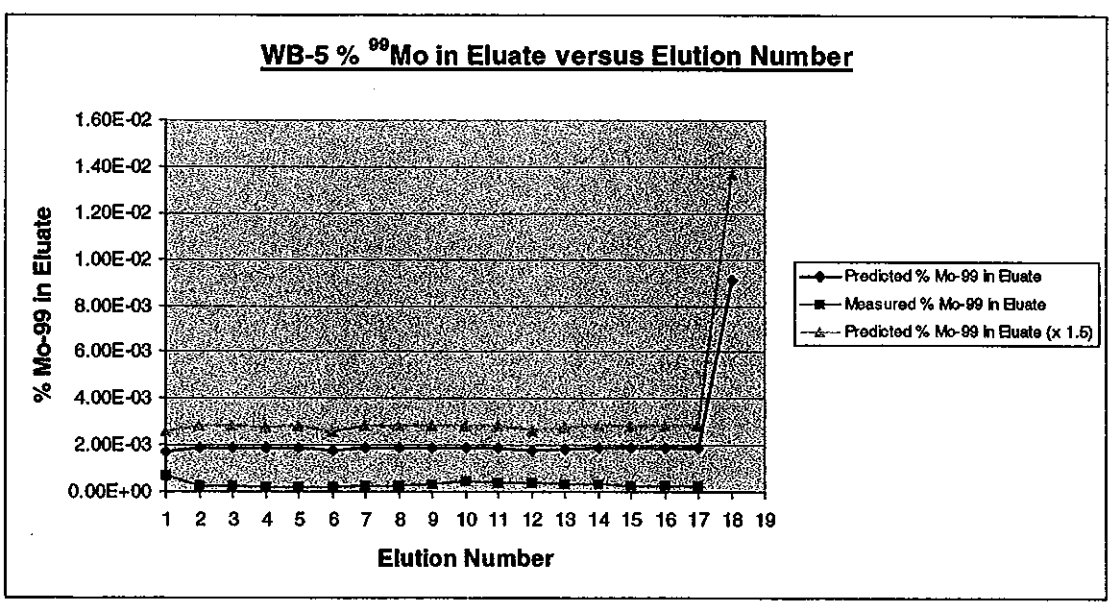
WB-5 % 99Mo in Eluate versus Elution Number
% Mo-99 in Eluate
1.60E-02
1.40E-02
1.20E-02
1.00E-02
8.00E-03
6.00E-03
4.00E-03
2.00E-03
0.00E+00
1 2 3 4 5 6 7 8 9 10 11 12 13 14 15 16 17 18 19
Elution Number
Predicted % Mo-99 in Eluate
Measured % Mo-99 in Eluate
Predicted % Mo-99 in Eluate (x 1.5)

Figure 3f.

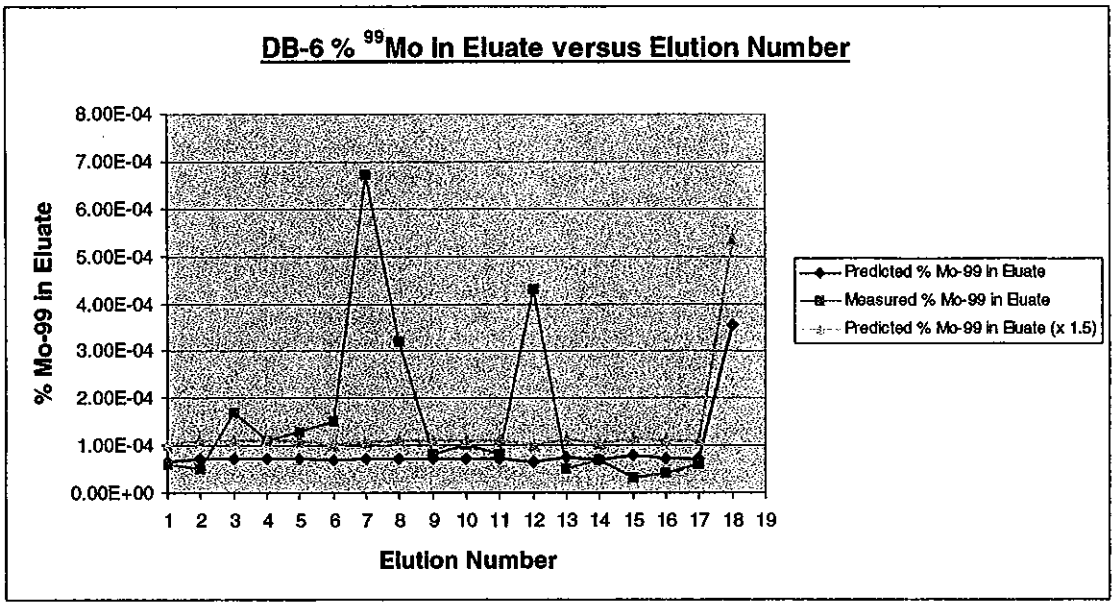
DB-6 % 99Mo In Eluate versus Elution Number
% Mo-99 in Eluate
8.00E-04
7.00E-04
6.00E-04
5.00E-04
4.00E-04
3.00E-04
2.00E-04
1.00E-04
0.00E+00
1 2 3 4 5 6 7 8 9 10 11 12 13 14 15 16 17 18 19
Elution Number
Predicted % Mo-99 in Eluate
Measured % Mo-99 in Eluate
Predicted % Mo-99 in Eluate (x 1.5)

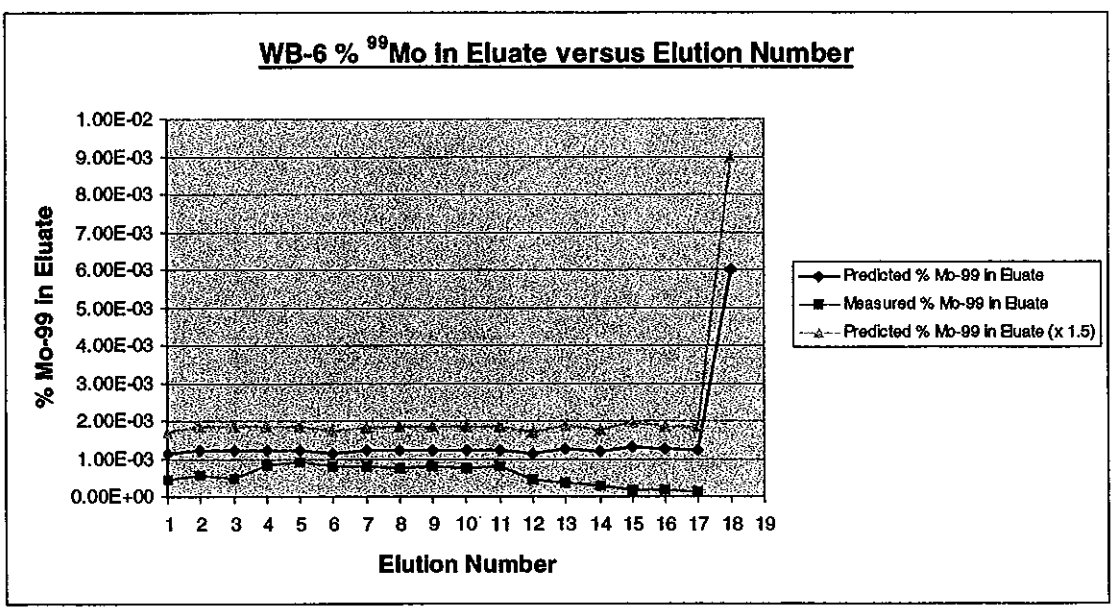
WB-6 % 99Mo In Eluate versus Elution Number
% Mo-99 in Eluate
1.00E-02
9.00E-03
8.00E-03
7.00E-03
6.00E-03
5.00E-03
4.00E-03
3.00E-03
2.00E-03
1.00E-03
0.00E+00
1 2 3 4 5 6 7 8 9 10 11 12 13 14 15 16 17 18 19
Elution Number
Predicted % Mo-99 in Eluate
Measured % Mo-99 in Eluate
Predicted % Mo-99 in Eluate (x 1.5)

Figure 3g.

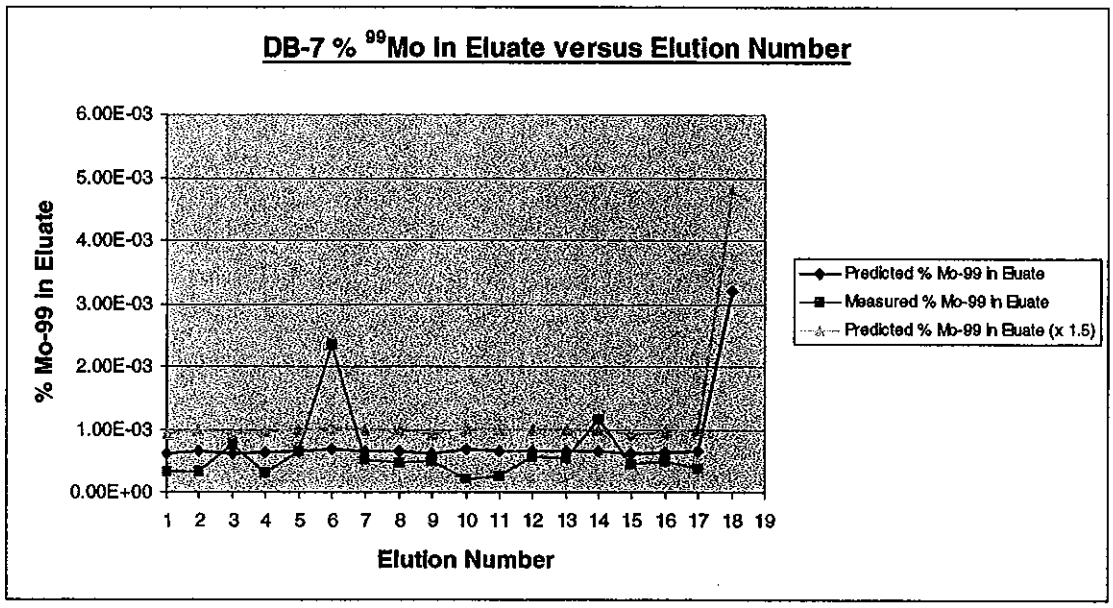
DB-7 % 99Mo In Eluate versus Elution Number
% Mo-99 In Eluate
6.00E-03
5.00E-03
4.00E-03
3.00E-03
2.00E-03
1.00E-03
0.00E+00
1 2 3 4 5 6 7 8 9 10 11 12 13 14 15 16 17 18 19
Elution Number
Predicted % Mo-99 in Eluate
Measured % Mo-99 in Eluate
Predicted % Mo-99 in Eluate (x 1.5)

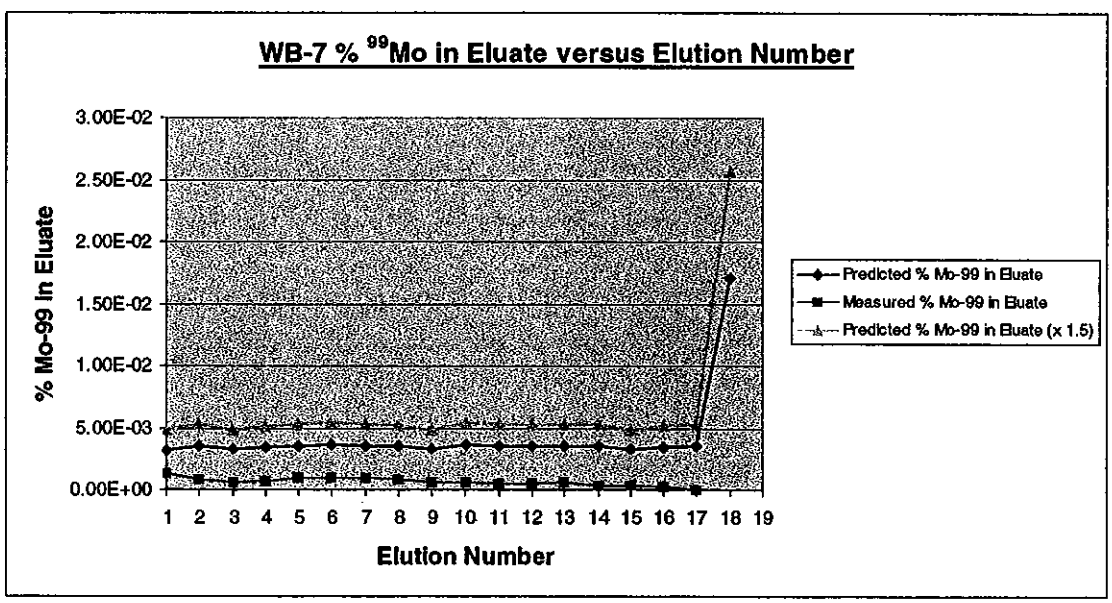
WB-7 % 99Mo in Eluate versus Elution Number
% Mo-99 In Eluate
3.00E-02
2.50E-02
2.00E-02
1.50E-02
1.00E-02
5.00E-03
0.00E+00
1 2 3 4 5 6 7 8 9 10 11 12 13 14 15 16 17 18 19
Elution Number
Predicted % Mo-99 in Eluate
Measured % Mo-99 in Eluate
Predicted % Mo-99 in Eluate (x 1.5)

Figure 3h.

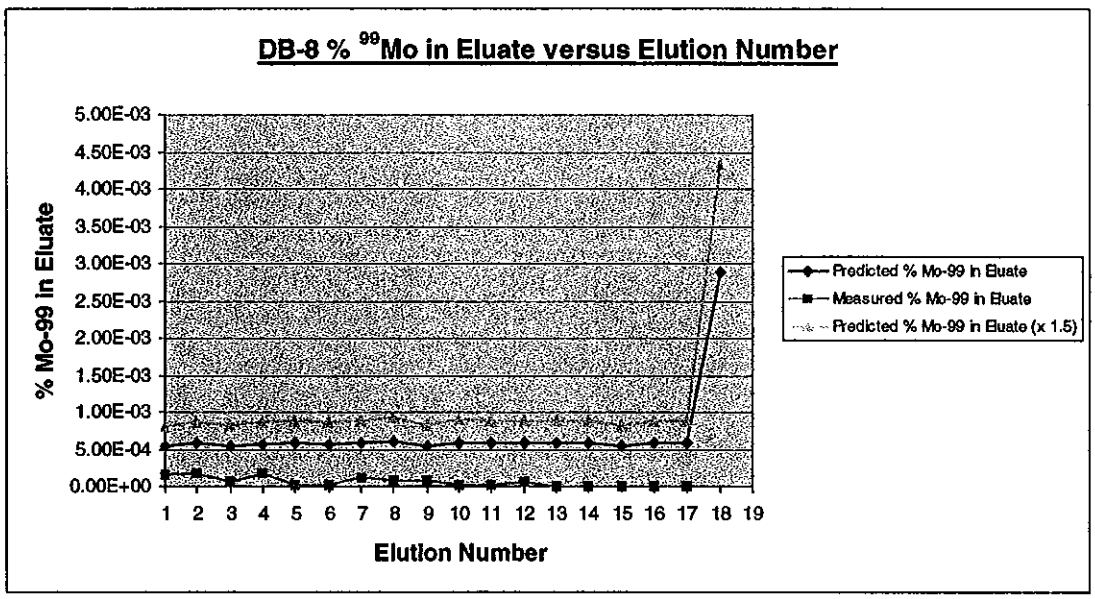
DB-8 % 99Mo in Eluate versus Elution Number
% Mo-99 in Eluate
5.00E-03
4.50E-03
4.00E-03
3.50E-03
3.00E-03
2.50E-03
2.00E-03
1.50E-03
1.00E-03
5.00E-04
0.00E+00
1 2 3 4 5 6 7 8 9 10 11 12 13 14 15 16 17 18 19
Elution Number
Predicted % Mo-99 in Eluate
Measured % Mo-99 in Eluate
Predicted % Mo-99 in Eluate (x 1.5)

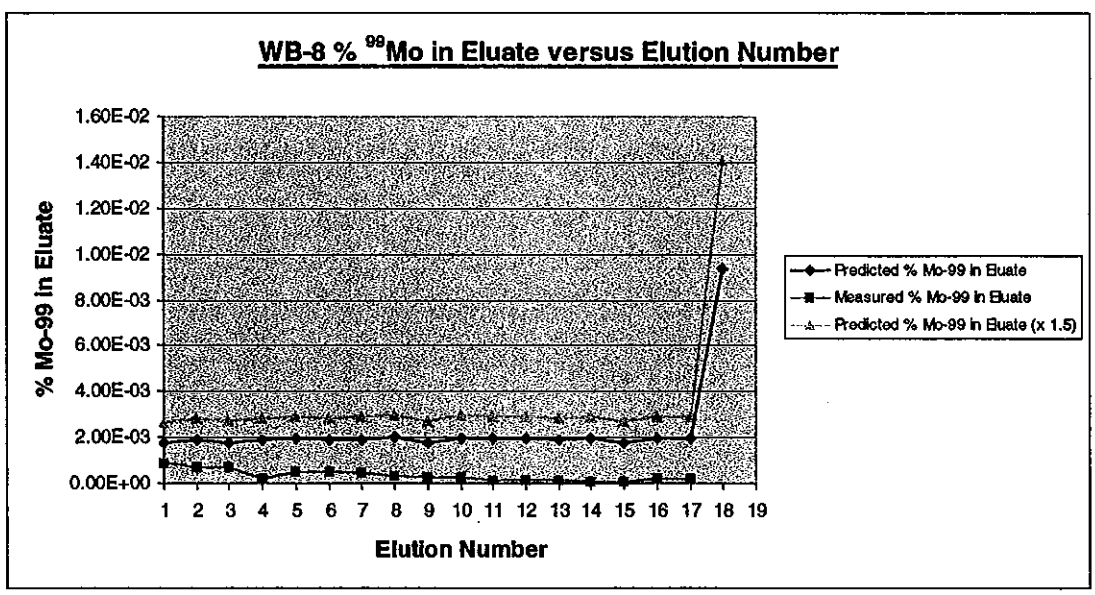
WB-8 % 99Mo in Eluate versus Elution Number
% Mo-99 in Eluate
1.60E-02
1.40E-02
1.20E-02
1.00E-02
8.00E-03
6.00E-03
4.00E-03
2.00E-03
0.00E+00
1 2 3 4 5 6 7 8 9 10 11 12 13 14 15 16 17 18 19
Elution Number
Predicted % Mo-99 in Eluate
Measured % Mo-99 in Eluate
Predicted % Mo-99 in Eluate (x 1.5)

Figure 3i.

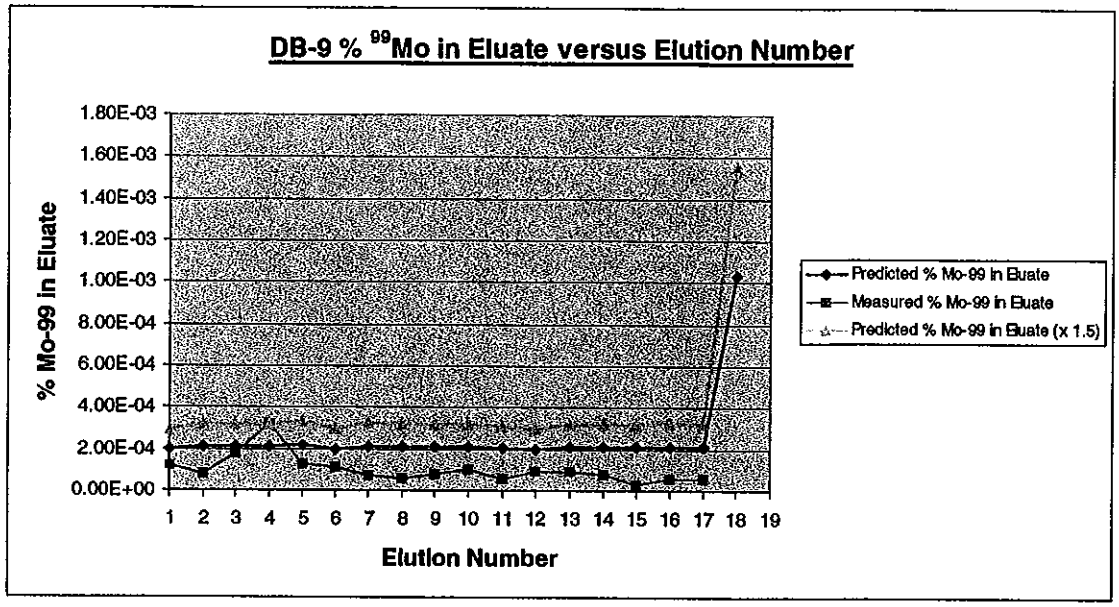
DB-9 % 99Mo in Eluate versus Elution Number
% Mo-99 in Eluate
1.80E-03
1.60E-03
1.40E-03
1.20E-03
1.00E-03
8.00E-04
6.00E-04
4.00E-04
2.00E-04
0.00E+00
1 2 3 4 5 6 7 8 9 10 11 12 13 14 15 16 17 18 19
Elution Number
Predicted % Mo-99 in Eluate
Measured % Mo-99 in Eluate
Predicted % Mo-99 in Eluate (x 1.5)

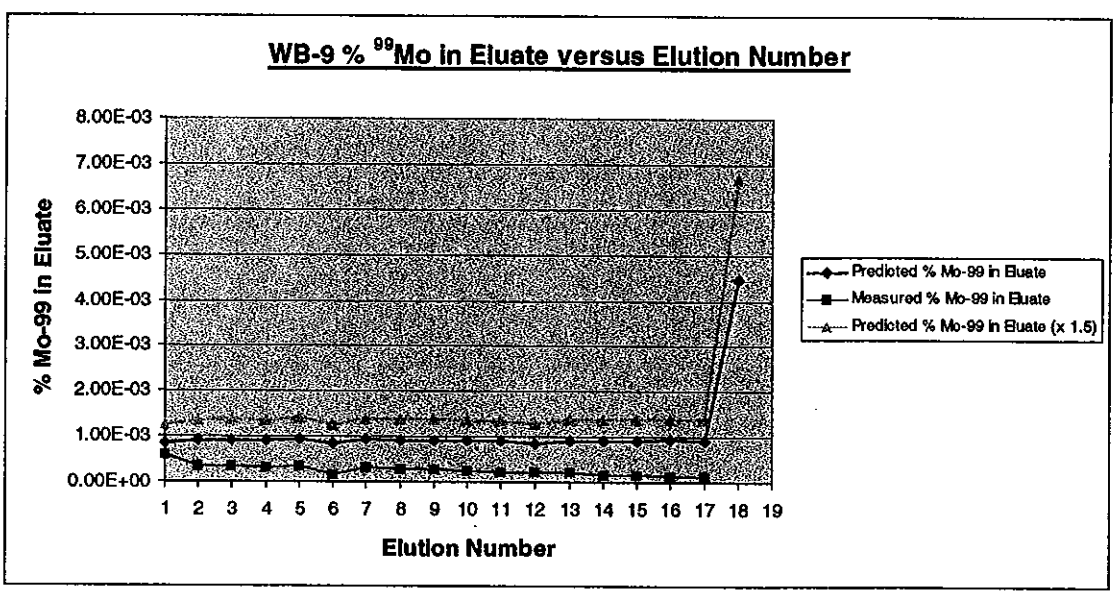
WB-9 % 99Mo in Eluate versus Elution Number
% Mo-99 in Eluate
8.00E-03
7.00E-03
6.00E-03
5.00E-03
4.00E-03
3.00E-03
2.00E-03
1.00E-03
0.00E+00
1 2 3 4 5 6 7 8 9 10 11 12 13 14 15 16 17 18 19
Elution Number
Predicted % Mo-99 in Eluate
Measured % Mo-99 in Eluate
Predicted % Mo-99 in Eluate (x 1.5)

Figure 3j.

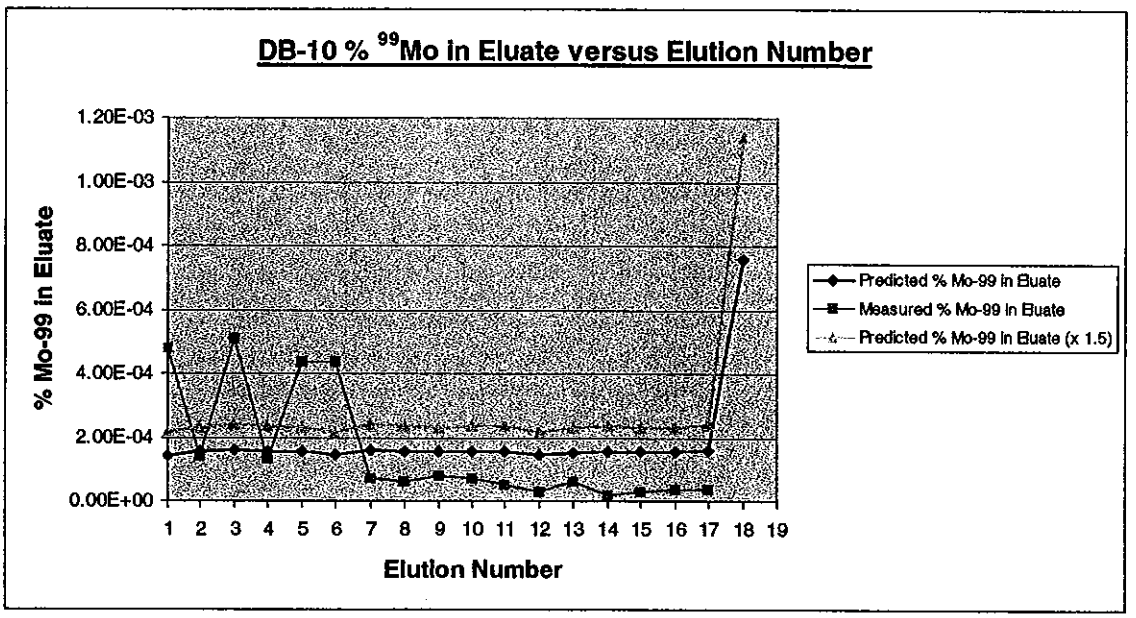
DB-10 % 99Mo in Eluate versus Elution Number
% Mo-99 in Eluate
1.20E-03
1.00E-03
8.00E-04
6.00E-04
4.00E-04
2.00E-04
0.00E+00
1 2 3 4 5 6 7 8 9 10 11 12 13 14 15 16 17 18 19
Elution Number
Predicted % Mo-99 in Eluate
Measured % Mo-99 in Eluate
Predicted % Mo-99 in Eluate (x 1.5)

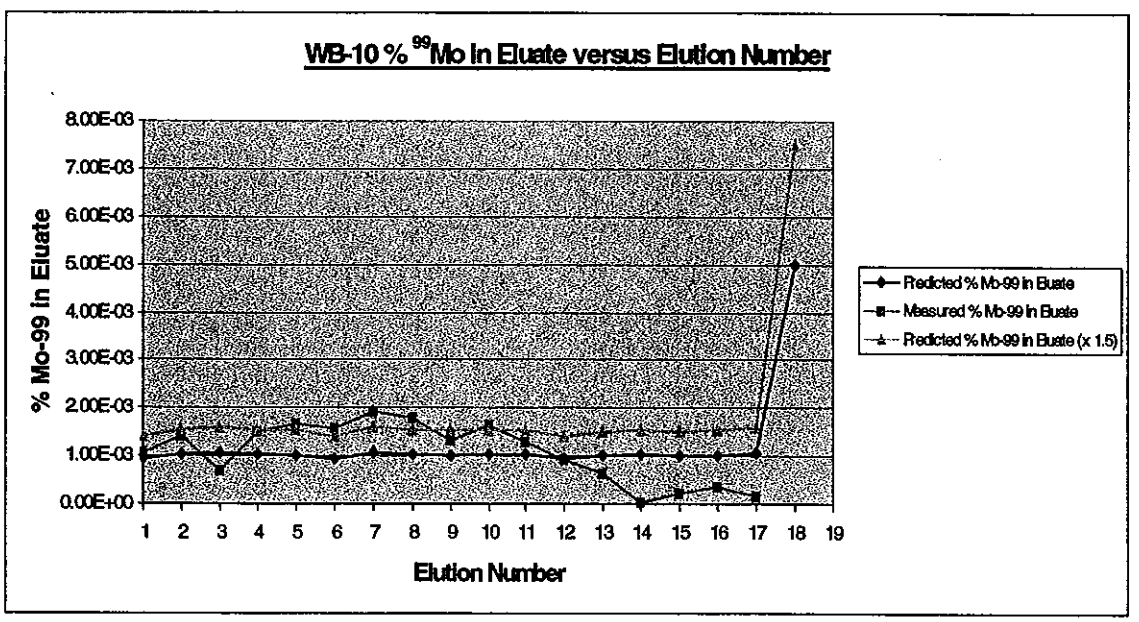
WB-10 % 99Mo in Eluate versus Elution Number
% Mo-99 in Eluate
8.00E-03
7.00E-03
6.00E-03
5.00E-03
4.00E-03
3.00E-03
2.00E-03
1.00E-03
0.00E+00
1 2 3 4 5 6 7 8 9 10 11 12 13 14 15 16 17 18 19
Elution Number
Predicted % Mo-99 in Eluate
Measured % Mo-99 in Eluate
Predicted % Mo-99 in Eluate (x 1.5)

Figure 4a.

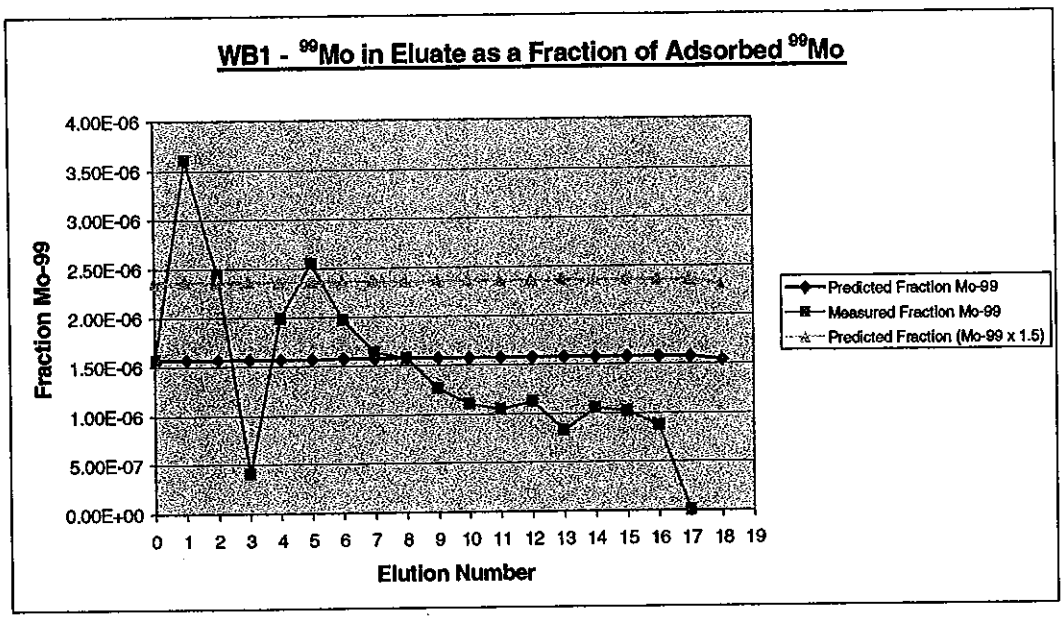
WB1 - 99Mo in Eluate as a Fraction of Adsorbed 99Mo
Fraction Mo-99
4.00E-06
3.50E-06
3.00E-06
2.50E-06
2.00E-06
1.50E-06
1.00E-06
5.00E-07
0.00E+00
0 1 2 3 4 5 6 7 8 9 10 11 12 13 14 15 16 17 18 19
Elution Number
Predicted Fraction Mo-99
Measured Fraction Mo-99
Predicted Fraction (Mo-99 x 1.5)

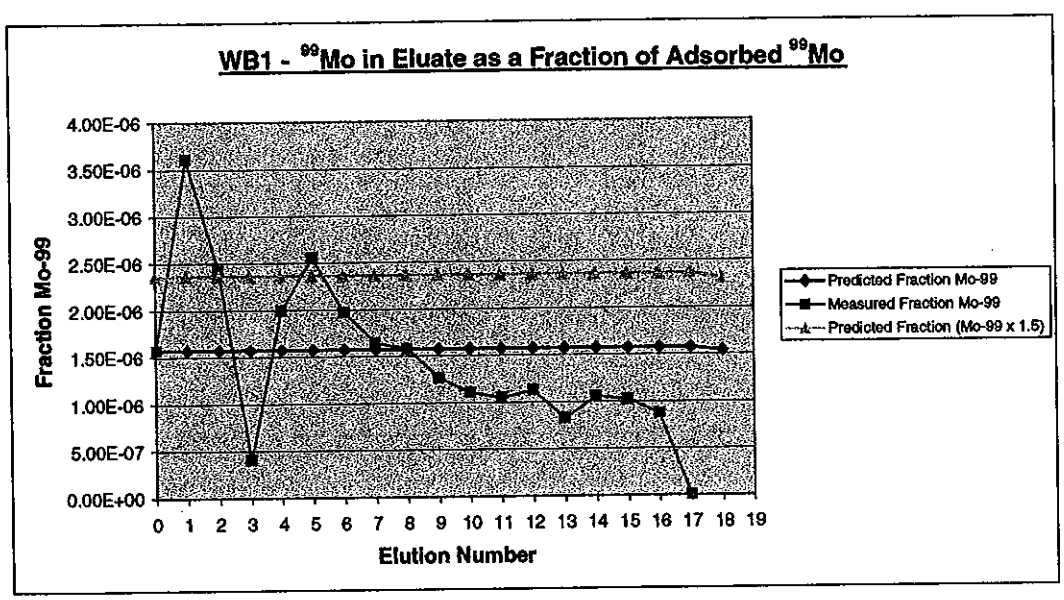
WB1 - 99Mo in Eluate as a Fraction of Adsorbed 99Mo
Fraction Mo-99
4.00E-06
3.50E-06
3.00E-06
2.50E-06
2.00E-06
1.50E-06
1.00E-06
5.00E-07
0.00E+00
0 1 2 3 4 5 6 7 8 9 10 11 12 13 14 15 16 17 18 19
Elution Number
Predicted Fraction Mo-99
Measured Fraction Mo-99
Predicted Fraction (Mo-99 x 1.5)

Figure 4b.

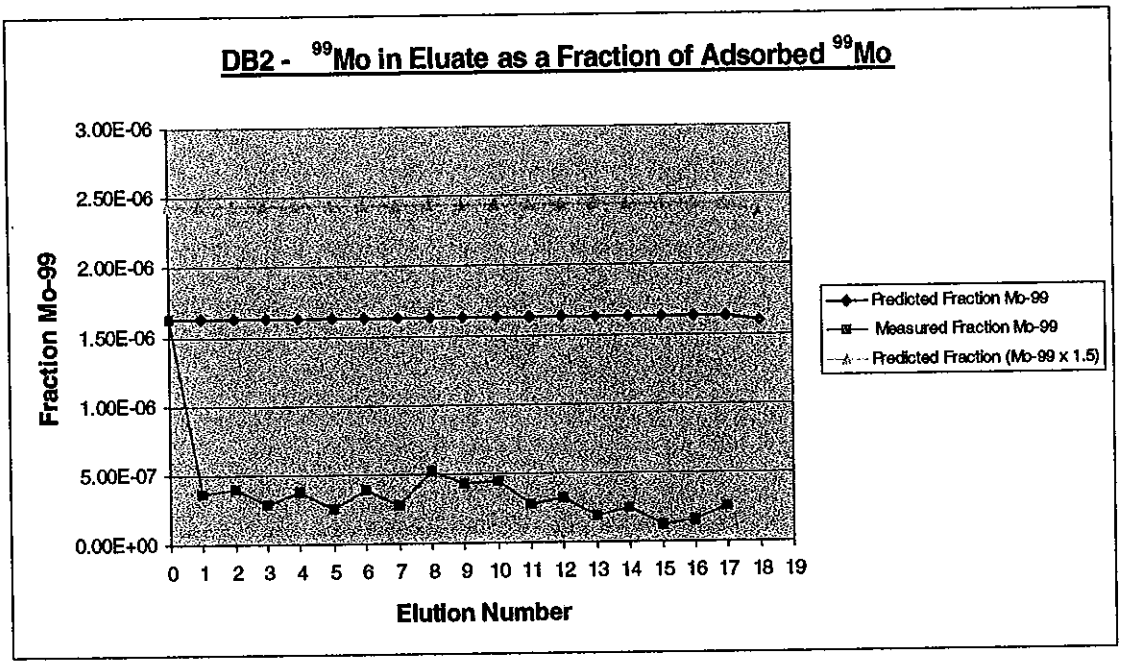
DB2 - 99Mo in Eluate as a Fraction of Adsorbed 99Mo
Fraction Mo-99
3.00E-06
2.50E-06
2.00E-06
1.50E-06
1.00E-06
5.00E-07
0.00E+00
0 1 2 3 4 5 6 7 8 9 10 11 12 13 14 15 16 17 18 19
Elution Number
Predicted Fraction Mo-99
Measured Fraction Mo-99
Predicted Fraction (Mo-99 x 1.5)

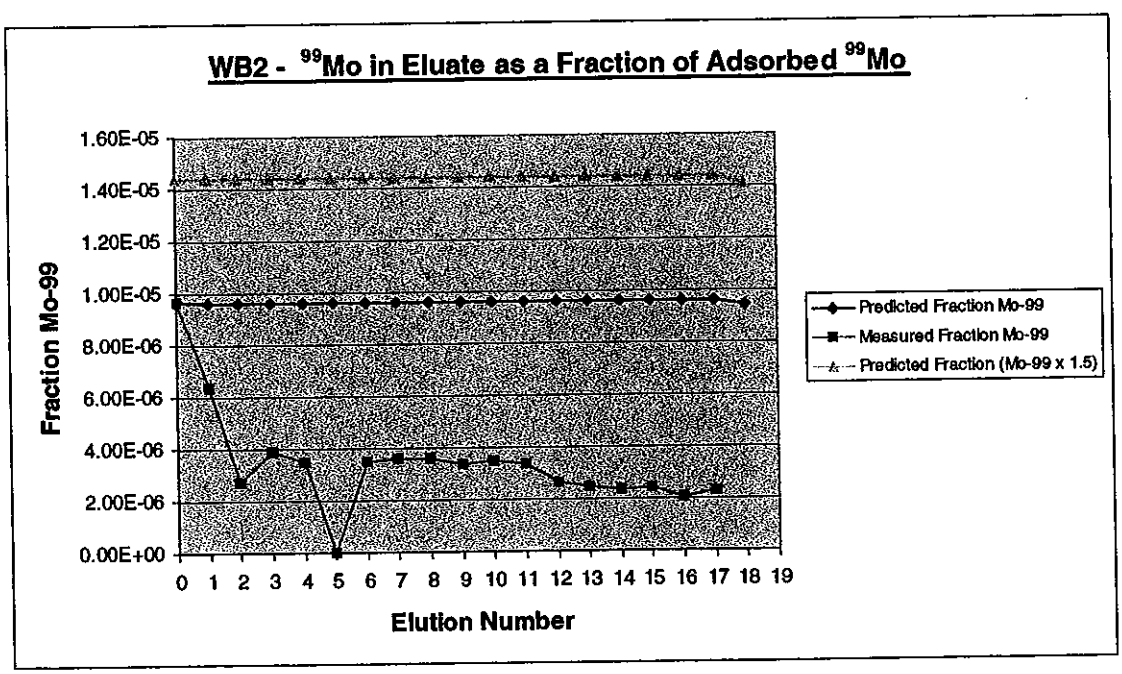
WB2 - 99Mo in Eluate as a Fraction of Adsorbed 99Mo
Fraction Mo-99
1.60E-05
1.40E-05
1.20E-05
1.00E-05
8.00E-06
6.00E-06
4.00E-06
2.00E-06
0.00E+00
0 1 2 3 4 5 6 7 8 9 10 11 12 13 14 15 16 17 18 19
Elution Number
Predicted Fraction Mo-99
Measured Fraction Mo-99
Predicted Fraction (Mo-99 x 1.5)

Figure 4c.

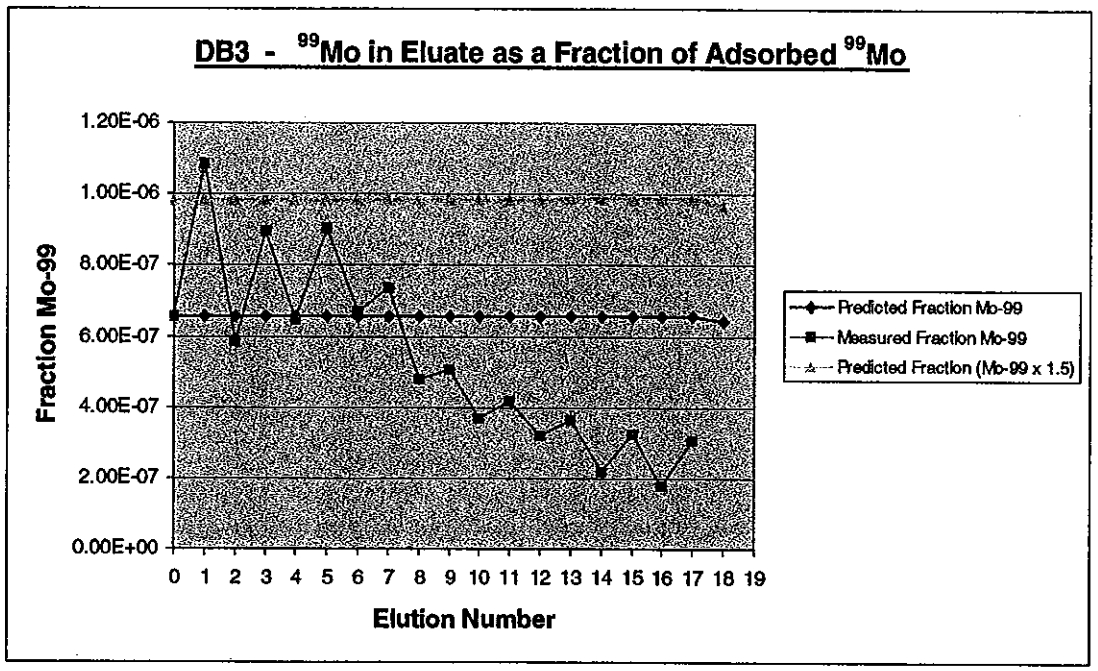
DB3 - 99Mo in Eluate as a Fraction of Adsorbed 99Mo
Fraction Mo-99
1.20E-06
1.00E-06
8.00E-07
6.00E-07
4.00E-07
2.00E-07
0.00E+00
0 1 2 3 4 5 6 7 8 9 10 11 12 13 14 15 16 17 18 19
Elution Number
Predicted Fraction Mo-99
Measured Fraction Mo-99
Predicted Fraction (Mo-99 x 1.5)

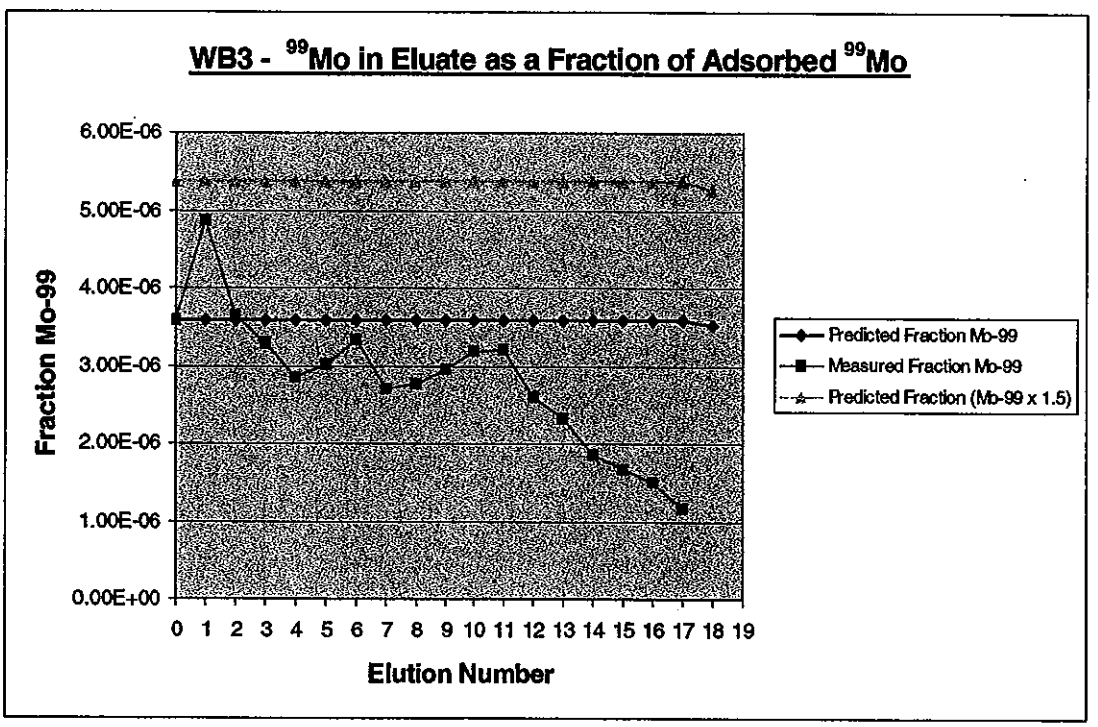
WB3 - 99Mo in Eluate as a Fraction of Adsorbed 99Mo
Fraction Mo-99
6.00E-06
5.00E-06
4.00E-06
3.00E-06
2.00E-06
1.00E-06
0.00E+00
0 1 2 3 4 5 6 7 8 9 10 11 12 13 14 15 16 17 18 19
Elution Number
Predicted Fraction Mo-99
Measured Fraction Mo-99
Predicted Fraction (Mo-99 x 1.5)

Figure 4d.

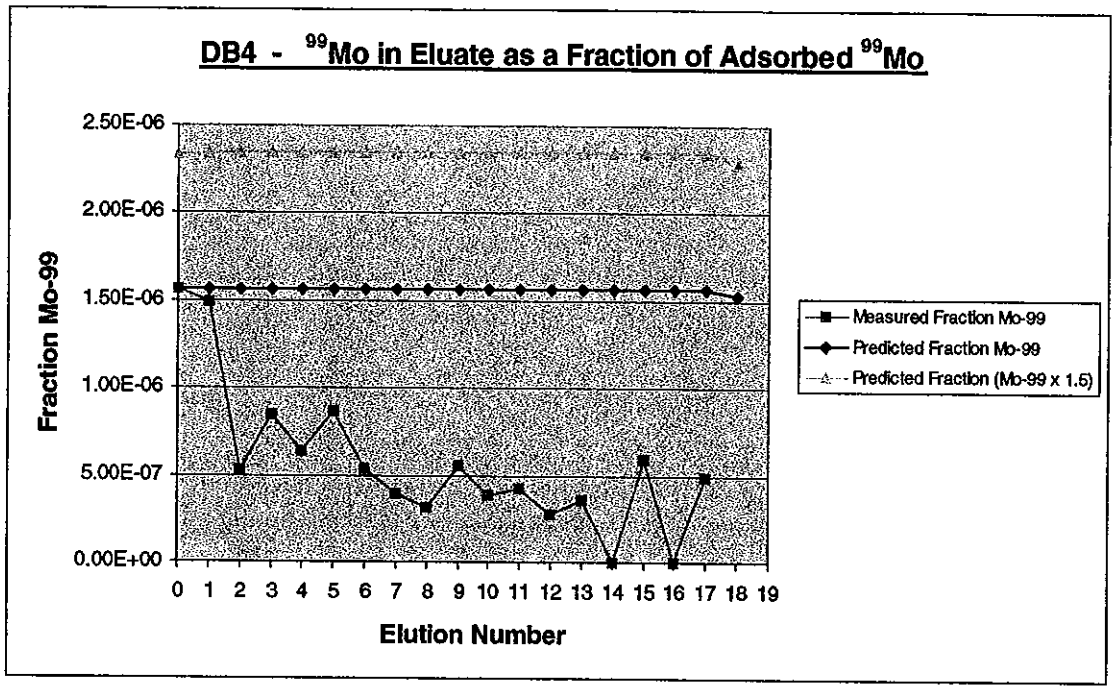
DB4 - 99Mo in Eluate as a Fraction of Adsorbed 99Mo
Fraction Mo-99
2.50E-06
2.00E-06
1.50E-06
1.00E-06
5.00E-07
0.00E+00
0 1 2 3 4 5 6 7 8 9 10 11 12 13 14 15 16 17 18 19
Elution Number
Measured Fraction Mo-99
Predicted Fraction Mo-99
Predicted Fraction (Mo-99 x 1.5)

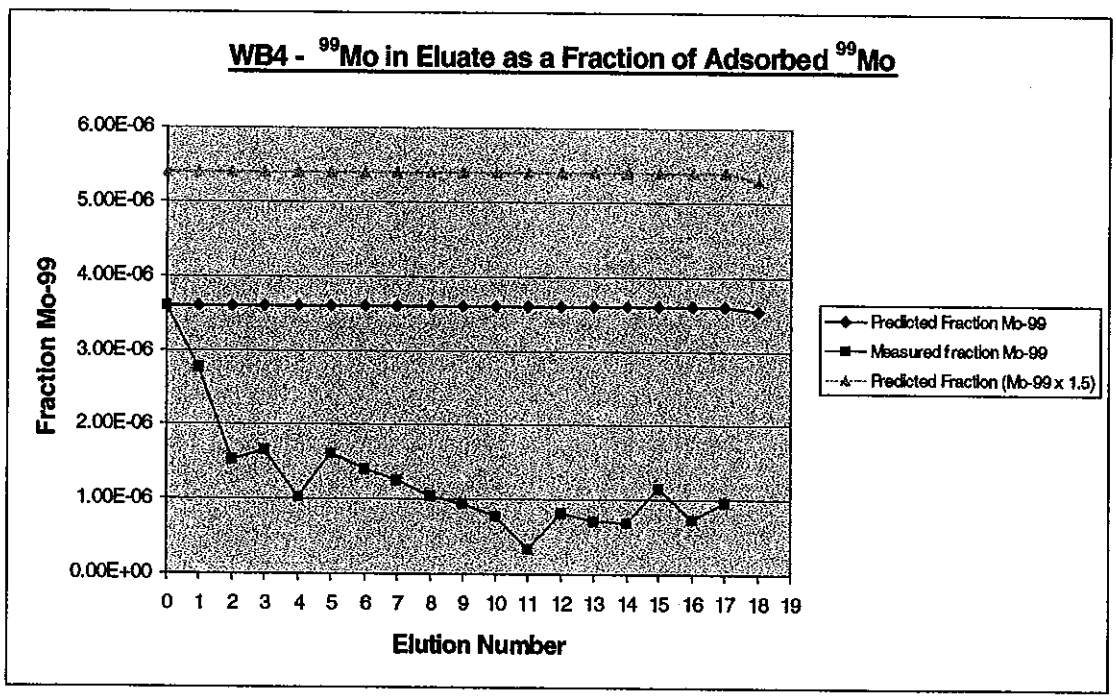
WB4 - 99Mo in Eluate as a Fraction of Adsorbed 99Mo
Fraction Mo-99
6.00E-06
5.00E-06
4.00E-06
3.00E-06
2.00E-06
1.00E-06
0.00E+00
0 1 2 3 4 5 6 7 8 9 10 11 12 13 14 15 16 17 18 19
Elution Number
Predicted Fraction Mo-99
Measured fraction Mo-99
Predicted Fraction (Mo-99 x 1.5)

Figure 4e.

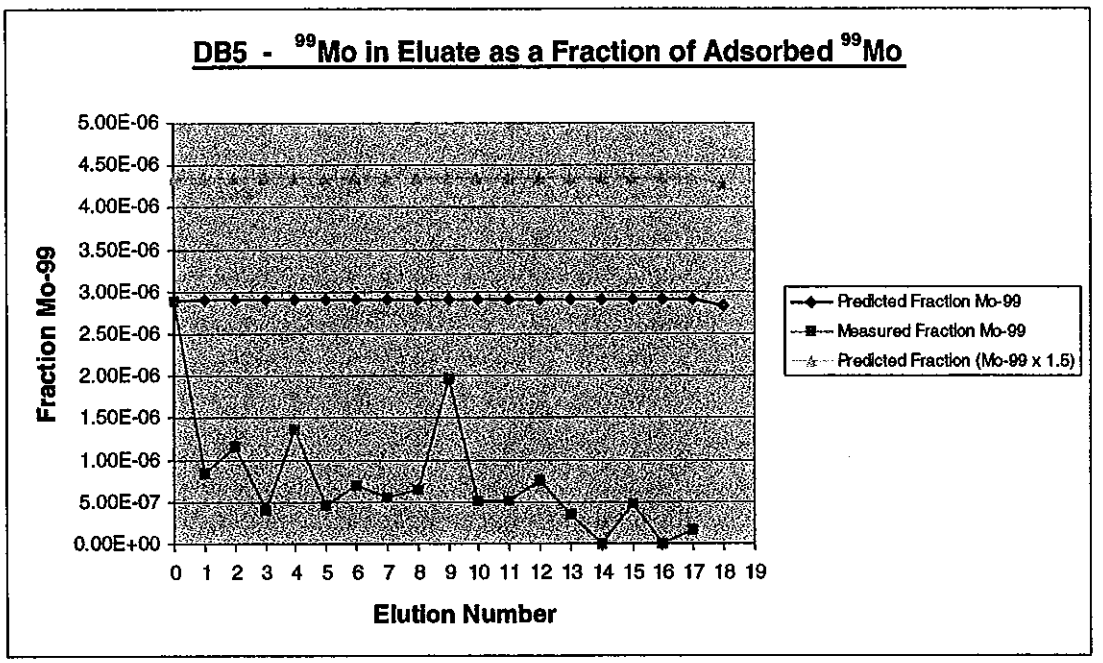
DB5 - 99Mo in Eluate as a Fraction of Adsorbed 99Mo
Fraction Mo-99
5.00E-06
4.50E-06
4.00E-06
3.50E-06
3.00E-06
2.50E-06
2.00E-06
1.50E-06
1.00E-06
5.00E-07
0.00E+00
0 1 2 3 4 5 6 7 8 9 10 11 12 13 14 15 16 17 18 19
Elution Number
Predicted Fraction Mo-99
Measured Fraction Mo-99
Predicted Fraction (Mo-99 x 1.5)

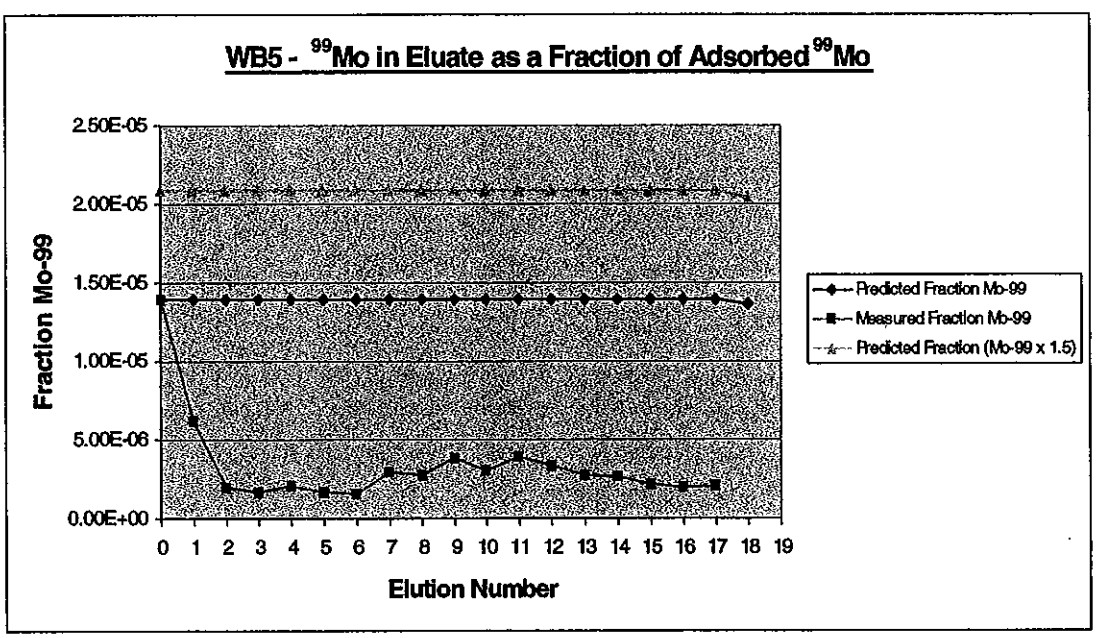
WB5 - 99Mo in Eluate as a Fraction of Adsorbed 99Mo
Fraction Mo-99
2.50E-05
2.00E-05
1.50E-05
1.00E-05
5.00E-06
0.00E+00
0 1 2 3 4 5 6 7 8 9 10 11 12 13 14 15 16 17 18 19
Elution Number
Predicted Fraction Mo-99
Measured Fraction Mo-99
Predicted Fraction (Mo-99 x 1.5)

Figure 4f.

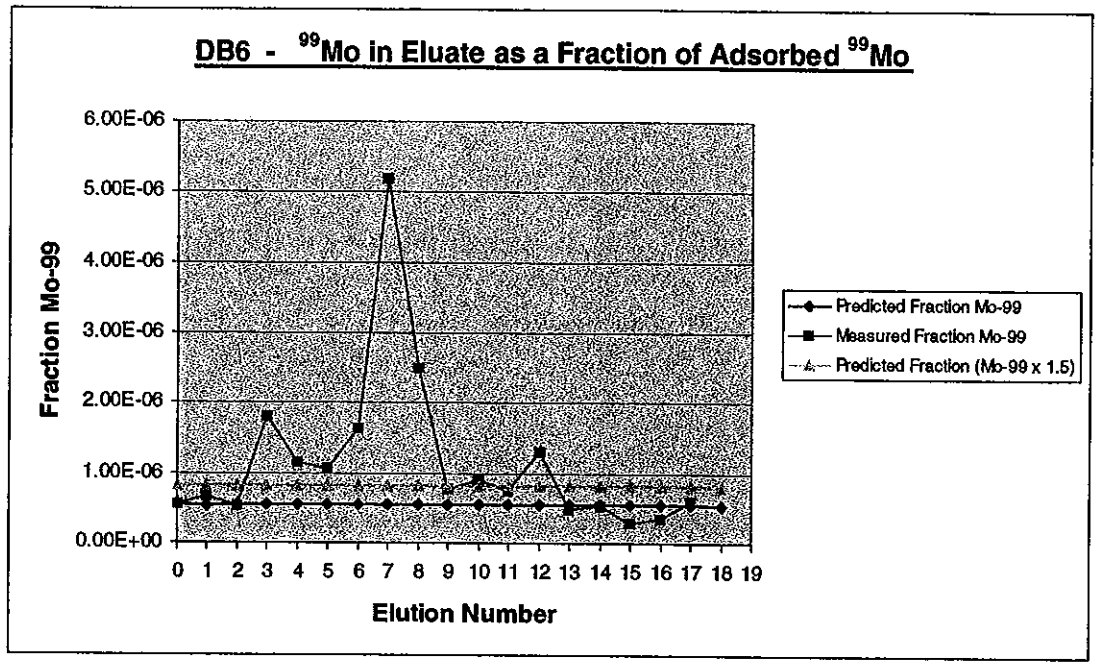
DB6 - 99Mo in Eluate as a Fraction of Adsorbed 99Mo
Fraction Mo-99
6.00E-06
5.00E-06
4.00E-06
3.00E-06
2.00E-06
1.00E-06
0.00E+00
0 1 2 3 4 5 6 7 8 9 10 11 12 13 14 15 16 17 18 19
Elution Number
Predicted Fraction Mo-99
Measured Fraction Mo-99
Predicted Fraction (Mo-99 x 1.5)

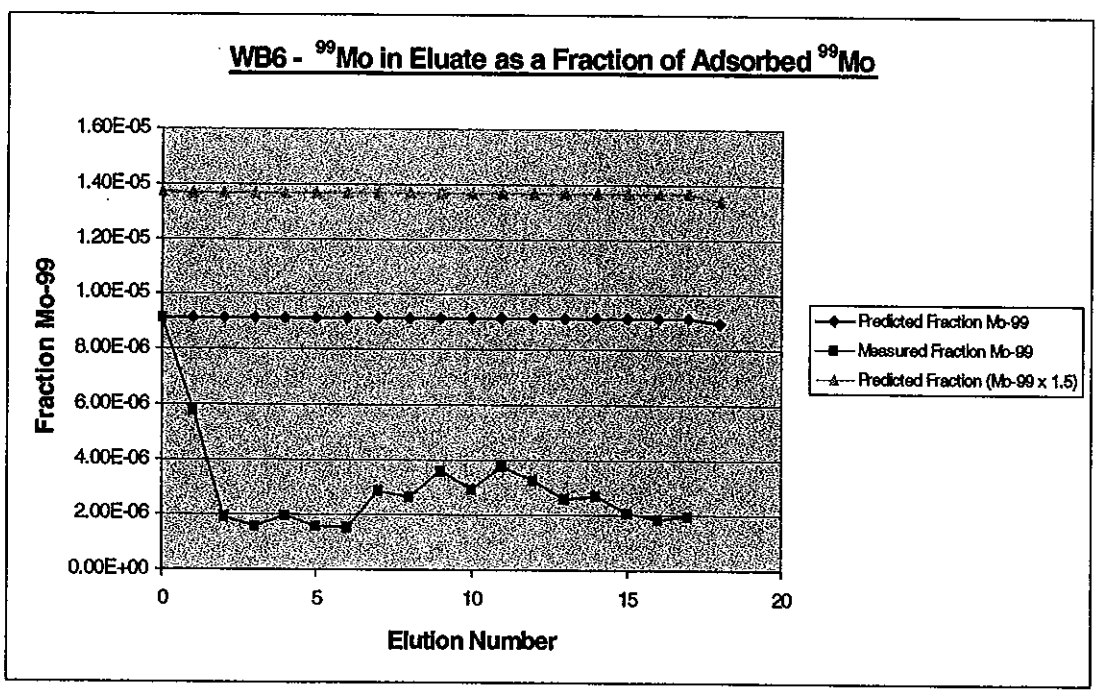
WB6 - 99Mo in Eluate as a Fraction of Adsorbed 99Mo
Fraction Mo-99
1.60E-05
1.40E-05
1.20E-05
1.00E-05
8.00E-06
6.00E-06
4.00E-06
2.00E-06
0.00E+00
0
5
10
15
20
Elution Number
Predicted Fraction Mo-99
Measured Fraction Mo-99
Predicted Fraction (Mo-99 x 1.5)

Figure 4g.

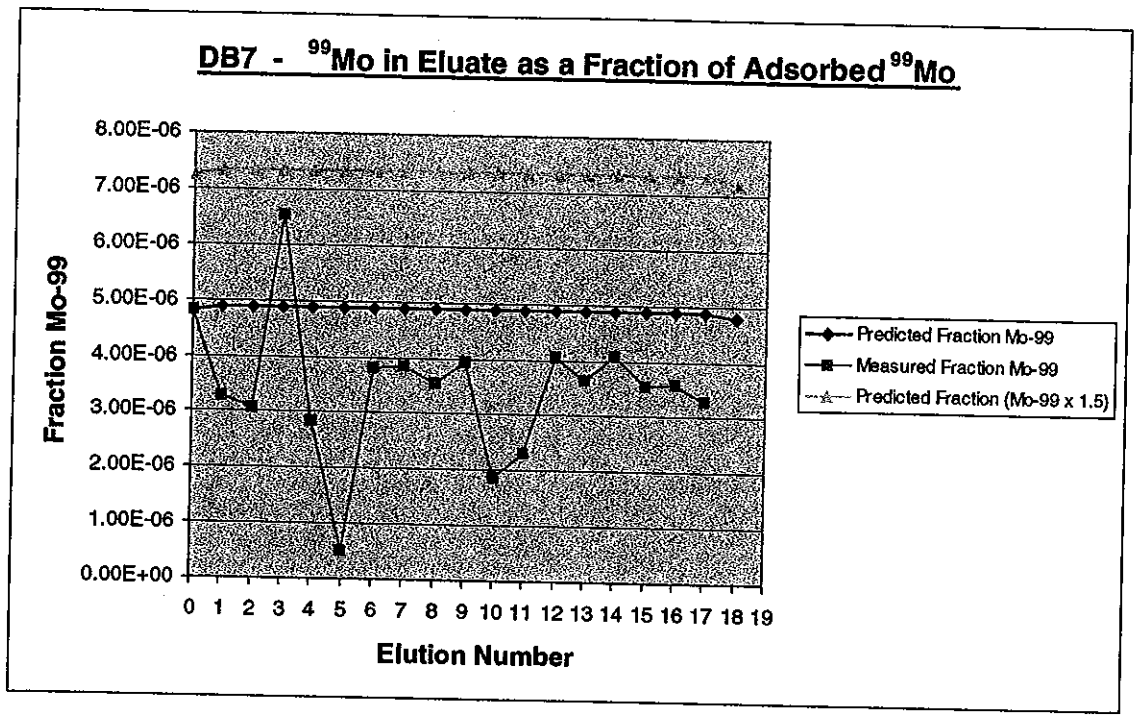
DB7 - 99Mo in Eluate as a Fraction of Adsorbed 99Mo
Fraction Mo-99
8.00E-06
7.00E-06
6.00E-06
5.00E-06
4.00E-06
3.00E-06
2.00E-06
1.00E-06
0.00E+00
0 1 2 3 4 5 6 7 8 9 10 11 12 13 14 15 16 17 18 19
Elution Number
Predicted Fraction Mo-99
Measured Fraction Mo-99
Predicted Fraction (Mo-99 x 1.5)

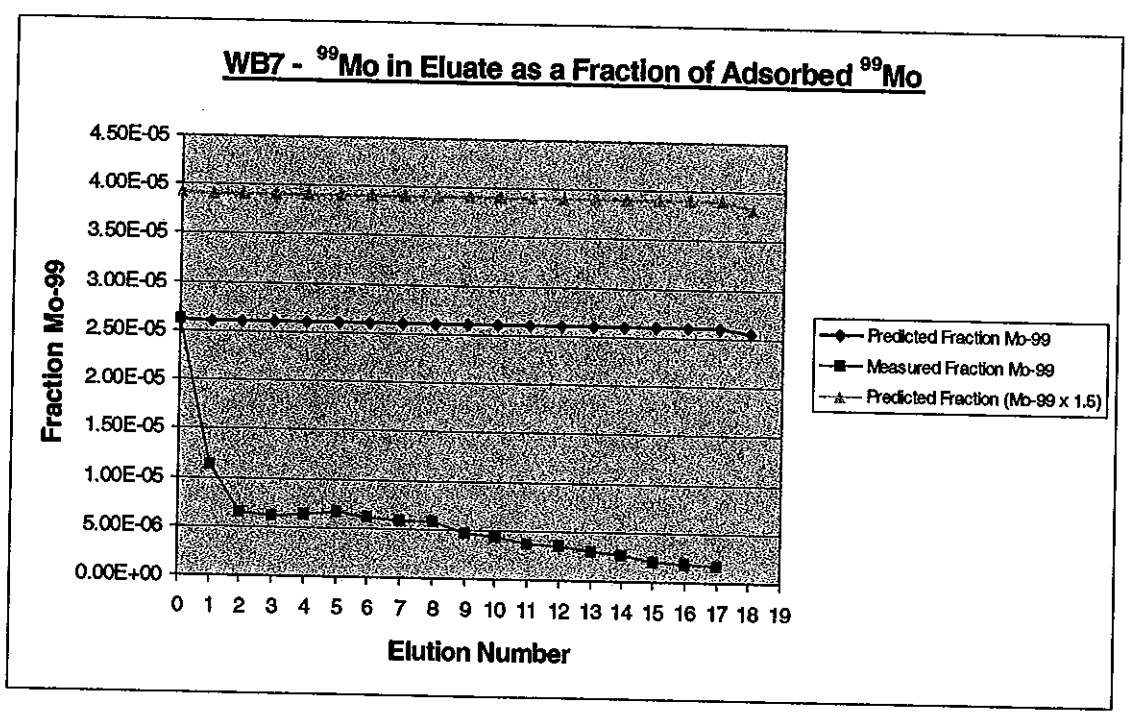
WB7 - 99Mo in Eluate as a Fraction of Adsorbed 99Mo
Fraction Mo-99
4.50E-05
4.00E-05
3.50E-05
3.00E-05
2.50E-05
2.00E-05
1.50E-05
1.00E-05
5.00E-06
0.00E+00
0 1 2 3 4 5 6 7 8 9 10 11 12 13 14 15 16 17 18 19
Elution Number
Predicted Fraction Mo-99
Measured Fraction Mo-99
Predicted Fraction (Mo-99 x 1.5)

Figure 4h.

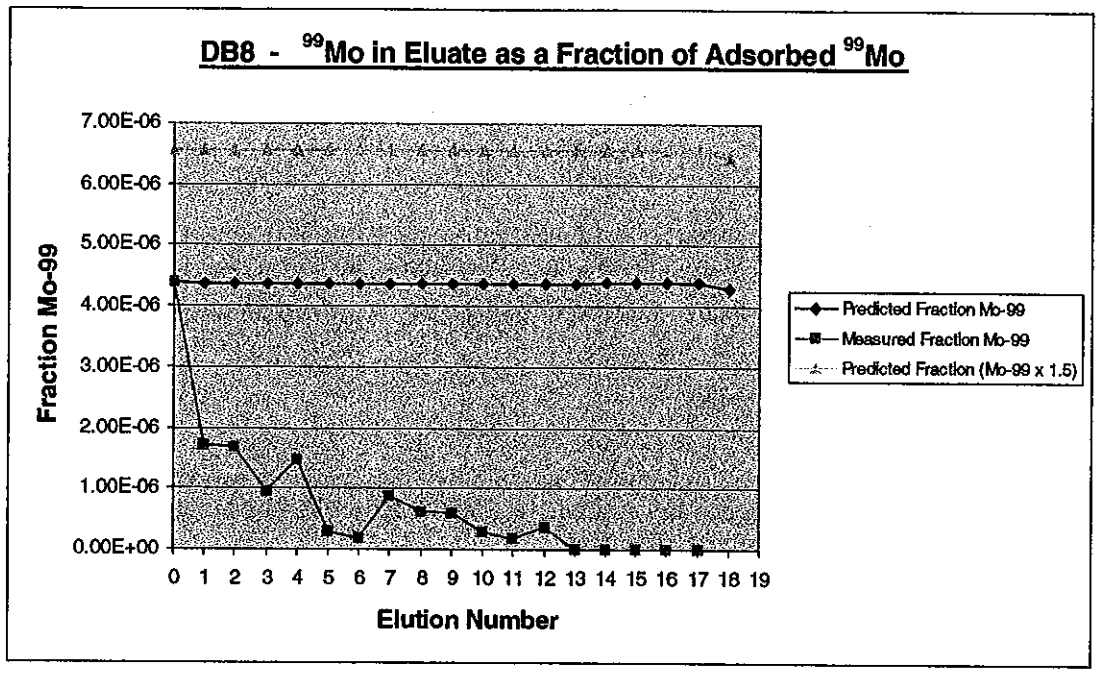
DB8 - 99Mo in Eluate as a Fraction of Adsorbed 99Mo
Fraction Mo-99
7.00E-06
6.00E-06
5.00E-06
4.00E-06
3.00E-06
2.00E-06
1.00E-06
0.00E+00
0 1 2 3 4 5 6 7 8 9 10 11 12 13 14 15 16 17 18 19
Elution Number
Predicted Fraction Mo-99
Measured Fraction Mo-99
Predicted Fraction (Mo-99 x 1.5)

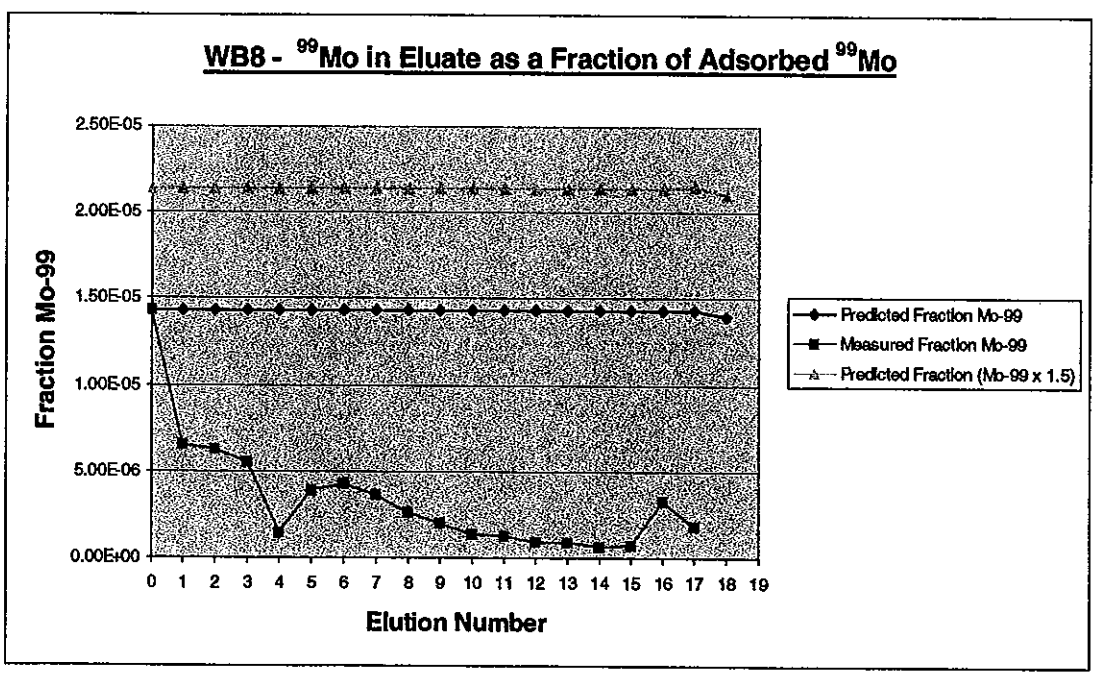
WB8 - 99Mo in Eluate as a Fraction of Adsorbed 99Mo
Fraction Mo-99
2.50E-05
2.00E-05
1.50E-05
1.00E-05
5.00E-06
0.00E+00
0 1 2 3 4 5 6 7 8 9 10 11 12 13 14 15 16 17 18 19
Elution Number
Predicted Fraction Mo-99
Measured Fraction Mo-99
Predicted Fraction (Mo-99 x 1.5)

Figure 4i.

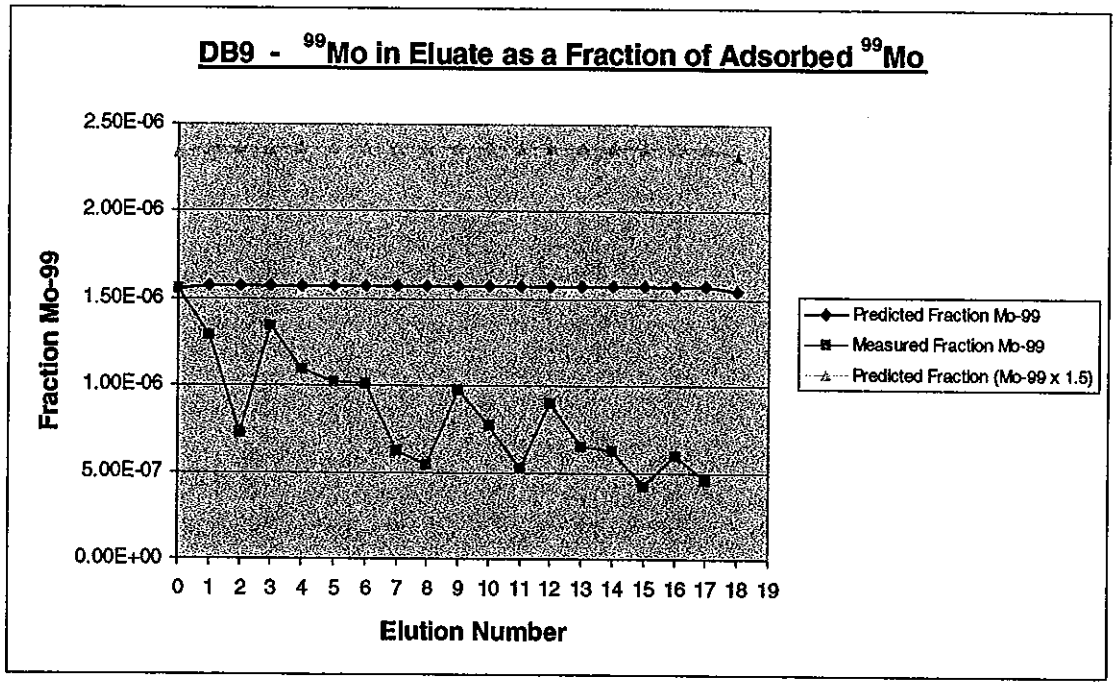
DB9 - 99Mo in Eluate as a Fraction of Adsorbed 99Mo
Fraction Mo-99
2.50E-06
2.00E-06
1.50E-06
1.00E-06
5.00E-07
0.00E+00
0 1 2 3 4 5 6 7 8 9 10 11 12 13 14 15 16 17 18 19
Elution Number
Predicted Fraction Mo-99
Measured Fraction Mo-99
Predicted Fraction (Mo-99 x 1.5)

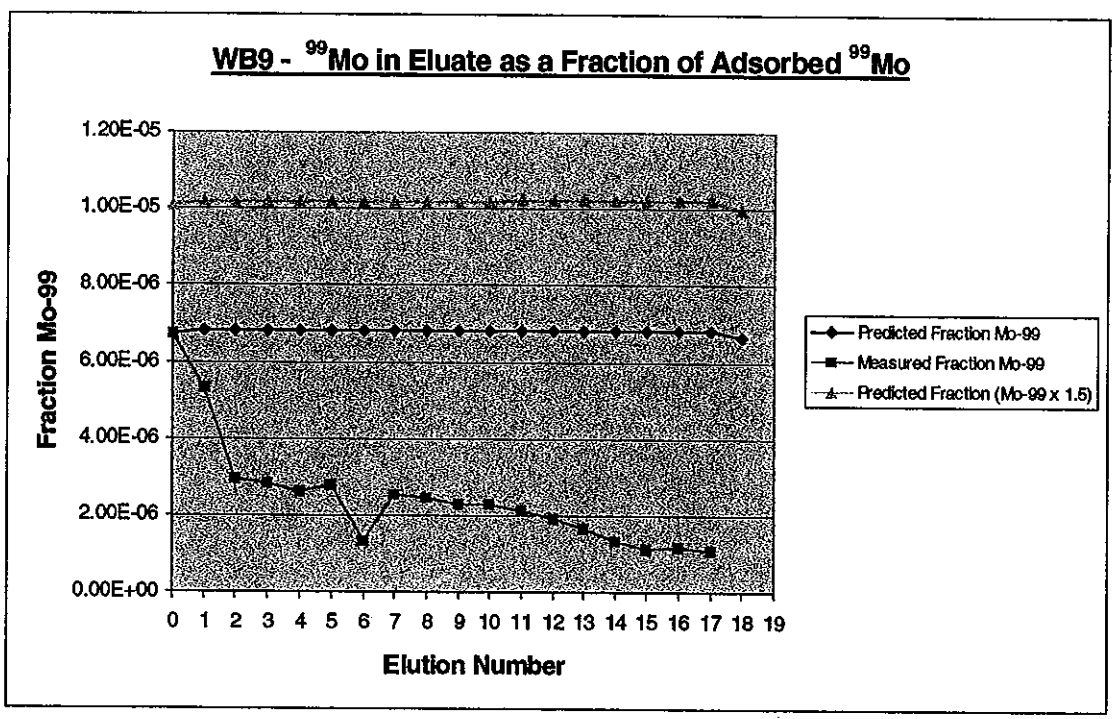
WB9 - 99Mo in Eluate as a Fraction of Adsorbed 99Mo
Fraction Mo-99
1.20E-05
1.00E-05
8.00E-06
6.00E-06
4.00E-06
2.00E-06
0.00E+00
0 1 2 3 4 5 6 7 8 9 10 11 12 13 14 15 16 17 18 19
Elution Number
Predicted Fraction Mo-99
Measured Fraction Mo-99
Predicted Fraction (Mo-99 x 1.5)

Figure 4i.

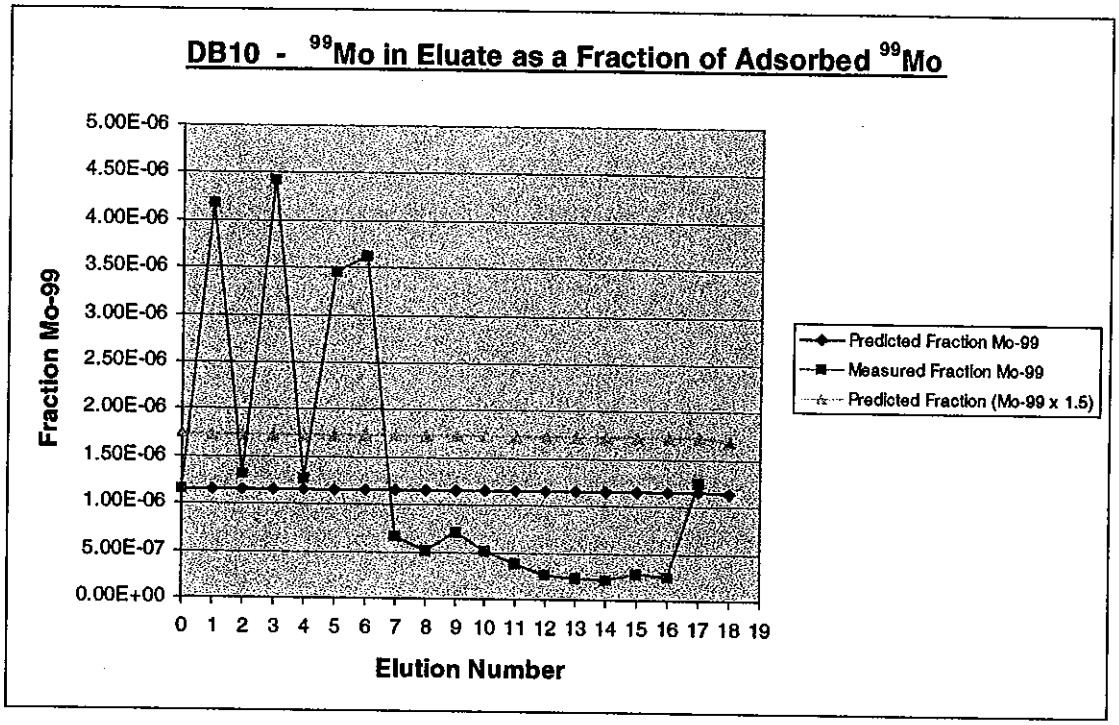
DB10 - 99Mo in Eluate as a Fraction of Adsorbed 99Mo
Fraction Mo-99
5.00E-06
4.50E-06
4.00E-06
3.50E-06
3.00E-06
2.50E-06
2.00E-06
1.50E-06
1.00E-06
5.00E-07
0.00E+00
0 1 2 3 4 5 6 7 8 9 10 11 12 13 14 15 16 17 18 19
Elution Number
Predicted Fraction Mo-99
Measured Fraction Mo-99
Predicted Fraction (Mo-99 x 1.5)

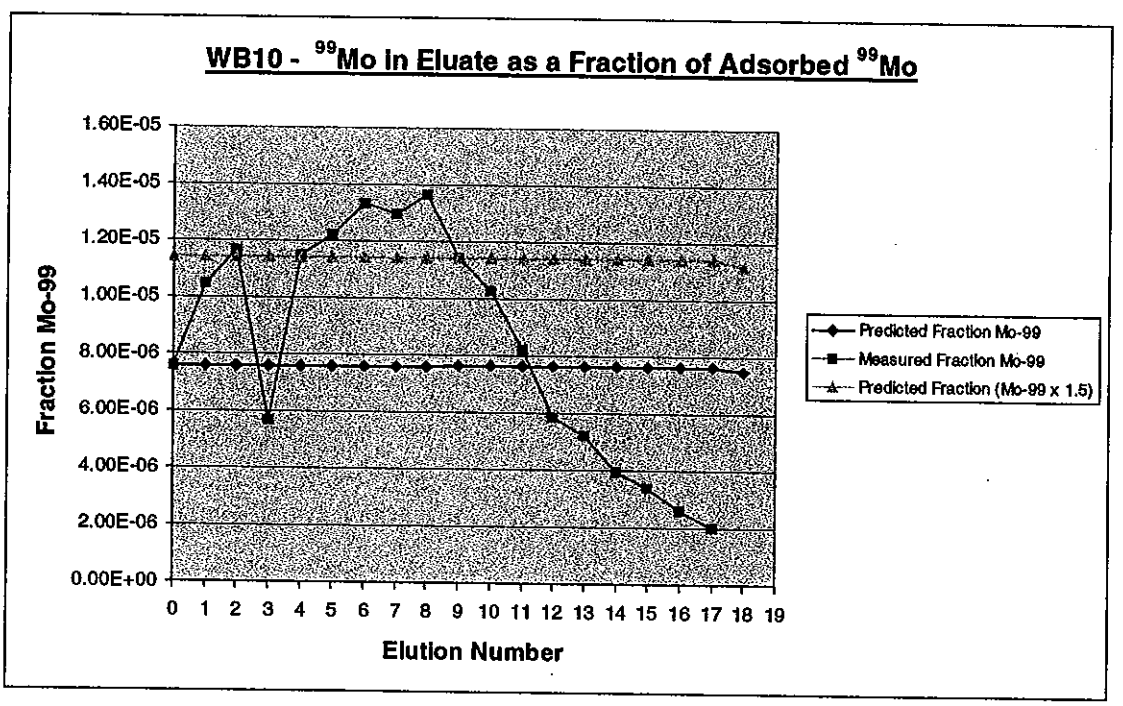
WB10 - 99Mo In Eluate as a Fraction of Adsorbed 99Mo
Fraction Mo-99
1.60E-05
1.40E-05
1.20E-05
1.00E-05
8.00E-06
6.00E-06
4.00E-06
2.00E-06
0.00E+00
0 1 2 3 4 5 6 7 8 9 10 11 12 13 14 15 16 17 18 19
Elution Number
Predicted Fraction Mo-99
Measured Fraction Mo-99
Predicted Fraction (Mo-99 x 1.5)

Figure 5.

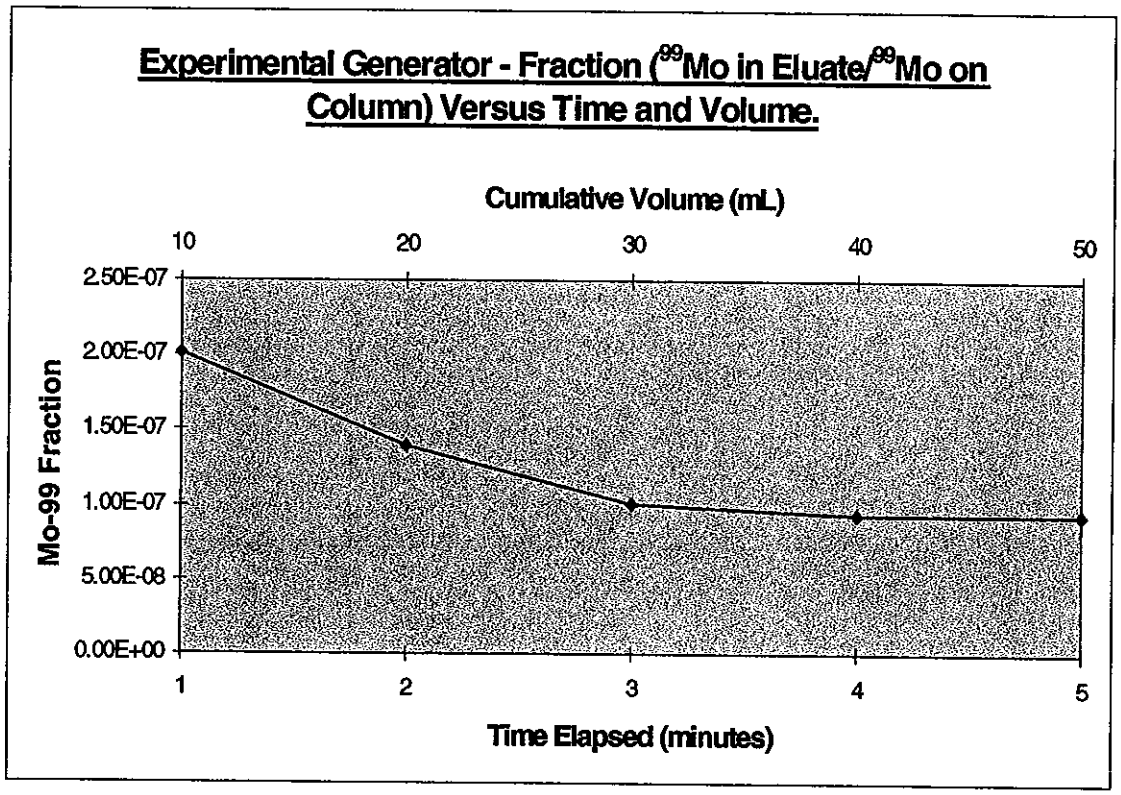
Experimental Generator - Fraction (^{99}Mo in Eluate/^{99}Mo on Column) Versus Time and Volume.
Cumulative Volume (mL)
10
20
30
40
50
2.50E-07
2.00E-07
1.50E-07
1.00E-07
5.00E-08
0.00E+00
Mo-99 Fraction
1
2
3
4
5
Time Elapsed (minutes)

Figure 6.

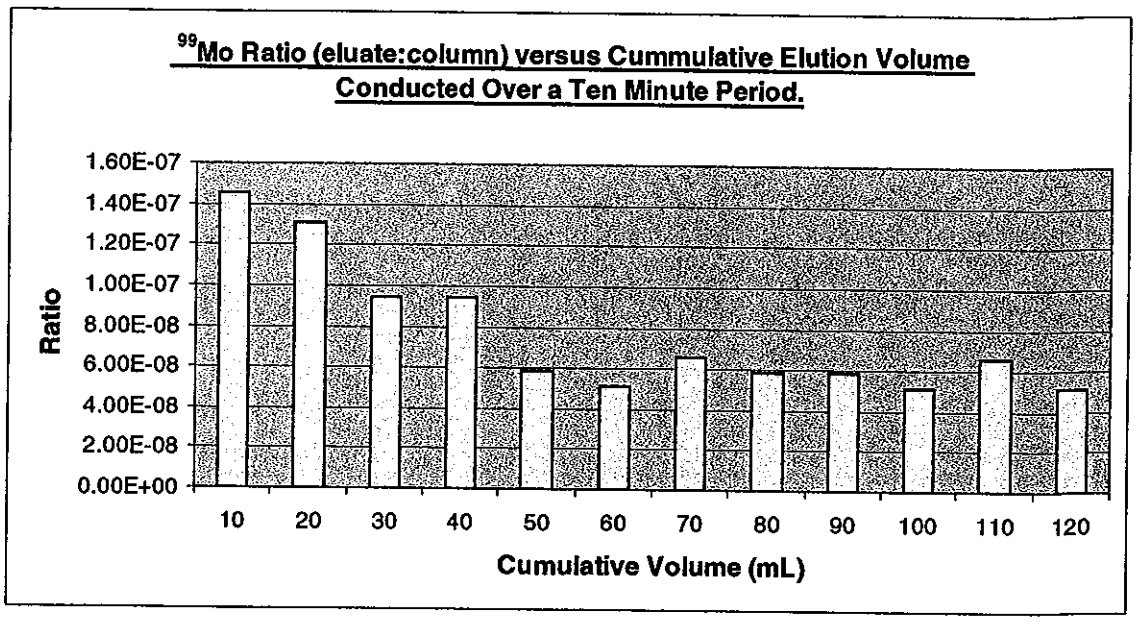
^{99}Mo Ratio (eluate:column) versus Cummulative Elution Volume
Conducted Over a Ten Minute Period.
Ratio
1.60E-07
1.40E-07
1.20E-07
1.00E-07
8.00E-08
6.00E-08
4.00E-08
2.00E-08
0.00E+00
10
20
30
40
50
60
70
80
90
100
110
120
Cumulative Volume (mL)

Figure 7a.

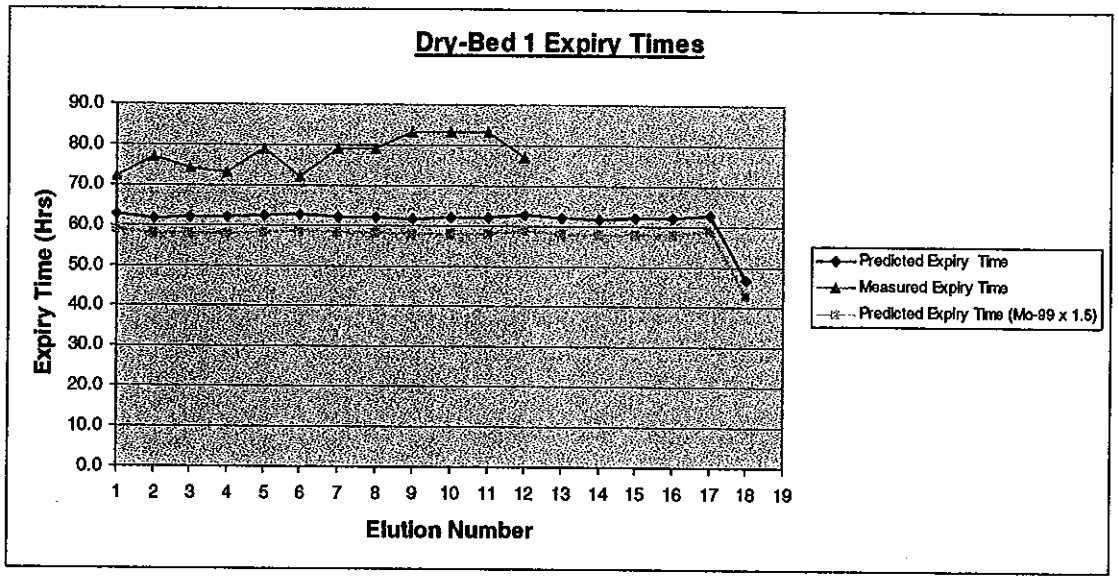
Dry-Bed 1 Expiry Times
Expiry Time (Hrs)
90.0
80.0
70.0
60.0
50.0
40.0
30.0
20.0
10.0
0.0
1 2 3 4 5 6 7 8 9 10 11 12 13 14 15 16 17 18 19
Elution Number
Predicted Expiry Time
Measured Expiry Time
Predicted Expiry Time (Mo-99 x 1.5)

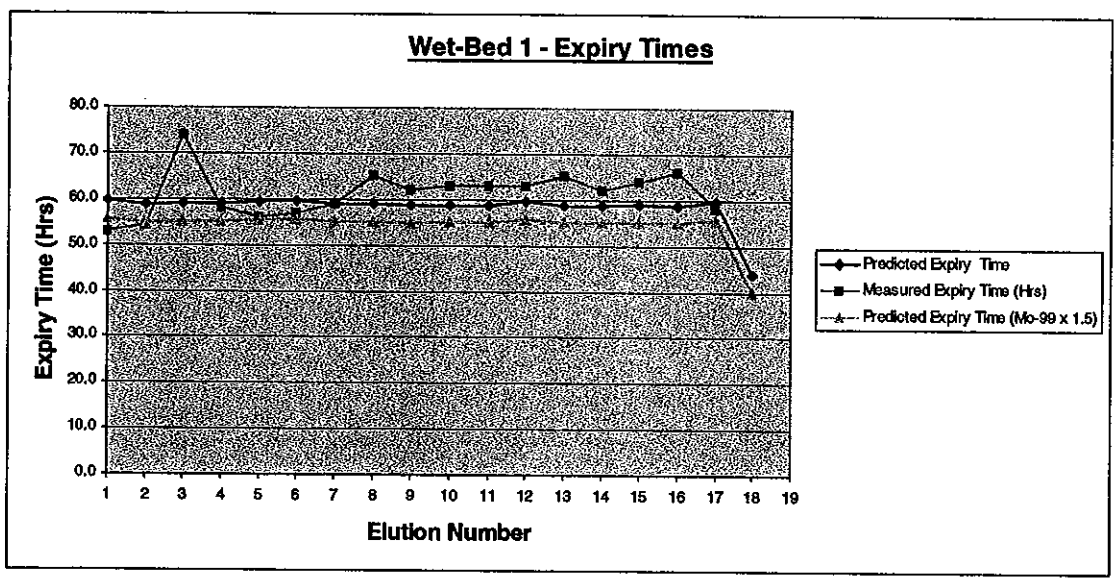
Wet-Bed 1 - Expiry Times
Expiry Time (Hrs)
80.0
70.0
60.0
50.0
40.0
30.0
20.0
10.0
0.0
1 2 3 4 5 6 7 8 9 10 11 12 13 14 15 16 17 18 19
Elution Number
Predicted Expiry Time
Measured Expiry Time (Hrs)
Predicted Expiry Time (Mo-99 x 1.5)

Figure 7b.

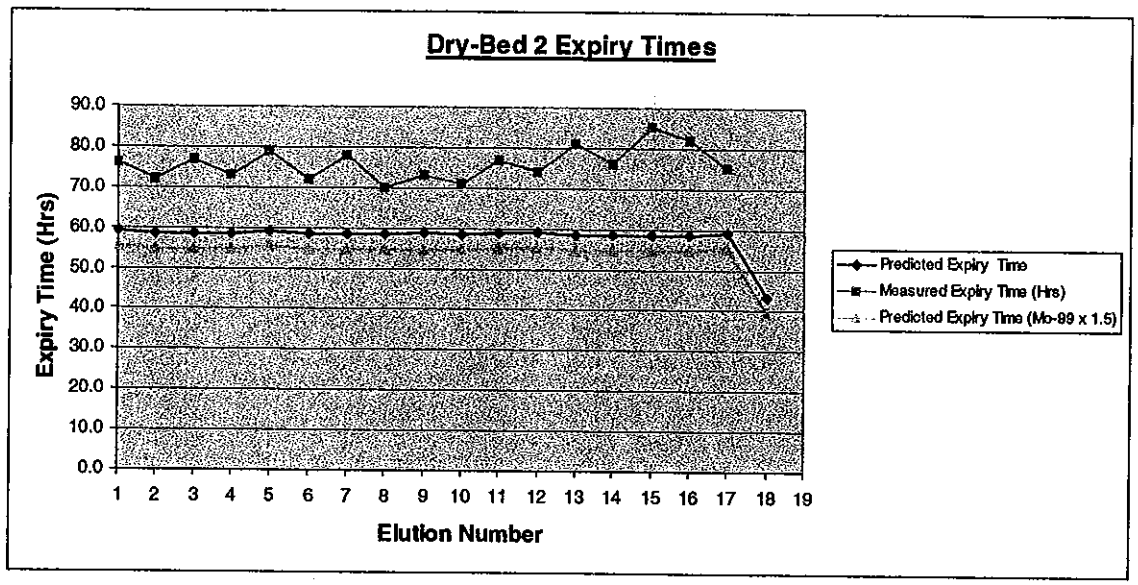
Dry-Bed 2 Expiry Times
Expiry Time (Hrs)
90.0
80.0
70.0
60.0
50.0
40.0
30.0
20.0
10.0
0.0
1 2 3 4 5 6 7 8 9 10 11 12 13 14 15 16 17 18 19
Elution Number
Predicted Expiry Time
Measured Expiry Time (Hrs)
Predicted Expiry Time (Mo-99 x 1.5)

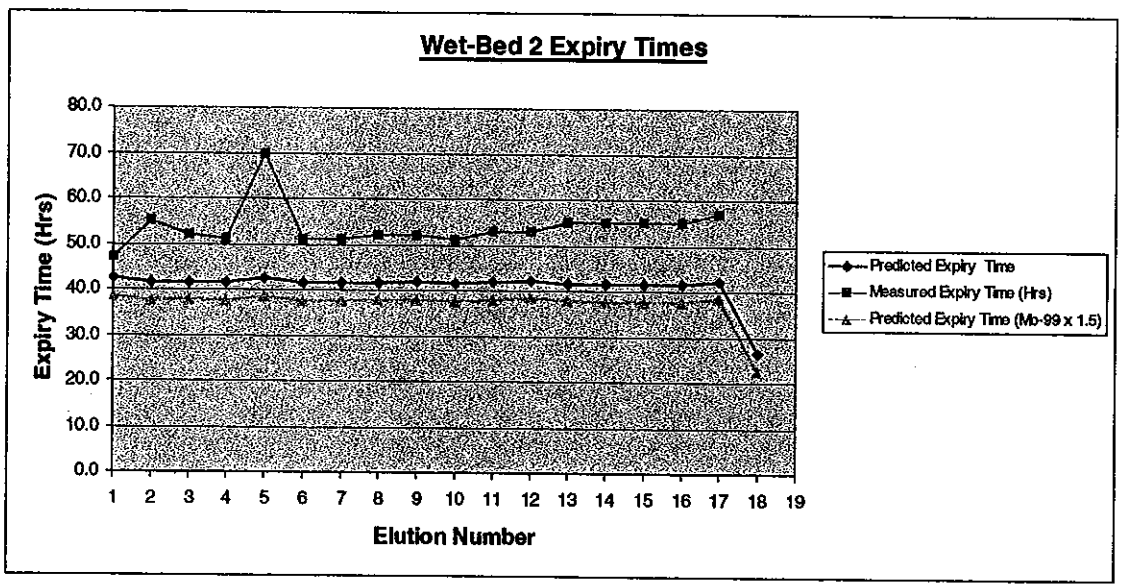
Wet-Bed 2 Expiry Times
Expiry Time (Hrs)
80.0
70.0
60.0
50.0
40.0
30.0
20.0
10.0
0.0
1 2 3 4 5 6 7 8 9 10 11 12 13 14 15 16 17 18 19
Elution Number
Predicted Expiry Time
Measured Expiry Time (Hrs)
Predicted Expiry Time (Mo-99 x 1.5)

Figure 7c.

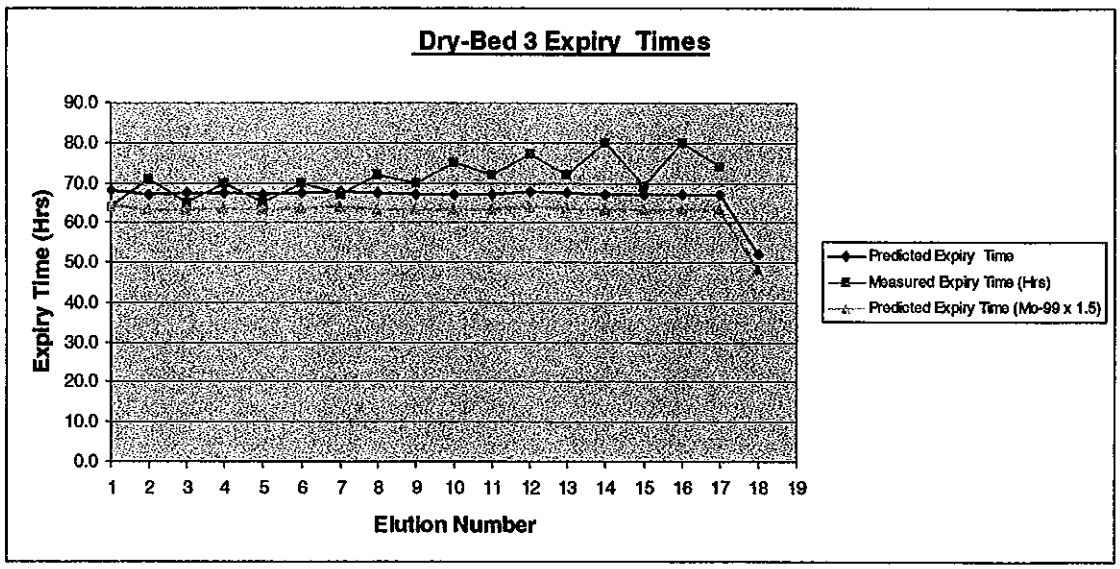
Dry-Bed 3 Expiry Times
Expiry Time (Hrs)
90.0
80.0
70.0
60.0
50.0
40.0
30.0
20.0
10.0
0.0
1 2 3 4 5 6 7 8 9 10 11 12 13 14 15 16 17 18 19
Elution Number
Predicted Expiry Time
Measured Expiry Time (Hrs)
Predicted Expiry Time (Mo-99 x 1.5)

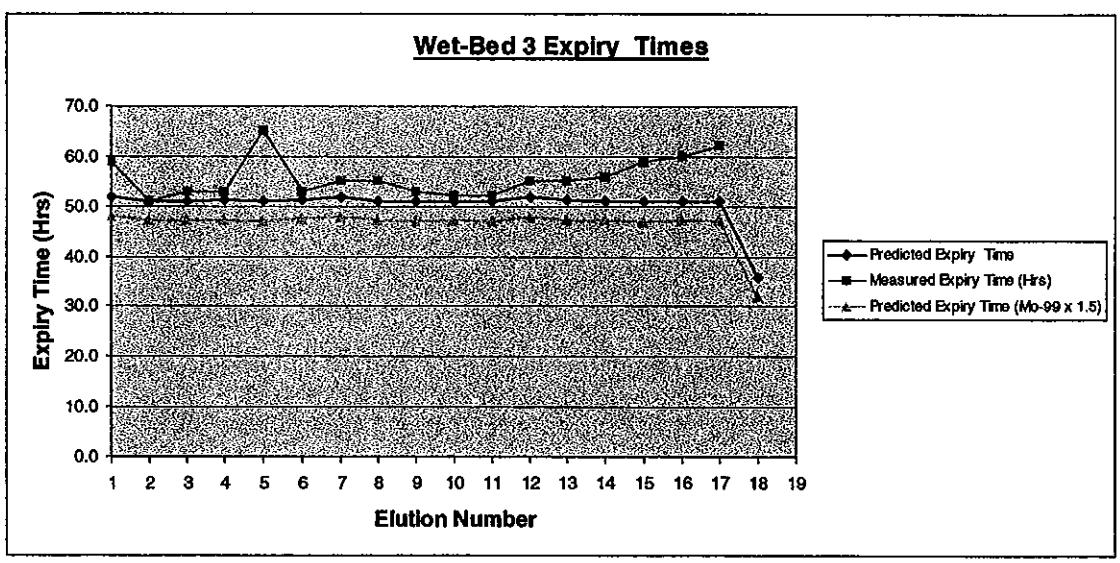
Wet-Bed 3 Expiry Times
Expiry Time (Hrs)
70.0
60.0
50.0
40.0
30.0
20.0
10.0
0.0
1 2 3 4 5 6 7 8 9 10 11 12 13 14 15 16 17 18 19
Elution Number
Predicted Expiry Time
Measured Expiry Time (Hrs)
Predicted Expiry Time (Mo-99 x 1.5)

Figure 7d.

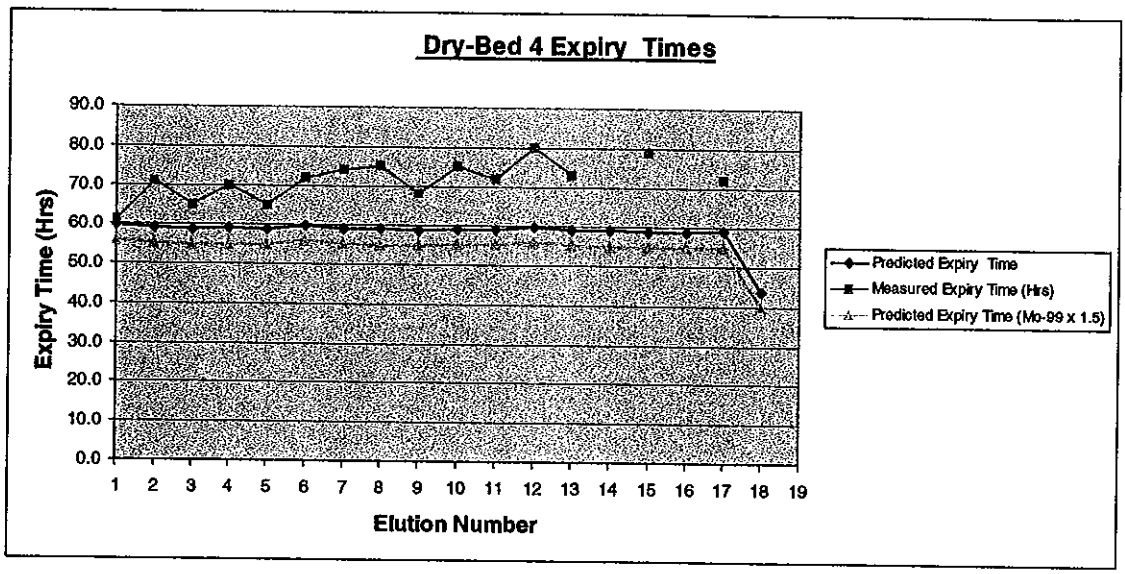
Dry-Bed 4 Expiry Times
Expiry Time (Hrs)
90.0
80.0
70.0
60.0
50.0
40.0
30.0
20.0
10.0
0.0
1 2 3 4 5 6 7 8 9 10 11 12 13 14 15 16 17 18 19
Elution Number
Predicted Expiry Time
Measured Expiry Time (Hrs)
Predicted Expiry Time (Mo-99 x 1.5)

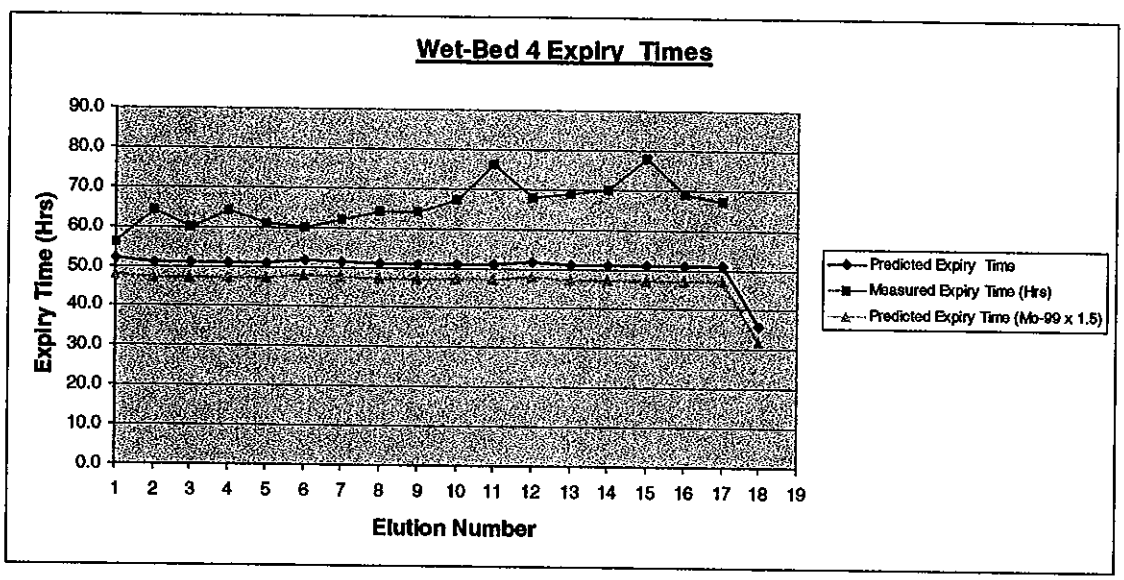
Wet-Bed 4 Expiry Times
Expiry Time (Hrs)
90.0
80.0
70.0
60.0
50.0
40.0
30.0
20.0
10.0
0.0
1 2 3 4 5 6 7 8 9 10 11 12 13 14 15 16 17 18 19
Elution Number
Predicted Expiry Time
Measured Expiry Time (Hrs)
Predicted Expiry Time (Mo-99 x 1.5)

Figure 7e.

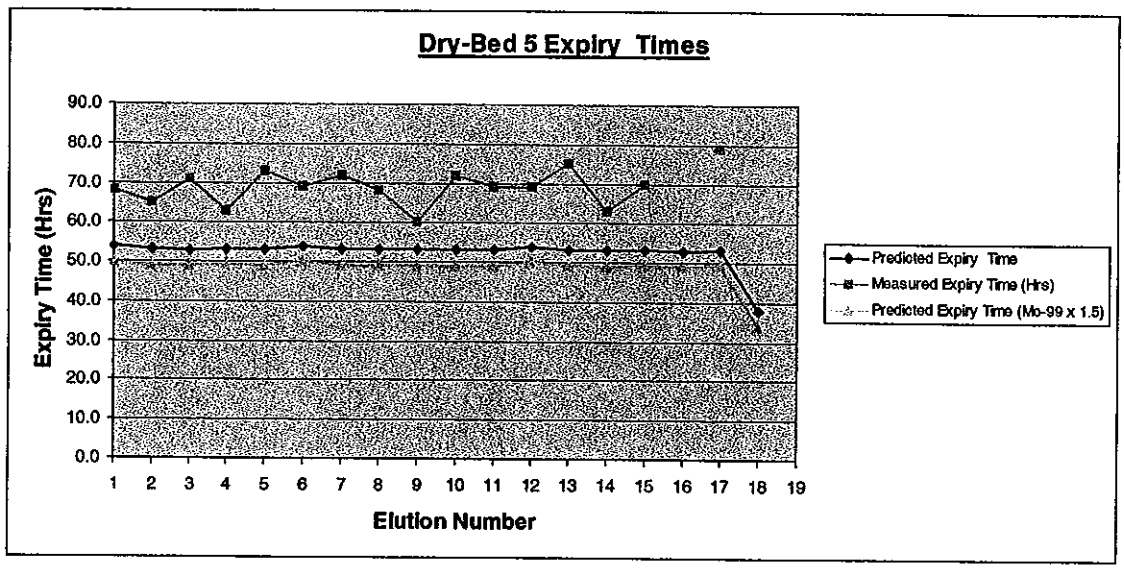
Dry-Bed 5 Expiry Times
Expiry Time (Hrs)
90.0
80.0
70.0
60.0
50.0
40.0
30.0
20.0
10.0
0.0
1 2 3 4 5 6 7 8 9 10 11 12 13 14 15 16 17 18 19
Elution Number
Predicted Expiry Time
Measured Expiry Time (Hrs)
Predicted Expiry Time (Mo-99 x 1.5)

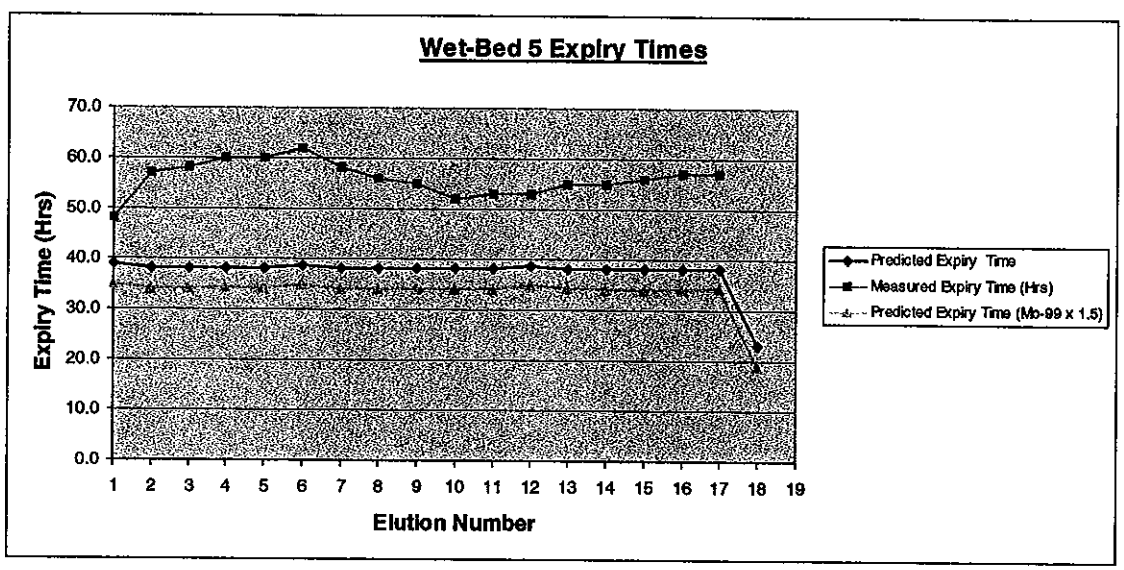
Wet-Bed 5 Expiry Times
Expiry Time (Hrs)
70.0
60.0
50.0
40.0
30.0
20.0
10.0
0.0
1 2 3 4 5 6 7 8 9 10 11 12 13 14 15 16 17 18 19
Elution Number
Predicted Expiry Time
Measured Expiry Time (Hrs)
Predicted Expiry Time (Mo-99 x 1.5)

Figure 7f.

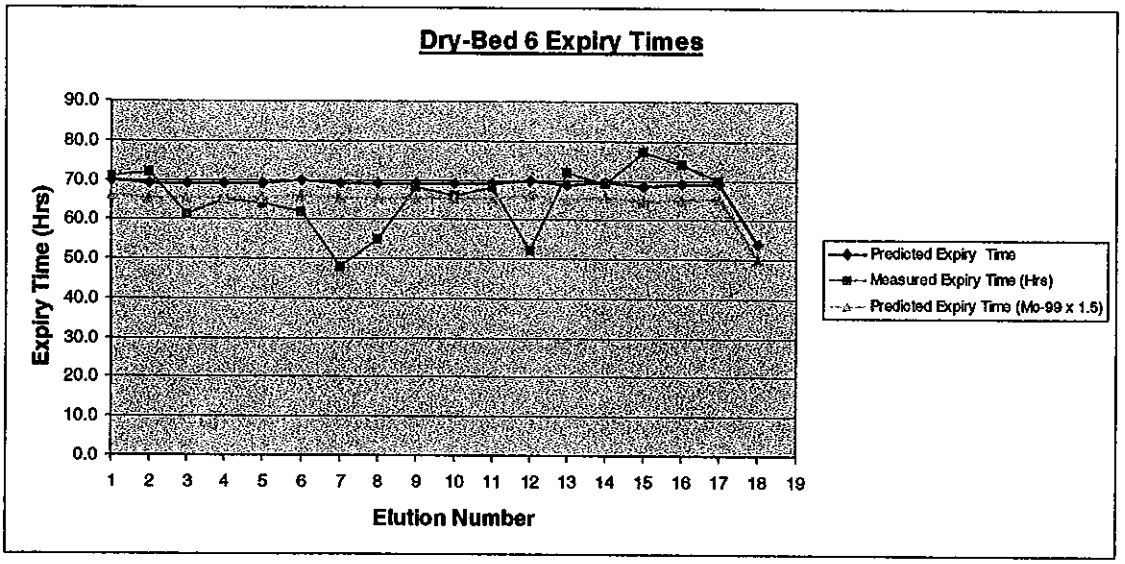
Dry-Bed 6 Expiry Times
Expiry Time (Hrs)
90.0
80.0
70.0
60.0
50.0
40.0
30.0
20.0
10.0
0.0
1 2 3 4 5 6 7 8 9 10 11 12 13 14 15 16 17 18 19
Elution Number
Predicted Expiry Time
Measured Expiry Time (Hrs)
Predicted Expiry Time (Mo-99 x 1.5)

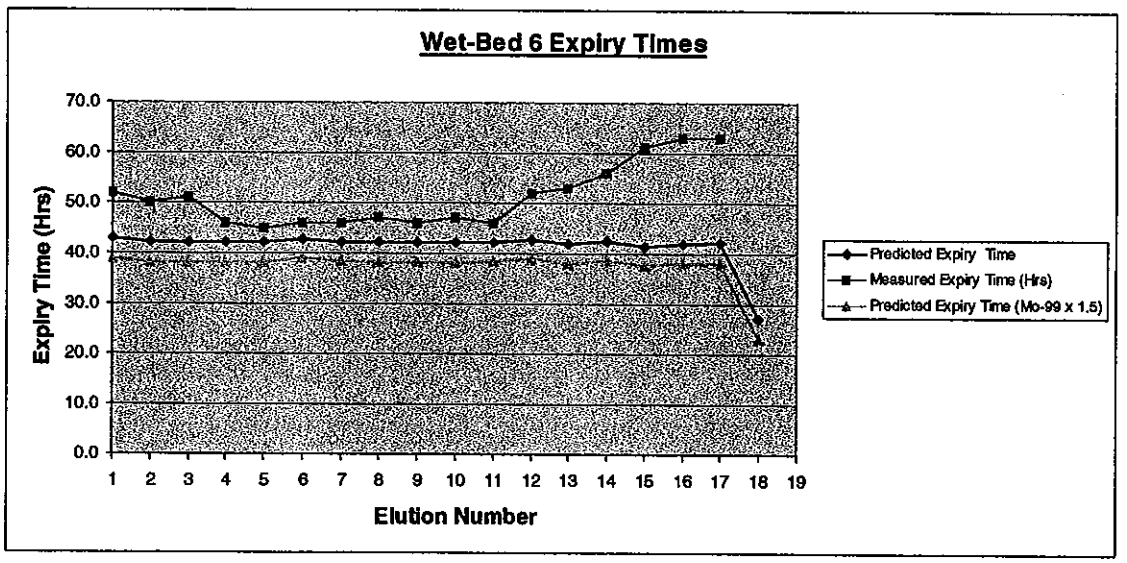
Wet-Bed 6 Expiry Times
Expiry Time (Hrs)
70.0
60.0
50.0
40.0
30.0
20.0
10.0
0.0
1 2 3 4 5 6 7 8 9 10 11 12 13 14 15 16 17 18 19
Elution Number
Predicted Expiry Time
Measured Expiry Time (Hrs)
Predicted Expiry Time (Mo-99 x 1.5)

Figure 7g.

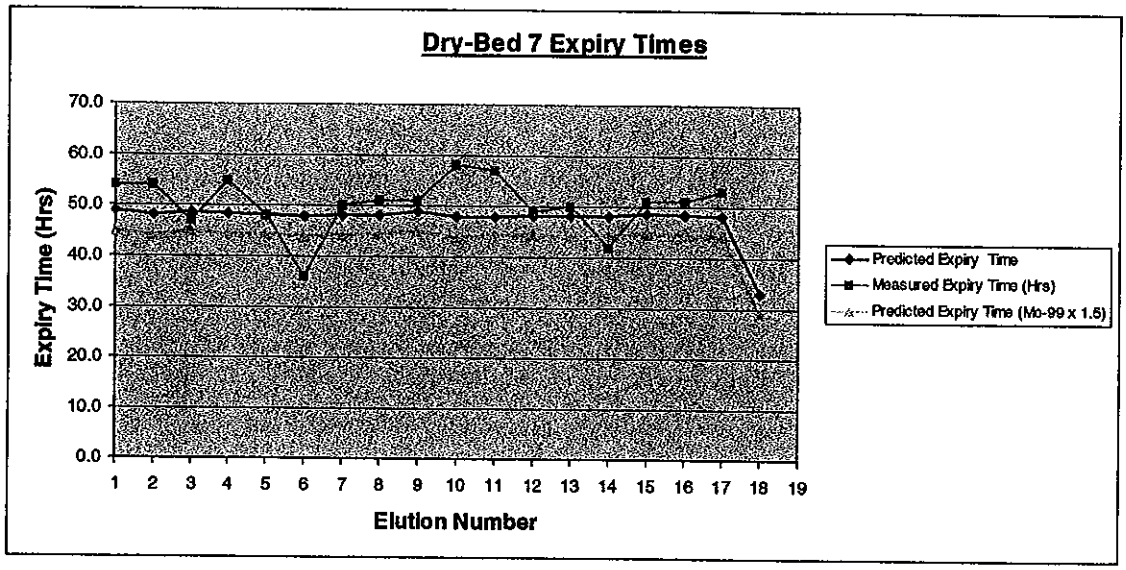
Dry-Bed 7 Expiry Times
Expiry Time (Hrs)
70.0
60.0
50.0
40.0
30.0
20.0
10.0
0.0
1 2 3 4 5 6 7 8 9 10 11 12 13 14 15 16 17 18 19
Elution Number
Predicted Expiry Time
Measured Expiry Time (Hrs)
Predicted Expiry Time (Mo-99 x 1.5)

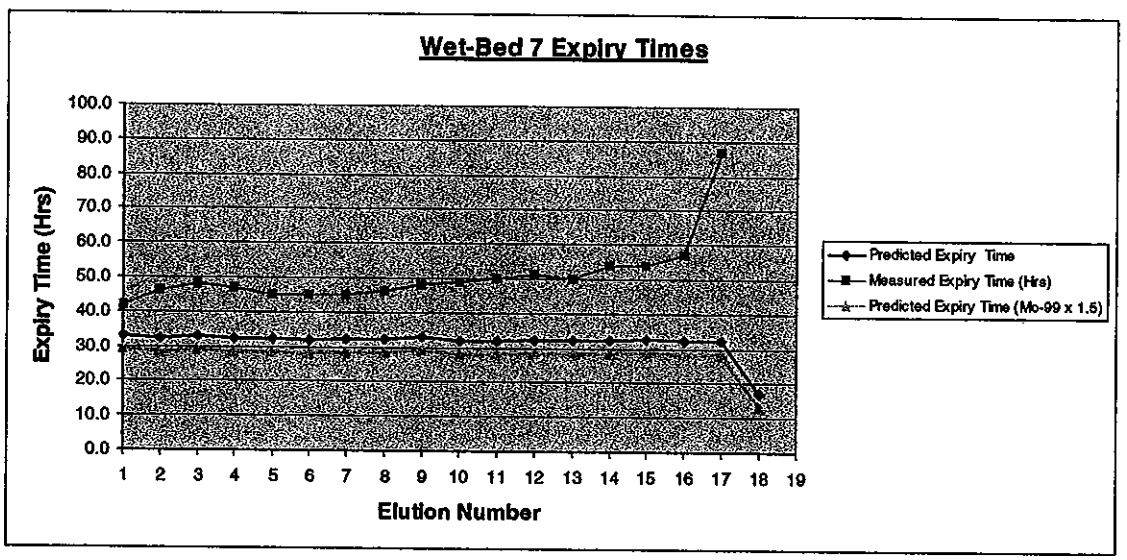
Wet-Bed 7 Expiry Times
Expiry Time (Hrs)
100.0
90.0
80.0
70.0
60.0
50.0
40.0
30.0
20.0
10.0
0.0
1 2 3 4 5 6 7 8 9 10 11 12 13 14 15 16 17 18 19
Elution Number
Predicted Expiry Time
Measured Expiry Time (Hrs)
Predicted Expiry Time (Mo-99 x 1.5)

Figure 7h.

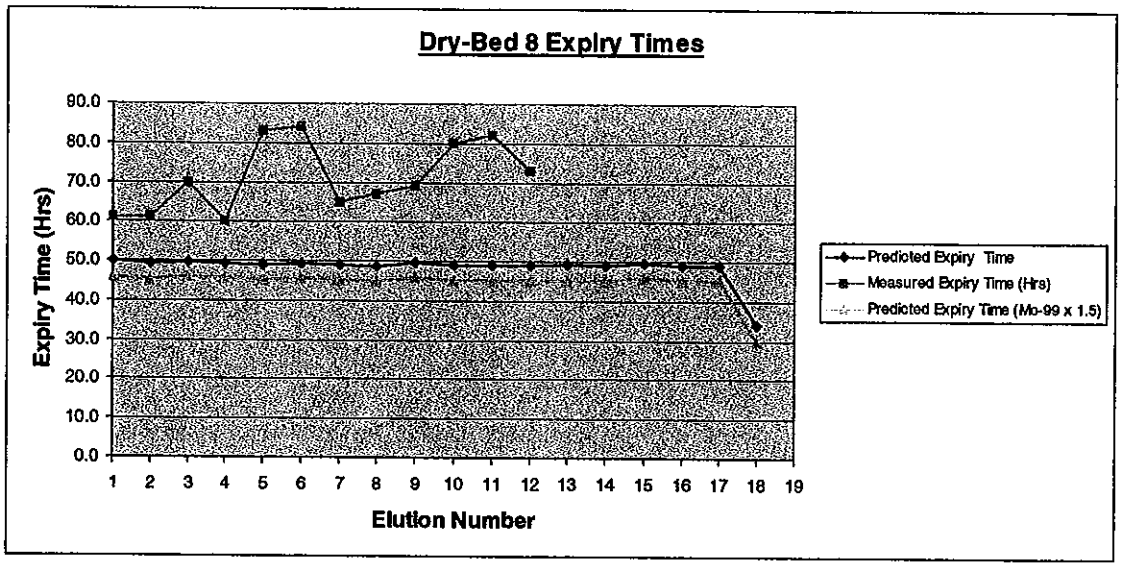
Dry-Bed 8 Expiry Times
Expiry Time (Hrs)
90.0
80.0
70.0
60.0
50.0
40.0
30.0
20.0
10.0
0.0
1 2 3 4 5 6 7 8 9 10 11 12 13 14 15 16 17 18 19
Elution Number
Predicted Expiry Time
Measured Expiry Time (Hrs)
Predicted Expiry Time (Mo-99 x 1.5)

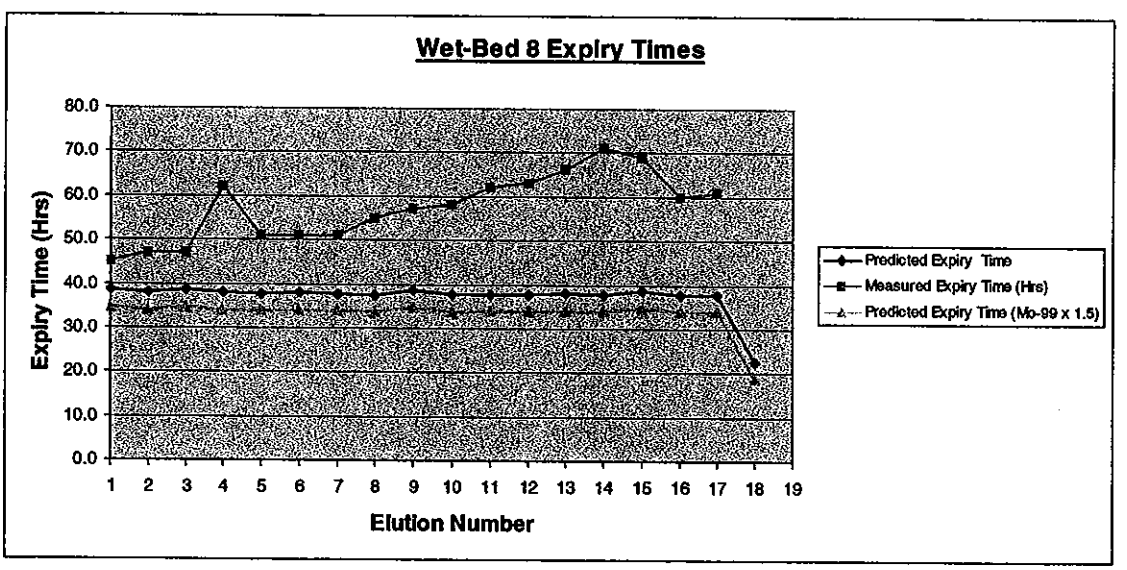
Wet-Bed 8 Expiry Times
Expiry Time (Hrs)
80.0
70.0
60.0
50.0
40.0
30.0
20.0
10.0
0.0
1 2 3 4 5 6 7 8 9 10 11 12 13 14 15 16 17 18 19
Elution Number
Predicted Expiry Time
Measured Expiry Time (Hrs)
Predicted Expiry Time (Mo-99 x 1.5)

Figure 7i.

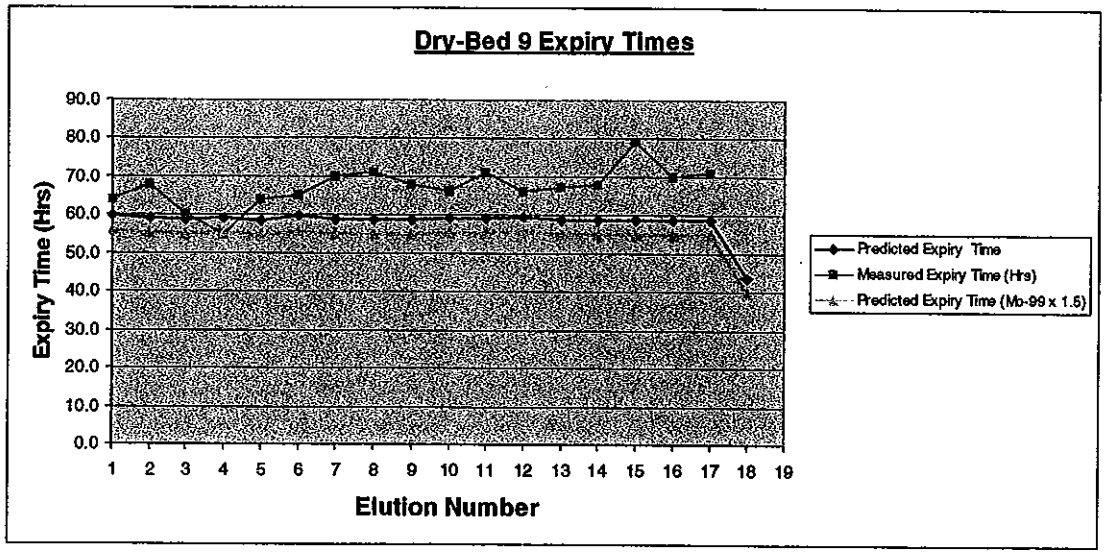
Dry-Bed 9 Expiry Times
Expiry Time (Hrs)
90.0
80.0
70.0
60.0
50.0
40.0
30.0
20.0
10.0
0.0
1 2 3 4 5 6 7 8 9 10 11 12 13 14 15 16 17 18 19
Elution Number
Predicted Expiry Time
Measured Expiry Time (Hrs)
Predicted Expiry Time (Mo-99 x 1.5)

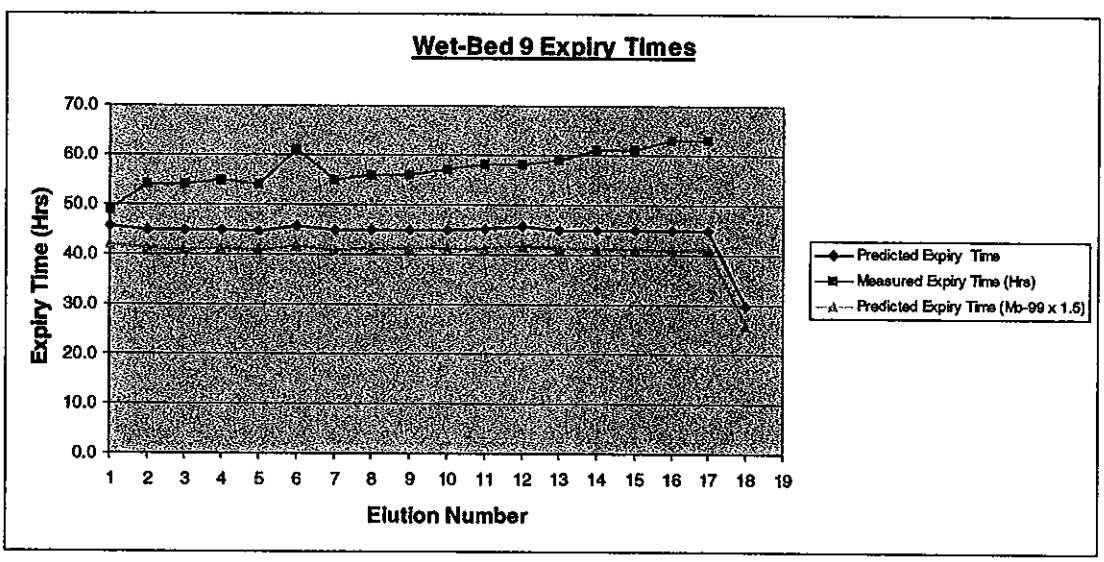
Wet-Bed 9 Expiry Times
Expiry Time (Hrs)
70.0
60.0
50.0
40.0
30.0
20.0
10.0
0.0
1 2 3 4 5 6 7 8 9 10 11 12 13 14 15 16 17 18 19
Elution Number
Predicted Expiry Time
Measured Expiry Time (Hrs)
Predicted Expiry Time (Mo-99 x 1.5)

Figure 8a.

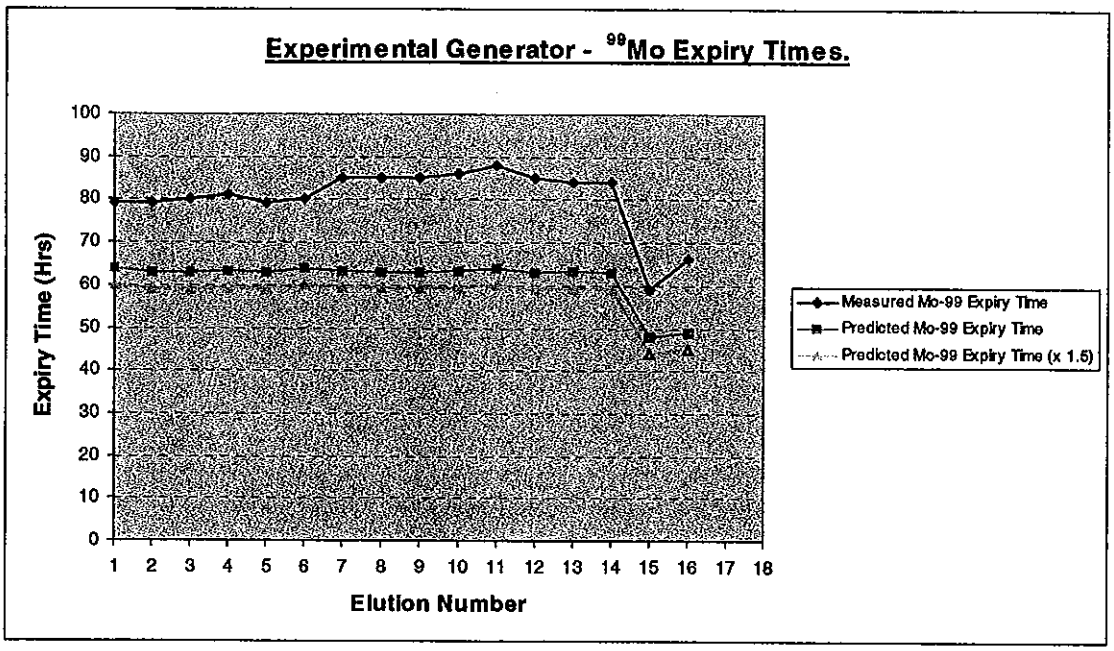

Figure 8b.

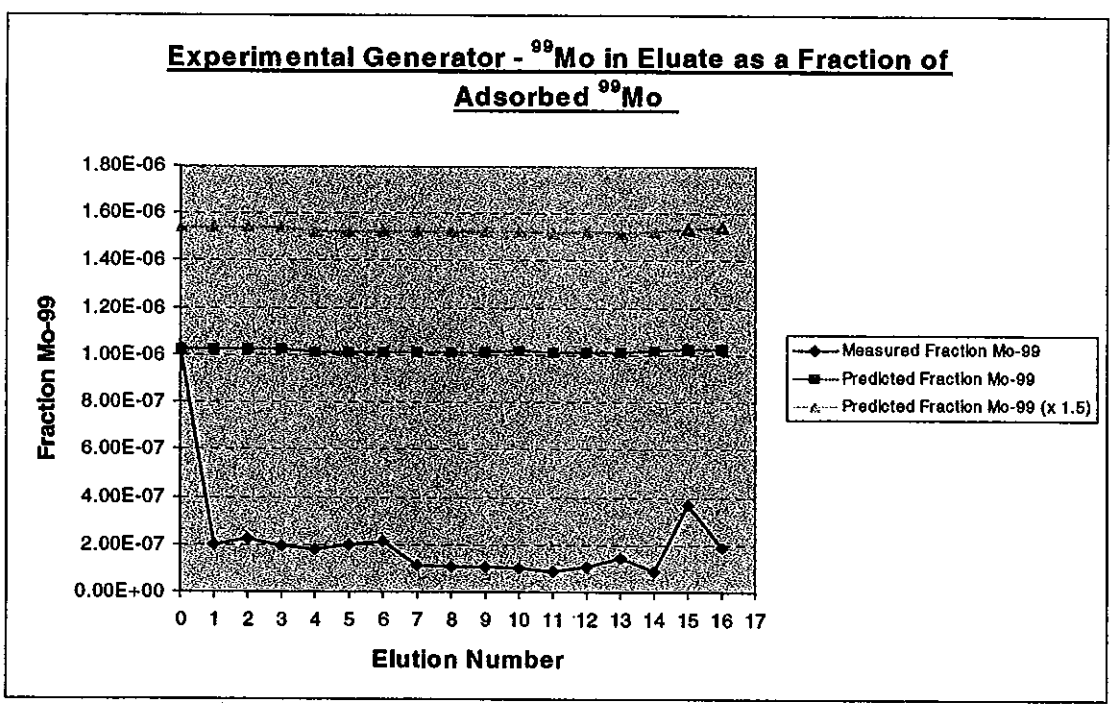

Figure 8c.

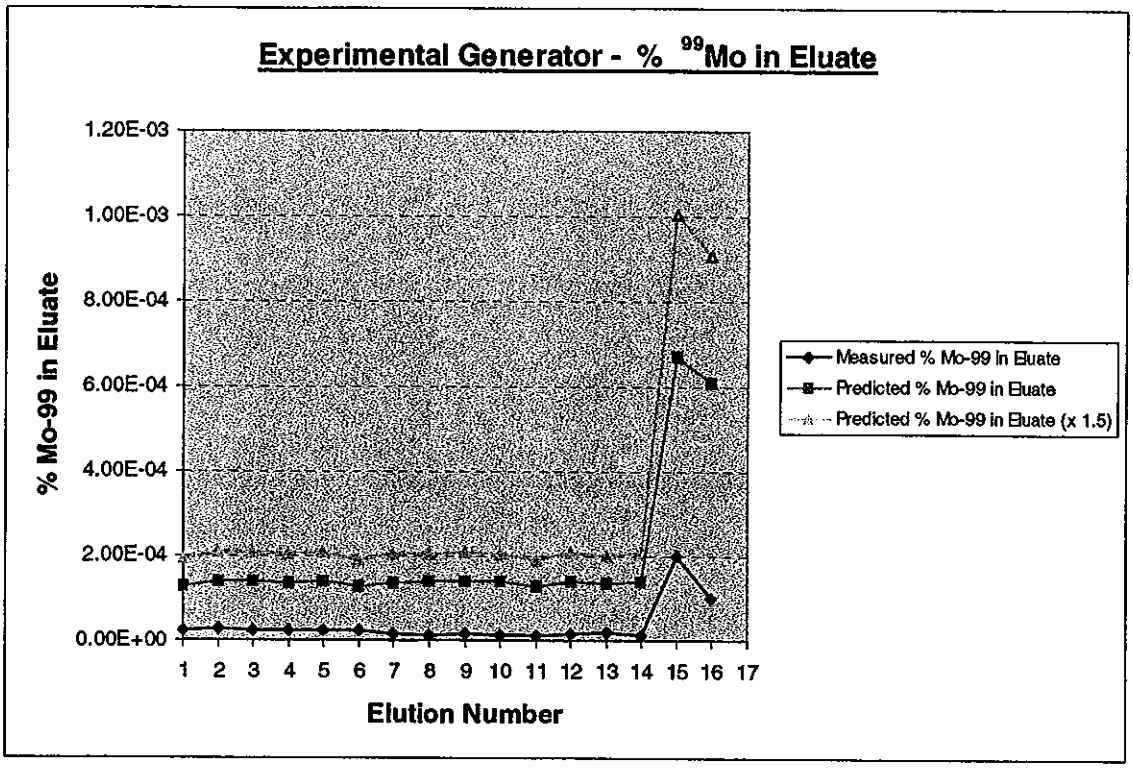
Experimental Generator - % 99Mo in Eluate
% Mo-99 in Eluate
1.20E-03
1.00E-03
8.00E-04
6.00E-04
4.00E-04
2.00E-04
0.00E+00
1 2 3 4 5 6 7 8 9 10 11 12 13 14 15 16 17
Elution Number
Measured % Mo-99 in Eluate
Predicted % Mo-99 in Eluate
Predicted % Mo-99 in Eluate (x 1.5)

TABLE 1

^{99}Mo ACTIVITY AND EXPIRATION TIME OF GENERATOR SETS

Generator	ACTIVITY AT CAL (GBq)	EXPIRY TIME (hours)	Generator	ACTIVITY AT CAL (GBq)	EXPIRY TIME (hours)
DB1	21.2	77.5 +/- 4.2	WB1	21.6	61.3 +/- 5.1
DB2	118.5	75.0 +/- 4.1	WB2	118.5	52.3 +/- 2.4
DB3	123.6	71.3 +/- 4.8	WB3	122.9	52.8 +/-3.9
DB4	19.4	71.4 +/- 5.4	WB4	19.8	66.1 +/- 5.7
DB5	58.9	66.1 +/- 5.8	WB5	59.9	55.9 +/- 3.3
DB6	62.2	65.5 +/- 7.9	WB6	63.3	51.2 +/- 6.2
DB7	118.7	50.4 +/- 5.3	WB7	120.4	48.6 +/- 4.0
DB8	21.6	71.3 +/- 9.0	WB8	20.1	58.3 +/- 7.9
DB9	122.0	66.7 +/- 6.5	WB9	121.5	57.3 +/-3.8
DB10	60.6	66.8 +/-10.0	WB10	60.6	44.2 +/- 13.3

DB = Dry Bed Generator

WB = Wet Bed Genrator

Each generator eluted a maximum of 17 cycles (N = 17)